



*Escuela Técnica Superior de Ingenieros de Caminos,
Canales y Puertos.*
UNIVERSIDAD DE CANTABRIA



Aplicación del hormigón con fibras a torres eólicas. Estado del arte y marco normativo.

Trabajo realizado por:

Pilar Melero Gallego

Dirigido:

Francisco Ballester Muñoz

Jokin Rico Arenal

Titulación:

**Máster Universitario en
Ingeniería de Caminos, Canales y
Puertos**

Santander, Septiembre de 2018

TRABAJO FINAL DE MASTER



RESUMEN

TÍTULO: Aplicación del hormigón con fibras a torres eólicas. Estado del arte y marco normativo. / Use of Fiber Reinforced Concrete in wind turbine towers. State of art and standards.

AUTOR: Pilar Melero Gallego

DIRECTORES: Francisco Ballester Muñoz y Jokin Rico Arenal

CONVOCATORIA: Septiembre 2018

PALABRAS CLAVE: Torre eólica, Hormigón con fibras, Estados límites, Caracterización mecánica, Hormigón convencional, Refuerzo, Esfuerzos, Diseño.

La continua evolución y desarrollo del sector eólico conduce a la utilización de turbinas de mayor potencia y peso, lo cual requiere de torres de mayor altura y capacidad portante. Cuando se requieren torres de alturas superiores a 100m, las torres metálicas pierden competitividad y las de hormigón aumentan sus ventajas.

Uno de los principales parámetros para la optimización de las torres de hormigón es el espesor, el cual puede reducirse con la utilización del hormigón con fibras, además de optimizar este espesor debido a los diferentes requisitos estructurales, la adición de fibras mejora otros parámetros como la durabilidad.

Debido a las ventajas estructurales y de construcción que presenta la técnica del hormigón reforzado con fibras, este documento desarrolla el estado del arte de este material, y el desarrollo normativo actual a nivel internacional, para marcar las guías para su diseño y aplicación a torres eólicas.

El estudio de la normativa refleja la limitación de esta frente al esfuerzo torsor, que no está debidamente desarrollado en ninguna normativa. Además, el comportamiento frente a cargas cíclicas que resulta sumamente importante en torres eólicas solamente es tratado por la normativa ACI, sin quedar definido completamente en ninguna normativa.

Se concluye que la aplicación del hormigón con fibras a torres eólicas resulta beneficiosa e interesante económicamente, si bien es necesario profundizar y definir correctamente el comportamiento a torsión y fatiga.

A continuación, se presenta la bibliografía consultada para la realización de este Trabajo Fin de Máster.



- [1] W. E. Foundation, «Wind Energy Foundation,» [En línea].
- [2] G. -. G. W. E. Council, «Global Wind Report, Annual Market Update 2017».
- [3] A. I. T. G. 9, «Report on Design of Concrete Wind Turbine Towers».
- [4] T. C. Centre, «Concrete Towers for Onshore and Offshore Wind Farms».
- [5] A. 544.1R-96, «Report on Fiber Reinforced Concrete,» R2009.
- [6] M. Joshua A. McMahon and Anna C. Birely, «Experimental Performance of Steel Fiber Reinforced Concrete Bridge Deck,» 2018.
- [7] J. V. N. A. J. B. H. R. Paulo A. L. Fernandes, «Study of a self-compacting fiber-reinforced concrete to be applied in the precast industry,» 2018.
- [8] P. P. J. M. X. S. Y. R. AC Birely, «Fiber Reinforced Concrete for Improved Performance of Transportation Infrastructure,» 2018.
- [9] M. d. Fomento, Instrucción de Hormigón Estructural EHE-08, 2008.
- [10] JSCE, «Recommendations for Design and Construction of High Performance Fiber Reinforced Cement Composites with Multiple Fine Cracks (HPFRCC),» 2008.
- [11] 544.9R-17, «Report on Measuring Mechanical Properties of Hardened Fiber-Reinforced Concrete,» 2017.
- [12] M. A. M. Muhammad I. Rjoub, «TORSIONAL STRENGTH OF STEEL FIBER,» Journal of Engineering Sciences, Assiut University, Vol. 35, No.1, pp.1-8, 2007.
- [13] D. R. S. T.D. Gunneswara Rao, «Torsion of steel fiber reinforced concrete members,» Cement and Concrete Research 33, 2003.
- [14] D. H. L. K. S. K. Hyunjin Ju, «Minimum torsional reinforcement ratio for reinforced concrete members with steel fiber,» Composite Structures, 2018.
- [15] R. T. 1. TDF, «Test and design methods for steel fibre reinforced concrete,» 2003.
- [16] CNR, «Guide for the Design and Construction of Fiber-Reinforced Concrete Structures,» 2007.



- [17] A. 544.2R-17, «Report on the Measurement of Fresh State Properties,» 2017.
- [18] A. 544.3R-08, «Guide for Specifying, Proportioning, and Production of Fiber-Reinforced Concrete,» 2008.
- [19] A. 544.4R-18, «Guide to Design with Fiber Reinforced Concrete,» 2018.
- [20] A. 544.R-10, «Report on the Physical Properties and durability of fiber reinforced concrete,» 2010.
- [21] A. 544.6R-15, «Report on Design and Construction of Steel Fiber-Reinforced Concrete Elevated Slabs,» 2015.
- [22] A. 544.7R-16, «Report on Design and Construction of Fiber-Reinforced Precast Concrete Tunnel Segments,» 2016.
- [23] ACI.8R-16, «Report on Indirect Method to Obtain Stress-Strain Response of Fiber-Reinforced Concrete,» 2016.



ABSTRACT

TITLE: Aplicación del hormigón con fibras a torres eólicas. Estado del arte y marco normativo. / Use of Fiber Reinforced Concrete in wind turbine towers. State of art and standards.

AUTHOR: Pilar Melero Gallego

DIRECTED BY: Francisco Ballester Muñoz y Jokin Rico Arenal

CALL: September 2018

KEYWORDS: Wind Turbine Tower, Fiber Reinforced Concrete, Limit States, Mechanical properties, Conventional concrete, Reinforcement, Forces, Design.

The development of the wind energy sector implies the use of bigger turbines which produce more energy, consequently higher towers with more capability requirements are necessary. When towers above 100m are required, steel towers become less competitive, while concrete towers increase their advantages.

One of the main parameters to optimize concrete towers is the thickness, which can be reduced with the use of fiber reinforced concrete, besides the thickness optimization, fiber reinforced concrete improve durability requirements.

Due to the structural and construction advantages of fiber reinforced concrete, this documents develop the state of art, and the international standards currently availables, to provide the guidelines for design and its application to wind turbine towers.

The standards analysis shows their limits for torsional efforts, which aren't properly developed in any standard. In addition, the behavior under fatigue loads that are very important in wind turbine towers, is only included in ACI standard, while the other standards don't define it completely.

In conclusion the use of fiber reinforced concrete in wind turbine towers is advantageous and economically attractive, although it's necessary to study and define the behavior under torsional and fatigue loads.

The references consulted in this report and listed below:

- [1] W. E. Foundation, «Wind Energy Foundation,» [En línea].
- [2] G. -. G. W. E. Council, «Global Wind Report, Annual Market Update 2017».
- [3] A. I. T. G. 9, «Report on Design of Concrete Wind Turbine Towers».



- [4] T. C. Centre, «Concrete Towers for Onshore and Offshore Wind Farms».
- [5] A. 544.1R-96, «Report on Fiber Reinforced Concrete,» R2009.
- [6] M. Joshua A. McMahon and Anna C. Birely, «Experimental Performance of Steel Fiber Reinforced Concrete Bridge Deck,» 2018.
- [7] J. V. N. A. J. B. H. R. Paulo A. L. Fernandes, «Study of a self-compacting fiber-reinforced concrete to be applied in the precast industry,» 2018.
- [8] P. P. J. M. X. S. Y. R. AC Birely, «Fiber Reinforced Concrete for Improved Performance of Transportation Infrastructure,» 2018.
- [9] M. d. Fomento, Instrucción de Hormigón Estructural EHE-08, 2008.
- [10] JSCE, «Recommendations for Design and Construction of High Performance Fiber Reinforced Cement Composites with Multiple Fine Cracks (HPFRCC),» 2008.
- [11] 544.9R-17, «Report on Measuring Mechanical Properties of Hardened Fiber-Reinforced Concrete,» 2017.
- [12] M. A. M. Muhammad I. Rjoub, «TORSIONAL STRENGTH OF STEEL FIBER,» Journal of Engineering Sciences, Assiut University, Vol. 35, No.1, pp.1-8, 2007.
- [13] D. R. S. T.D. Gunneswara Rao, «Torsion of steel fiber reinforced concrete members,» Cement and Concrete Research 33, 2003.
- [14] D. H. L. K. S. K. Hyunjin Ju, «Minimum torsional reinforcement ratio for reinforced concrete members with steel fiber,» Composite Structures, 2018.
- [15] R. T. 1. TDF, «Test and design methods for steel fibre reinforced concrete,» 2003.
- [16] CNR, «Guide for the Design and Construction of Fiber-Reinforced Concrete Structures,» 2007.
- [17] A. 544.2R-17, «Report on the Measurement of Fresh State Properties,» 2017.
- [18] A. 544.3R-08, «Guide for Specifying, Proportioning, and Production of Fiber-Reinforced Concrete,» 2008.



- [19] A. 544.4R-18, «Guide to Design with Fiber Reinforced Concrete,» 2018.
- [20] A. 544.R-10, «Report on the Physical Properties and durability of fiber reinforced concrete,» 2010.
- [21] A. 544.6R-15, «Report on Design and Construction of Steel Fiber-Reinforced Concrete Elevated Slabs,» 2015.
- [22] A. 544.7R-16, «Report on Design and Construction of Fiber-Reinforced Precast Concrete Tunnel Segments,» 2016.
- [23] ACI.8R-16, «Report on Indirect Method to Obtain Stress-Strain Response of Fiber-Reinforced Concrete,» 2016.



TABLA DE CONTENIDOS

RESUMEN	2
ABSTRACT.....	5
TABLA DE CONTENIDOS	8
LISTA DE ACRÓNIMOS.....	11
LISTA DE FIGURAS	11
LISTA DE TABLAS	14
1. INTRODUCCIÓN.....	15
1.1. Energía eólica.....	15
1.2. Torres eólicas de hormigón	16
1.2.1. Clasificación	16
1.2.2. Procedimiento constructivo	17
1.2.3. Ventajas	19
1.2.4. Diseño	20
2. ESTADO DEL ARTE DEL HORMIGÓN CON FIBRAS	22
2.1. Aspectos históricos.....	22
2.2. Aplicaciones actuales.....	23
2.3. Tipos de fibras	23
3. MARCO NORMATIVO	25
3.1. EHE 08.....	28
3.1.1. Caracterización mecánica	28
3.1.2. Estado Límite Último.....	34
3.1.3. Estado Límite de Servicio	37
3.1.4. Cuantías mínimas.....	37
3.2. Model Code 2010	38
3.2.1. Caracterización mecánica	38
3.2.2. Estado Límite Último.....	45
3.2.3. Estado Límite de Servicio	50
3.2.4. Cuantías mínimas.....	54
3.3. ACI.....	56



3.3.1.	Caracterización mecánica	56
3.3.1.	Estado Límite Último.....	58
3.3.2.	Estado Límite de Servicio	68
3.3.3.	Cuantías mínimas.....	69
3.4.	RILEM	71
3.4.1.	Caracterización mecánica	71
3.4.2.	Estado Límite Último.....	74
3.4.3.	Estado Límite de Servicio	82
3.4.4.	Cuantías mínimas.....	85
3.5.	CNR	88
3.5.1.	Caracterización mecánica	88
3.5.1.	Estado Límite Último.....	93
3.5.2.	Estado Límite de Servicio	99
3.5.3.	Cuantías mínimas.....	100
3.6.	JSCE	102
3.6.1.	Caracterización mecánica	102
3.6.2.	Estado Límite Último.....	106
3.6.3.	Estado Límite de Servicio	113
3.6.4.	Cuantías mínimas.....	117
3.7.	COMPARATIVA.....	120
	Coeficiente de Poisson.....	122
	Tracción.....	123
	Compresión.....	124
	ELU – Flexión compuesta	125
	ELU - Cortante	126
	ELU - Torsión	127
	ELU - Fatiga	128
	ELS - Fisuración	129
	ELS – Compresión máxima	130
	Cuantías mínimas - Flexión	131
	Cuantías mínimas - Cortante	132



Aplicación del hormigón con fibras a torres eólicas
Trabajo Fin de Máster – Pilar Melero Gallego



3.8.	COMPORTAMIENTO EN TORSIÓN	136
4.	CONCLUSIONES.....	139
5.	REFERENCIAS.....	140



LISTA DE ACRÓNIMOS

FRC – Fiber Reinforced Contrete
SFRC – Steel Fiber Reinforced Concrete
CFRM – Continuos Fiber Reinforced Materials
GFRC – Glass Fiber Reinforced Concrete
GWEC – Global Wind Energy Council
CMOD – Crack Mouth Opening Displacement
ULS – Ultimate Limit State
SLS – Service Limit State
HPFRCC – High Performance Fiber Reinforced Cementitious Composites
EQ - Earthquake forces

LISTA DE FIGURAS

Ilustración 1.- Capacidad instalada 2001-2017 (Fuente GWEC) [2]	15
Ilustración 2.- Pronóstico de capacidad instalada acumulada (Fuente GWEC) [2] ...	15
Ilustración 3.- Torre híbrida de hormigón (Fuente ACI ITG 9)	16
Ilustración 4.- Fibras metálicas (Fuente ACI)	23
Ilustración 5.- Línea temporal de la publicación de las normativas referentes al hormigón con fibras.....	26
Ilustración 6.- Figura 39.6 de la EHE08 - Representación esquemática de la relación tensodeformacional del hormigón	28
Ilustración 7.- EHE 08 Anejo 14 - Figura A14.1 Diagrama tipo carga apertura de fisuras	29
Ilustración 8.- EHE 08 Anejo 14 - Figura A.14.2 Diagrama del cálculo rectangular ...	30
Ilustración 9.- EHE 08 Anejo 14 - Figura A.14.3 Diagrama del cálculo multilineal	30
Ilustración 10.- EHE 08 Anejo 14 - Tabla A.14.1 Valores de referencia para s_m	31
Ilustración 11.- EHE 08 - Figura 39.5.a. Diagrama de cálculo parábola-rectángulo ..	32
Ilustración 12.- EHE 08 - Figura 39.5.b. Diagrama de cálculo rectángular	34
Ilustración 13.- Model Code 2010 - Figure 5.6-4: Inverse analysis of beam in bending performed to obtain stress - crack relation	39
Ilustración 14.- Model Code 2010 - Figure 5.6-5: Test set-up required by EN 14651(dimensions in [mm])	39
Ilustración 15.- Model Code 2010 - Figure 5.6-6: Typical F-CMOD curve for FRC.....	40



Ilustración 16.- Model Code 2010 – Figure 5.6-8 <i>Simplified model adopted to compute the ultimate residual tensile strength in uniaxial tension f_{Ftu} by means of the residual nominal bending strength f_{R3}</i>	41
Ilustración 17.- Figure 5.6-8 <i>Simplified post-cracking constitutive laws: stress-crack opening (continuous and dashed lines refer to softening and hardening post-cracking behaviour, respectively)</i>	41
Ilustración 18.- Model Code 2010 – Figure 5.6-9: <i>Stress diagrams for the determination of the residual tensile strength f_{Fts} (b) and f_{Ftu} (c) for the linear model, respectively</i>	42
Ilustración 19.- Model Code 2010 - Figure 5.6-10: Typical results from a bending test on a softening material (a); linear post-cracking constitute law(b)	43
Ilustración 20.- Model Code 2010 - Figure 5.6-3: Main differences between plain and fibre reinforced concrete having both normal and high strength under uniaxial compression.	45
Ilustración 21.- Model Code 2010 – Figure 7.7-3: <i>ULS for bending moment and axial force: use of the simplified stress/strain relationship (λ and η coefficient in accordance Eq. (7.2-15) to (7.2-18) in subclause 7.2.3.1.5).</i>	46
Ilustración 22.-Model Code 2010 - <i>Stress-strain relations at SLS for softening (a) and softening or hardening (b, c) behaviour of FRC</i>	52
Ilustración 23.- ACI 544.4R - Fig. 4.2 Schematic of a typical stress-strain diagram for FRC inn uniaxial tension and compression, according to RILEM TC 162-TDF (2003) and Vandewalle (2003).	57
Ilustración 24.- ACI 544.4R - Fig. 4.2 Schematic of a typical stress-strain diagram for FRC inn uniaxial tension and compression, according to RILEM TC 162-TDF (2003) and Vandewalle (2003).	58
Ilustración 25.- ACI 544.1R - Fig.2.4 - Shear behavior of reinforced SFRC beams.....	59
Ilustración 26.- ACI 544.4R - Fig. 4.4—Schematics of stress block for a cracked reinforced concrete flexural member without fibers: (a) reinforced concrete beam section; (b) actual distribution of normal stresses; and (c) simplified distribution of normal stresses.....	60
Ilustración 27.- ACI 544.4R - Fig. 4.5—Schematics of stress block for a cracked FRC flexural member. (a) FRC beam section; (b) actual distribution of normal stresses; and (c) simplified distribution of normal stresses.....	60
Ilustración 28.- ACI 544.4R - Table 4.5 - Typical calculation of FRC residual strength values for crack control	62
Ilustración 29.- ACI 544.4R - Fig. 4.6—Schematics of stress block for a cracked FRC flexural member: (a) FRC beam section; (b) distribution of flexural stresses; and (c) simplified distribution of normal stresses.....	63



Ilustración 30.- ACI 544.4R - Fig. 4.7—Schematics of stress block for a cracked flexural member with hybrid reinforcement: (a) beam section; and (b) distribution of normal stresses and forces from fibers and reinforcing bar.	65
Ilustración 31.- ACI 544.4 - Fig. 4.9c Design chart for normalized ultimate momento capacity (determined at $\lambda = \lambda_{cu}$) for different levels of postcrack tensile strength μ and reinforcement ratio.....	70
Ilustración 32.- RILEM TC 162 - Modulus of elasticity	71
Ilustración 33.- RILEM TC 162 - Fig 2 Stress-strain diagram and size factor k_h	72
Ilustración 34.- RILEM TC 162 – Fig 1.1 Stress distribution	73
Ilustración 35.- RILEM TC 162-TDF – Fig. 4 Arrangement of displacement monitoring gauges.....	74
Ilustración 36.- RILEM TC 162 – Fig 3 Stress and strain distribution	76
Ilustración 37.- RILEM TC 162 – Fig 6 Strut and tie model	78
Ilustración 38.- RILEM TC 162 – Fig.7 ρl for V_{cd}	79
Ilustración 39.- CNR-DT 204/2006 - Figure 2-1-Tensile behaviour.....	89
Ilustración 40.- CNR-DT 204/2006 - Figure 2-2 - Four point bending test as suggested in UNI 11039.....	91
Ilustración 41.- CNR-DT 204/2006 - Figure 2-3 – Definition of point and mean residual strength	91
Ilustración 42.- CNR-DT 204/2006 - Figure 2-4 - Simplified constitutive laws: tension-crack opening.....	92
Ilustración 43.- CNR-DT 204/2006 - Figure 4-1 – ULS for bending moment and axial force: use of the simplified stress/strain relationship (<i>stress-block</i> with η e λ coefficient in accordance with EC2).	95
Ilustración 44.- JSCE - Fig 3.5.1 Example of determination of Young's modulus	102
Ilustración 45.- JSCE - Fig 3.5.1 Example of determination of Poisson's ratio.....	103
Ilustración 46.- JSCE - Fig 3.3.1 Tensile stress-strain relationship	103
Ilustración 47.- JSCE - Fig 3.3.2 Compressive stress-strain relationship.....	105
Ilustración 48.- JSCE - Fig. 6.2.1 Schematic representations of strain and stress distributions.....	107
Ilustración 49.- JSCE - Fig. 3.9.1 Example of flexural fatigue test of HPFRCC.....	112
Ilustración 50.- JSCE - Fig. 6.5.1 Flow diagram for wxamining the limit state fatigue	113
Ilustración 51.- EHE 08 - Figura 39.5.b. Diagrama de cálculo rectangular	124
Ilustración 52.- ACI 544.9R - Fig. 11a Schematic of setup for torsion test on FRC beams (di Prisco et al. 2014).	136
Ilustración 53.- ACI 544.9R - Fig. 11b Torsional hinge (di Prisco et al. 2014).	137



Ilustración 54.- Figure 1 Experimental values of torsion (T_{exp}) versus calculated torsion (T_{cal}) according, first according to proposed equation, then according to ACI equation..... 138

LISTA DE TABLAS

Tabla 1.- Coste estimado de instalación para 50 torres (Fuente ACI ITG 9 – adapted from LaNier 2005)..... 19

Tabla 2.- Model Code 2010 - Table 4.5-7 *Partial safety factors γ_F for loads in the design of structural members not involving geotechnical actions: alternative combination of values*..... 47

Tabla 3.- RILEM TC 162 – Table 3 Criteria for crack with..... 83



1. INTRODUCCIÓN

1.1. Energía eólica

Según la Wind Energy Foundation la energía eólica es el segundo recurso energético que más rápido crece en el mundo, con una capacidad instalada global de 539,581 (MW) a finales de 2017. [1]

Como se muestra en la siguiente ilustración la energía eólica se ha desarrollado enormemente en los últimos años llegando a quintuplicar la energía instalada hace diez años.

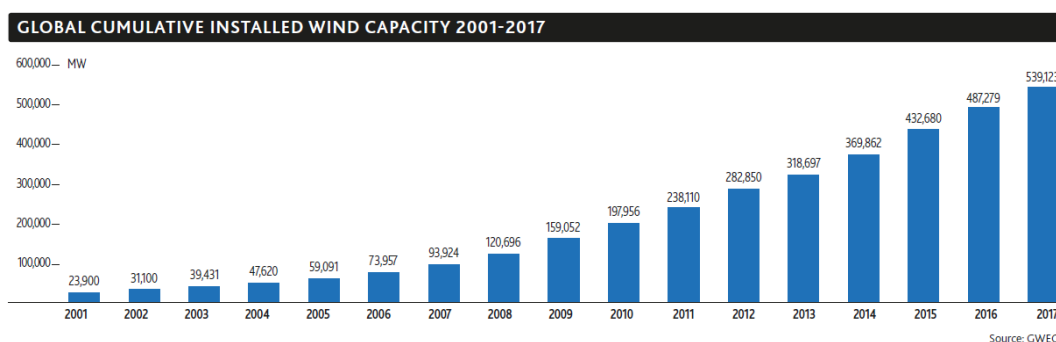


Ilustración 1.- Capacidad instalada 2001-2017 (Fuente GWEC) [2]

Se pronostica que la capacidad instalada acumulada siga creciendo como refleja la siguiente gráfica por regiones:

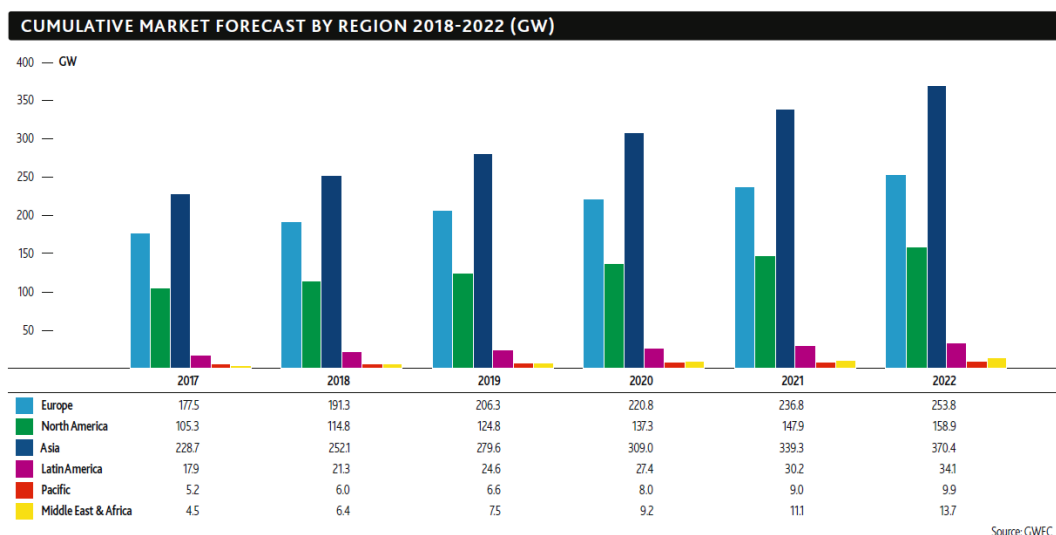


Ilustración 2.- Pronóstico de capacidad instalada acumulada (Fuente GWEC) [2]

El continuo crecimiento y la evolución del sector eólico conducen a la instalación de turbinas de mayor potencia.



Cuando el nivel de potencia de una turbina supera los 2,5 MW, las torres necesarias para mantenerlas exceden los 100m. Para esta altura muchas de las ventajas de las tradicionales torres metálicas desaparecen, debido al mayor tamaño, la menor rigidez, y la necesidad de acabado en obra. [2]

Bajo estas condiciones, las torres de hormigón son alternativas aplicables y económicamente atractivas. Según Engström et al. (2010), usando una altura de góndola de 125m, es posible ahorrar hasta un 30% del coste de la torre seleccionando una tecnología distinta a la convencional de torres metálicas soldadas. [2]

Umut et al. (2011) señaló que según se aumenta la altura de la torre, la demanda de rigidez es crítica. Las torres de hormigón tienen mayor capacidad que las metálicas para adaptar la rigidez y así conseguir el comportamiento requerido por los fabricantes. [3]

1.2. Torres eólicas de hormigón

1.2.1. Clasificación

Siguiendo la clasificación que se propone en ACI ITG 9, las torres de hormigón pueden clasificarse de la siguiente forma: [3]

Torres híbridas de hormigón

Las torres híbridas de hormigón consisten en una torre de hormigón base, con una torre metálica instalada sobre ella, que a su vez soporta la turbina como se muestra en la figura:

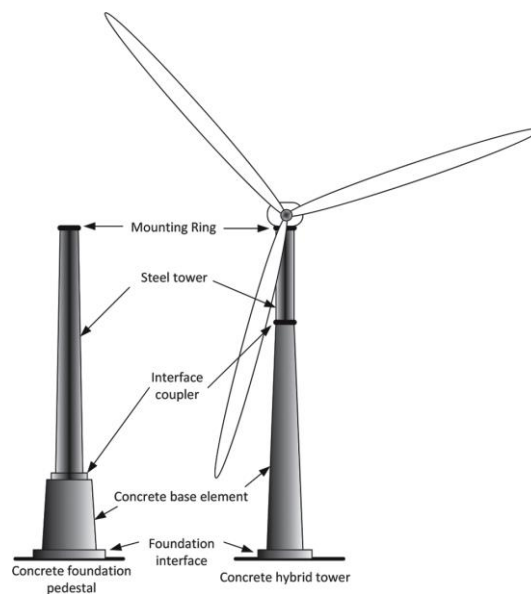


Ilustración 3.- Torre híbrida de hormigón (Fuente ACI ITG 9)



Los sistemas de torres híbridas se diseñan para optimizar el costo económico de la parte metálica prefabricada y colocada in situ. La parte de hormigón de la torre proporciona la altura adicional.

Torres de hormigón

Se consideran torres completas de hormigón aquellas que conectan desde la cimentación hasta la góndola. Para torres construidas de hormigón con alturas de 100 a 150m, el diámetro de la base oscila de los 8 a los 10m, la máxima dimensión condiciona la segmentación, transporte y los costes de montaje.

1.2.2. Procedimiento constructivo

Prefabricadas

Las torres prefabricadas se producen antes de su emplazamiento en obra. Su fabricación puede empezar poco después de adjudicar el contrato, y debe realizarse mientras se desarrolla la preparación del emplazamiento y la cimentación. Los elementos prefabricados pueden ser secciones anulares completas o elementos placa que formen una parte de la torre, con paneles de ancho variable para sistemas avanzados.

El tamaño de los elementos prefabricados afecta al sitio de fabricación. Si se prefabrican elementos de gran tamaño, la operación completa de prefabricado puede desplazarse al parque eólico para evitar el transporte por carretera.

El tiempo de montaje para torres prefabricadas de 135m se estima en 3 días por torre, asumiendo que todos los componentes se encuentran en la obra y están rápidamente disponibles. El tiempo total de construcción del parque eólico es atribuible a la disponibilidad de moldes y grúas.

Construcción in situ

Dos procedimientos convencionales de construcción in situ pueden aplicarse a la construcción de torres eólicas: encofrado trepante o deslizante. La construcción in situ requiere la consideración de dos restricciones en la planificación. Primero, la construcción de la torre no puede empezar hasta que la cimentación está preparada para la siguiente secuencia de trabajo. Segundo, la velocidad de construcción depende de la resistencia del hormigón inferior. Ambos procedimientos requieren un continuo suministro de hormigón y deben justificar una dosificación in situ.

Encofrado trepante

El encofrado trepante se ajusta al hormigón recién colocado para crear un nuevo nivel de encofrado. Puede diseñarse para variar tanto el diámetro como el espesor a medida



que avanza. Una medida estándar de encofrado es de 3 a 6m, pueden desplazarse tan pronto como el hormigón haya curado lo suficiente para soportar el movimiento.

En construcción de edificios normalmente se desplaza el encofrado una vez por semana, sin embargo, en la construcción de torres puede desplazarse diariamente, puesto que la única carga es el peso axial de la sección superior. Con un desplazamiento diario de 4m una torre de 100m puede culminarse en 25 días. El número de turbinas en el parque eólico dictará el número de sistemas de encofrado requeridos para alcanzar el plazo de construcción deseado.

Encofrado deslizante

El encofrado deslizante, que incluye la continua colocación del hormigón, ha sido usado exitosamente en chimeneas y grandes silos. Se colocan en el hormigón varillas metálicas y gatos hidráulicos se anclan en las varillas para ascender el encofrado mientras el hormigón es colocado. Se consiguen ratios de 180 a 300mm por hora para encofrados de 1.2 a 2m. Con estas ratios de movimientos una torre de 100m puede fabricarse en aproximadamente 20 días. Con 2m por día, el procedimiento incluye el tiempo requerido para instalar el anillo superior. El encofrado deslizante es una operación continua con control limitado sobre el desvío lateral.

Se requiere de experiencia en construcción con encofrado deslizante para mantener la alineación vertical.

Hormigón proyectado

La proyección de hormigón es un procedimiento que coloca el hormigón mediante una manguera sobre un contorno. El hormigón proyectado tiene la ventaja de solo requerir un encofrado interno o externo. El encofrado puede ser ajustable para variar el diámetro según asciende el encofrado, y puede ser continuo con un encofrado interior móvil. Las estructuras de hormigón proyectado de magnitud similar a torres eólicas requieren inversión en investigación, desarrollo y control de calidad, puesto que las torres eólicas son mayores que las actuales construcciones de hormigón proyectado. El tiempo de construcción es similar al de las opciones de construcción in situ.

Hormigón centrifugado

El hormigón centrifugado es una variante especial del prefabricado que usa la rotación para colocar el hormigón en una configuración densa. El proceso se ha usado satisfactoriamente para torres de transmisión de alto voltaje, pero no para dimensiones como las de una torre eólica (Rodgers 1972; Fouad and Detwiler 2012). La dimensión de los elementos depende de la capacidad de elevación in situ. Los plazos de construcción son similares a las opciones prefabricadas.



A continuación, se muestra una comparativa del coste de instalación según el estudio realizado por el National Renewable Energy Laboratory (NREL), el estudio considera emplazamientos condicionados por fuerzas sísmicas (EQ) y emplazamientos sólo influenciados por el viento.

Tabla 1.- Coste estimado de instalación para 50 torres (Fuente ACI ITG 9 – adapted from LaNier 2005)

Turbine/tower size, construction method, and condition	MW	Installed cost	Percent all-tubular steel cost
Hybrid steel concrete (EQ)	1.5	\$1,402,721	103
All-precast concrete (Wind)	1.5	\$1,581,707	115
All-precast concrete (EQ)	1.5	\$1,943,472	142
All-cast-in-place concrete (EQ)	1.5	\$1,394,300	102
All-cast-in-place concrete (wind)	1.5	\$1,188,150	87
All-tubular steel (wind)	1.5	\$1,369,656	100
Hybrid steel concrete (EQ)	3.6	\$2,380,653	104
All-precast concrete (wind)	3.6	\$2,026,608	88
All-cast-in-place concrete (wind)	3.6	\$1,550,472	68
All-tubular steel (wind)	3.6	\$2,293,759	100
Hybrid steel concrete (EQ)	5.0	\$3,242,075	110
All-precast concrete (wind)	5.0	\$2,402,928	81
All-precast concrete (EQ)	5.0	\$2,949,155	100
All-cast-in-place concrete (wind)	5.0	\$1,872,036	63
All-cast-in-place concrete (EQ)	5.0	\$2,126,524	72
All-tubular steel (wind)	5.0	\$2,956,356	100

**EQ (Earthquake forces), considerando cargas sísmicas.*

Wind, considerando sólo las cargas debidas al viento.

**Estos costes incluyen todos los costes relevantes de la construcción de una torre eólica excepto los costes de suministro de la turbina, el rotor y la conexión eléctrica de la turbina a la red de distribución.*

Como se puede observar para todas las potencias consideradas, las torres de hormigón in situ son la opción más económica, aumentando su rentabilidad proporcionalmente con la altura.

1.2.3. Ventajas

Además de la competitividad económica, el hormigón presenta las siguientes ventajas: [4]



Bajo mantenimiento

El hormigón es un material inherentemente durable. Cuando el diseño y la construcción se realizan correctamente, el hormigón puede mantener sus propiedades ingenieriles deseadas bajo condiciones extremas de exposición.

Económicamente competitivo

Las soluciones con hormigón pueden combinar el bajo coste con un ciclo de vida significativamente mayor.

Flexibilidad en diseño y construcción

La versatilidad del hormigón permite diseños sin restricciones de altura o tamaño para lograr los requisitos del emplazamiento.

Flexibilidad en dosificación

El hormigón es un material de construcción adaptable que puede ajustarse mediante alteraciones en la dosificación para modificar los parámetros esenciales como resistencia, rigidez y densidad.

Excelente comportamiento dinámico

El hormigón tiene buenas propiedades de amortiguamiento. En particular el hormigón pretensado tiene una alta resistencia a fatiga, aportando más tolerancia y menos riesgo de un fallo dinámico.

Bajo impacto ambiental

No solo si se trata de hormigón reciclado, sino porque su incorporación de CO₂ y energía puede ser mucho menor que en otros materiales de construcción. Además, una torre eólica de hormigón tiene la capacidad de consumir CO₂ de la atmósfera durante su vida de servicio.

1.2.4. Diseño

Es necesario minimizar el peso de la torre para alcanzar una solución competitiva en el diseño de una torre de hormigón. Para ello se debe optimizar el espesor, que depende de varios factores como la resistencia, la rigidez, la estabilidad local y los requisitos de durabilidad, que definen los recubrimientos mínimos del acero. Además, debe de considerarse el espesor necesario para albergar el pretensado. [4]

Para la consecución de este objetivo, el presente trabajo plantea la utilización del Hormigón Reforzado con Fibras, las cuales pueden sustituir a la tradicional armadura pasiva, minimizando el espesor de la torre. Además, esta técnica presenta las siguientes ventajas estructurales: [5]



Comportamiento bajo cargas estáticas

Como consecuencia de la naturaleza de las fibras, estas aportan ductilidad tras la fisuración, evitando la rotura frágil. Las fibras metálicas mejoran la ductilidad del hormigón bajo todos los modos de carga, pero la efectividad en la modificación de la resistencia, varía en compresión, tracción, cortante, torsión y flexión.

- Compresión: la resistencia última no varía significativamente con la presencia de fibras.
- Tracción: la resistencia mejora significativamente con la adición de fibras.
- Cortante y torsión: las fibras metálicas generalmente mejoran la resistencia del hormigón a cortante y torsión.
- Flexión: El aumento de la resistencia a flexión del hormigón con fibras metálicas es sustancialmente mayor que en tracción o compresión debido al comportamiento dúctil en la zona traccionada altera la distribución elástica de tensión y deformación en la sección. El diagrama de tensiones es esencialmente plástico en la zona traccionada y elástico en la zona comprimida, desplazando el eje neutro hacia la zona comprimida.

Comportamiento bajo cargas de impacto

Para caracterizar el comportamiento del hormigón bajo cargas de impacto los dos parámetros más importantes son la resistencia y la energía de fractura. Las fibras metálicas aumentan la energía a fractura bajo impacto por un factor de 2.5 para hormigón de resistencia normal y 3.5 para hormigones de alta resistencia.

Comportamiento en fatiga

La adición de fibras a vigas convencionales reforzadas aumenta la vida en fatiga y disminuye el ancho de fisura bajo cargas de fatiga.

Tenacidad

La tenacidad es una de las características que más diferencia al hormigón reforzado con fibras metálicas del convencional.



2. ESTADO DEL ARTE DEL HORMIGÓN CON FIBRAS

2.1. Aspectos históricos

Los antecedentes históricos del hormigón con fibras pueden remontarse a 1540 con la incorporación de paja o pelo de caballo para reforzar los adobes. Posteriormente en el Año 1898 comienzan a usarse las fibras de asbesto en la pasta de cemento, técnica que actualmente está en desuso por sus efectos perjudiciales sobre la salud. Posiblemente esto es lo que ha motivado que de los años 1960 a 1980 se hayan desarrollado tipos de fibras alternativos.

En la actualidad un gran rango de materiales de ingeniería incorpora fibras para mejorar las propiedades del compuesto. Ensayos experimentales y patentes que incluyen el uso de refuerzo metálico discontinuo para mejorar las propiedades del hormigón se han desarrollado desde 1910. Durante los primeros años de los 60 la investigación en Estados Unidos se ha centrado en evaluar el potencial de las fibras metálicas como refuerzo en el hormigón. Desde entonces se ha desarrollado la investigación, desarrollo, experimentación y aplicaciones industriales del hormigón reforzado con fibras metálicas.

Numerosas investigaciones y aplicaciones del hormigón con fibras se están desarrollando en todo el mundo. El interés de la industria y las oportunidades potenciales de negocio se han evidenciado con los continuos desarrollos de materiales de construcción reforzados con fibras. [5]



2.2. Aplicaciones actuales

Conforme se desarrolla la experiencia con el hormigón reforzado con fibras metálicas, más aplicaciones son aceptadas en el campo de la ingeniería. Las propiedades más importantes del hormigón reforzado con fibras metálicas son la tenacidad a flexión (debido a la capacidad de absorber energía tras la fisuración), la resistencia a impacto, y la resistencia a fatiga en flexión. Por esta razón ha sido utilizado en losas de hormigón donde está sujeto a altas cargas e impacto.

El hormigón reforzado con fibras metálicas también es utilizado en numerosas aplicaciones de hormigón proyectado, como estabilización de tierras y taludes en roca, túneles, minas y reparaciones. [5]

Si bien las aplicaciones tradicionales son:

- Pavimentos
- Estructuras hidráulicas
- Hormigón proyectado

El reciente desarrollo normativo y las líneas de investigación conducen al uso del hormigón reforzado con fibras con fines estructurales, sustituyendo parcial o completamente el refuerzo tradicional. Algunos de los estudios actuales son:

- Experimental Performance of Steel Fiber Reinforced Concrete Bridge Deck [6].
- Study of a self-compacting fiber-reinforced concrete to be applied in the precast industry [7]
- Fiber Reinforced Concrete for Improved Performance of Transportation Infrastructure [8]

2.3. Tipos de fibras

- Fibras de acero, este tipo de refuerzo puede presentar distintas geometrías que se le confieren para mejorar la adherencia.



Ilustración 4.- Fibras metálicas (Fuente ACI)



Aplicación del hormigón con fibras a torres eólicas
Trabajo Fin de Máster – Pilar Melero Gallego



- Fibras poliméricas, las fibras plásticas están formadas por un material polimérico (polipropileno, polietileno de alta densidad, aramida, alcohol de polivinilo, acrílico, nylon, poliéster) extrusionado y posteriormente cortado. [9]
- Fibras de vidrio, de alta resistencia a tracción cuyo principal inconveniente es que son atacadas por los álcalis de los cementos portland. [5]
- Fibras sintéticas, derivadas de polímeros orgánicos, algunos tipos son: acrílicas, de carbono, nylon, poliéster, polietileno o polipropileno. [5]
- Fibras naturales, como fibra de coco, plátano, palma, o derivada de la caña de azúcar. [5]

La normativa actual centra su formulación en fibras metálicas, por lo cual de aquí en adelante se desarrollará esta tipología.



3. MARCO NORMATIVO

Para la correcta caracterización y diseño del hormigón con fibras se ha analizado la normativa actual existente a nivel internacional, para ello se han seleccionado los siguientes organismos:

- Ministerio de Fomento del Gobierno de España.
 - EHE 08 – Instrucción del hormigón estructural.
- AENOR - Asociación Española de Normalización y Certificación.
 - UNE-EN 14651:2007+A1 – Método de ensayo para hormigón con fibras metálicas. Determinación de la resistencia a la tracción por flexión (límite de proporcionalidad (LOP), resistencia residual).
 - UNE-EN 14889-1 – Fibras para hormigón. Parte 1: Fibras de acero. Definiciones, especificaciones y conformidad.
 - UNE-EN 14889-2 – Fibras para hormigón. Parte 2: Fibras poliméricas. Definiciones, especificaciones y conformidad.
- FIB - Federación internacional del hormigón, de sus siglas en francés, (Fédération Internationale du Béton).
 - Model Code 2010
- ACI – Instituto Americano del Hormigón (American Concrete Institute).
 - ITG-9R-16 - Report on Design of Concrete Wind Turbine Towers
 - 318.RS-14 - Requisitos de Reglamento para Concreto Estructural
 - 544.1R-96_09 - Report on Fiber Reinforced Concrete
 - 544.2R-17 - Report on the Measurement of Fresh State Properties
 - 544.3R-08 - Guide for Specifying, Proportioning, and Production of Fiber-Reinforced Concrete
 - 544.4R-18 - Guide to Design with Fiber Reinforced Concrete
 - 544.5R-10 - Report on the Physical Properties and durability of fiber reinforced concrete
 - 544.6R-15 - Report on Design and Construction of Steel Fiber-Reinforced Concrete Elevated Slabs
 - 544.7R-16 - Report on Design and Construction of Fiber-Reinforced Precast Concrete Tunnel Segments
 - 544.8R-16 - Report on Indirect Method to Obtain Stress-Strain Response of Fiber-Reinforced Concrete
 - 544.9R-17 - Report on Measuring Mechanical Properties of Hardened Fiber-Reinforced Concrete
- RILEM - Unión Internacional de Laboratorios y Expertos en Materiales de Construcción (Réunion Internationale des Laboratoires et Experts des Matériaux).



- RILEM TC 162-TDF: ‘Test and design methods for steel fibre reinforced concrete’
- CNR – Consejo Nacional de Investigación (Consiglio Nazionale delle Ricerche) dependiente del Ministerio de Educación, Universidades e Investigación de Italia.
 - CNR-DT 204/2006 Guide for the Design and Construction of Fiber-Reinforced Concrete Structures
- JSCE – Sociedad Japonesa de Ingenieros Civiles (Japan Society of Civil Engineers).
 - JSCE Guidelines for concrete nº 15 - Standard specifications for concrete structures – 2007 “Design”
 - JSCE Guidelines for concrete nº 16 - Standard specifications for concrete structures – 2007 “Materials and construction”
 - JSCE Recommendations for Design and Construction of High Performance Fiber Reinforced Cement Composites with Multiple Fine Cracks (HPFRCC)

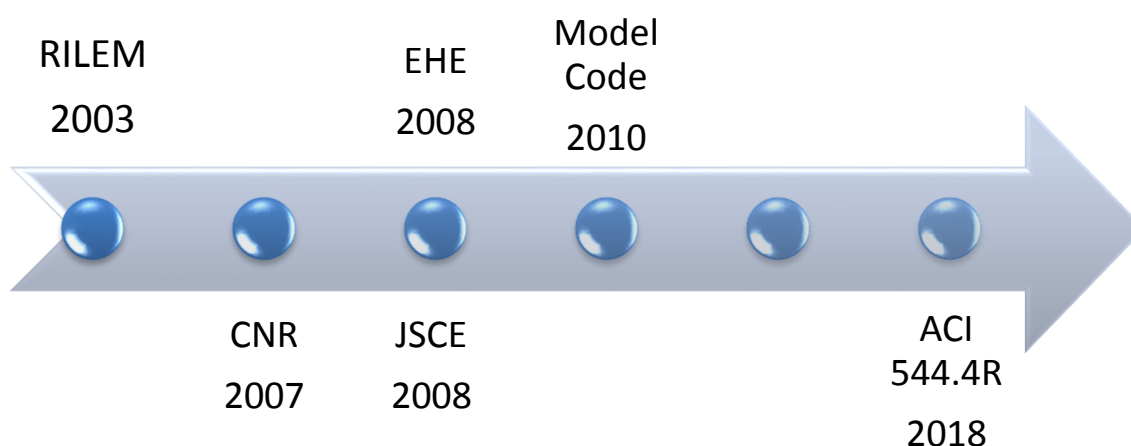


Ilustración 5.- Línea temporal de la publicación de las normativas referentes al hormigón con fibras

En la ilustración anterior podemos observar la secuencia de publicación de las diferentes normativas relativas al hormigón reforzado con fibras.



A continuación, se presentan para cada normativa los apartados de interés para el cálculo de una torre eólica de hormigón con fibras, por ello se incluyen los tipos de esfuerzos, geometrías y condiciones de contorno esperables en este tipo de estructuras.

Para ello se han extraído de las distintas normas aquellos fragmentos relevantes para el diseño de esta tipología estructural. Al tratarse de normativa de distintos países de procedencia y por tanto editadas en distintos idiomas, se ha recurrido a la versión en inglés de todas ellas, salvo la normativa española. Por lo cual en los siguientes apartados se recogen extractos en inglés no traducidos al castellano por su carácter normativo.

El esquema realizado para cada normativa contiene los siguientes apartados comunes:

- Caracterización mecánica: en el cual se definen el módulo de elasticidad, coeficiente de Poisson, comportamiento en tracción y compresión.
- Estado Límite Último: definido como aquello que produce el fallo en la estructura por pérdida de equilibrio, colapso o rotura de la misma o de una parte de ella [9]. Se han analizado la flexión compuesta, cortante, torsión y fatiga.
- Estado Límite de Servicio: aquello para lo que no se cumplen los requisitos de funcionalidad, de comodidad o de aspecto requeridos [9]. Distinguiendo fisuración y compresión máxima.
- Cuantías mínimas: se presentan los requisitos de armadura mínima para los esfuerzos de flexión, cortante y torsión.



3.1. EHE 08

3.1.1. Caracterización mecánica

Módulo de elasticidad

El anejo 14 de la EHE 08 no propone ninguna modificación respecto al módulo de elasticidad por lo que se recurre a la formulación para hormigón convencional.

[EHE 08 39.6 Módulo de deformación longitudinal del hormigón]

Como módulo de deformación longitudinal secante E_{cm} a 28 días (pendiente de la secante de la curva real s-e), se adoptará:

$$E_{cm} = 8500 \sqrt[3]{f_{cm}}$$

Dicha expresión es válida siempre que las tensiones, en condiciones de servicio, no sobrepasen el valor de $0,40 f_{cm}$, siendo f_{cm} la resistencia media a compresión del hormigón a 28 días de edad.

Para cargas instantáneas o rápidamente variables, el módulo de deformación longitudinal inicial del hormigón (pendiente de la tangente en el origen) a la edad de 28 días, puede tomarse aproximadamente igual a:

$$E_c = \beta_E \cdot E_{cm}$$

$$\beta_E = 1,30 - \frac{f_{ck}}{400} \leq 1,175$$

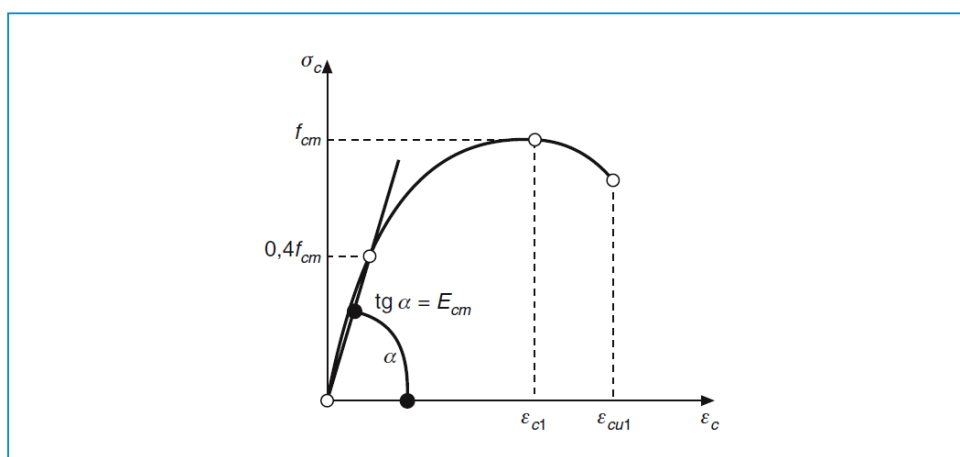


Ilustración 6.- Figura 39.6 de la EHE08 - Representación esquemática de la relación tensodeformacional del hormigón



Coeficiente de Poisson

[EHE 08 Anejo 14 – 39.9 Coeficiente de Poisson]

Las fibras individualmente, o como grupo, deberán tener un coeficiente de Poisson similar al del hormigón si se quiere tener en cuenta el efecto red a nivel estructural.

Tracción

[EHE 08 Anejo 14 – 31.3 Características mecánicas]

Del ensayo propuesto en UNE-EN 14651 se obtiene el diagrama carga-abertura de fisura del hormigón (figura A.14.1). A partir de los valores de carga correspondiente al límite de proporcionalidad (F_L) y a las aberturas de fisura 0,5 mm y 2,5 mm (F_1 y F_3 respectivamente), se obtiene el valor de resistencia a flexo tracción ($f_{ct,fl}$) y los valores de resistencia residual a flexo tracción correspondientes: $f_{R,1}$ y $f_{R,3}$.

El cálculo de los valores de resistencia a flexo tracción y de resistencia residual a flexo tracción según la citada norma UNE-EN 14651 se realiza asumiendo una distribución elástico lineal de tensiones en la sección de rotura.

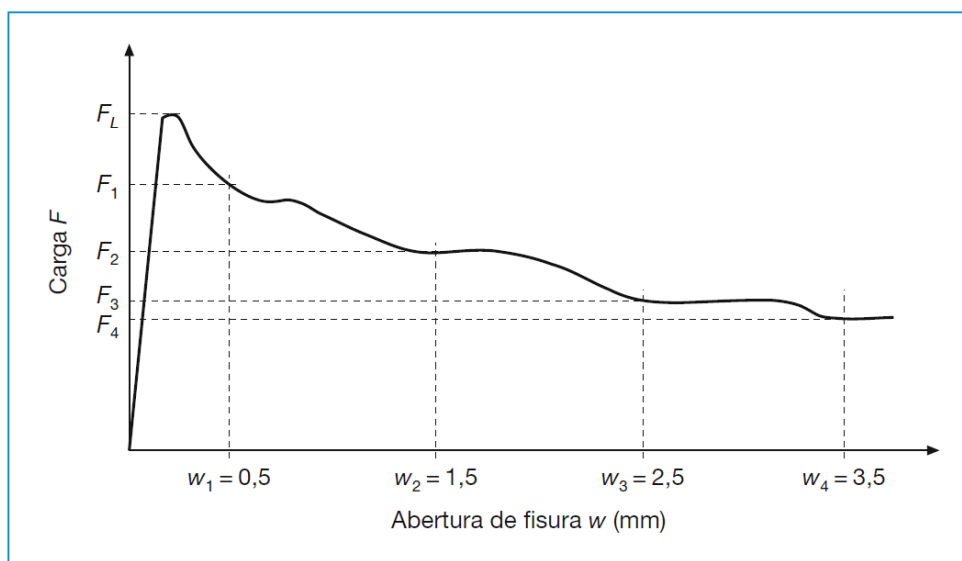


Ilustración 7.- EHE 08 Anejo 14 - Figura A14.1 Diagrama tipo carga apertura de fisuras

A partir de estos valores se determinará el diagrama de cálculo a tracción según lo indicado en el Artículo 39°. También, se podrán incorporar otros diagramas que definan dichas ecuaciones constitutivas de forma directa siempre y cuando los resultados vengan avalados por campañas concluyentes de tipo experimental y bibliografía especializada.



[EHE 08 Anejo 14 – 39.5 Diagrama tensión – deformación en tracción de cálculo del hormigón con fibras]

Para el cálculo de secciones sometidas a sollicitaciones normales, en los Estados Límite Últimos se adoptará uno de los diagramas siguientes:

- Diagrama rectangular: De forma general se aplicará el diagrama de la figura A.14.2 caracterizado por la resistencia residual a tracción de cálculo $f_{ctR,d}$:

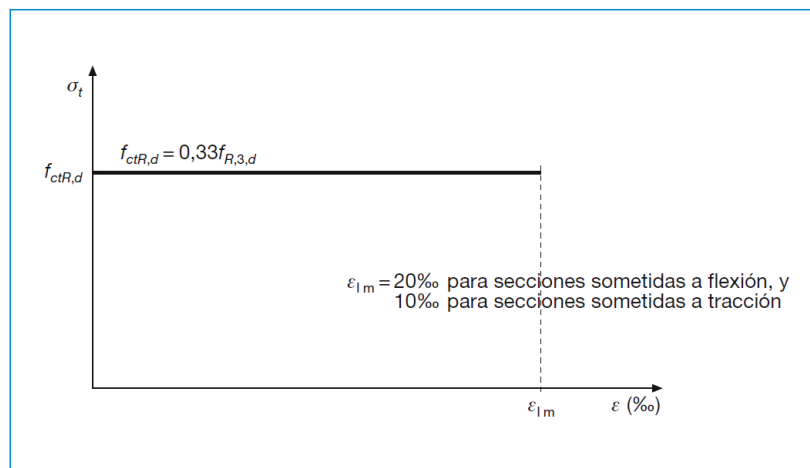


Ilustración 8.- EHE 08 Anejo 14 - Figura A.14.2 Diagrama del cálculo rectangular

- Diagrama multilíneal: Para aplicaciones que exigen un cálculo ajustado, se propone el diagrama tensión (σ)- deformación (ϵ) de la figura A.14.3, definido por una resistencia a tracción de cálculo $f_{ct,d}$ y de las resistencias residuales a tracción de cálculo: $f_{ctR1,d}$, $f_{ctR3,d}$, asociadas a sendas deformaciones ϵ_1 y ϵ_2 en el régimen de post-pico, donde:

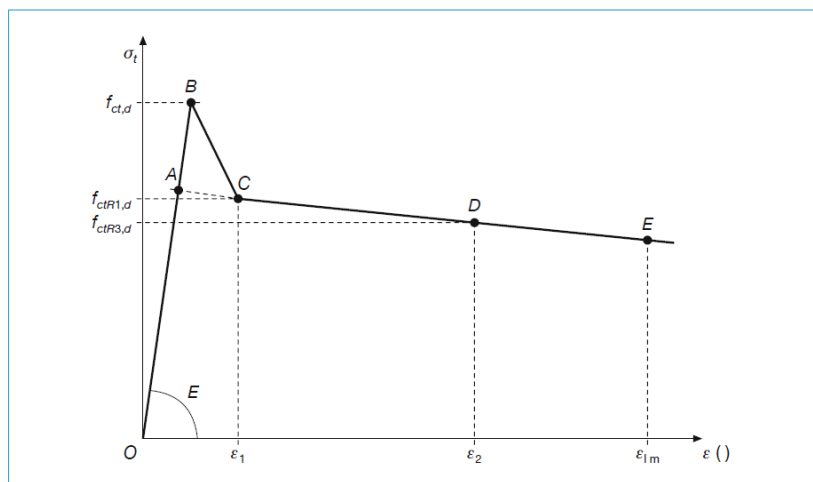


Ilustración 9.- EHE 08 Anejo 14 - Figura A.14.3 Diagrama del cálculo multilíneal



donde:

f_L = Carga correspondiente al límite de proporcionalidad

$$f_{ct,d} = 0,6 f_{ct,fl,d}$$

$$f_{ctR1,d} = 0,45 f_{R,1,d}$$

$$f_{ctR3,d} = k_1 (0,5 f_{R,1,d} - 0,2 f_{R,1,d})$$

$k_1 = 1$ para secciones sometidas a flexión y $0,7$ para secciones sometidas a tracción.

$$\varepsilon_1 = 0,1 + 1.000 f_{ct,d} / E_{c,0}$$

$$\varepsilon_2 = 2,5 / l_{cs}$$

$\varepsilon_{lim} = 20\text{‰}$ para secciones sometidas a flexión y 10‰ para secciones sometidas a tracción

l_{cs} = Longitud crítica (en metros) del elemento calculado que puede determinarse por la expresión:

$$l_{cs} = \min(s_m, h - x)$$

siendo:

x profundidad del eje neutro

$h - x$ distancia del eje neutro al extremo más traccionado

s_m distancia media entre fisuras. Salvo que se disponga de datos justificados se podrá utilizar para s_m los valores de la tabla A.14.1.

Elementos sin armadura tradicional, o poco armados y hormigón de fibras con comportamiento a flexión con ablandamiento ($f_{R1} < f_L$ y $f_{R2} < f_L$).	H (canto de la pieza).
Hormigón de fibras armado, con $f_{R3,d} < 2 \text{ kN/mm}^2$.	s_m calculado de acuerdo con 49.2.4.
Elementos con hormigón de fibras con comportamiento a flexión con endurecimiento ($f_{R1} > f_L$ y/o $f_{R2} > f_L$).	Se determinará de forma experimental según lo indicado en 31.3.
Otros casos.	Se consultará la bibliografía especializada.

Nota: De forma simplificada, se considerarán elementos poco armados aquéllos cuya cuantía geométrica de armadura tradicional a tracción sea inferior al uno por mil.

Ilustración 10.- EHE 08 Anejo 14 - Tabla A.14.1 Valores de referencia para s_m



El efecto del pico A-B-C puede ser importante cuando se aplique un análisis no lineal, especialmente para pequeñas deformaciones. En otros casos, para el cálculo en rotura puede utilizarse el diagrama bilineal simplificado, formado por las rectas correspondientes al tramo elástico O-A y la prolongación de la recta C-E hasta el punto A, e incluso considerando un comportamiento rígido con $E = \infty$.

Se aceptarán otros diagramas de cálculo siempre que los resultados con ellos obtenidos concuerden de manera satisfactoria con los correspondientes a los del diagrama rectangular indicado en la figura A.14.2, o queden del lado de la seguridad.

Compresión

[EHE 08 Anejo 14 – 31.3 Características mecánicas]

En solicitaciones de compresión, el diagrama tensión-deformación del hormigón con fibras no se modifica respecto al del articulado, ya que se puede considerar que la adición de las fibras no varía de forma significativa el comportamiento del hormigón en compresión.

[EHE 08 – 39.5 Diagrama tensión-deformación de cálculo del hormigón]

Para el cálculo de secciones sometidas a solicitaciones normales, en los Estados Límite Últimos se adoptará uno de los diagramas siguientes:

a) Diagrama parábola rectángulo

Está formado por una parábola de grado n y un segmento rectilíneo (Figura 39.5.a). El vértice de la parábola se encuentra en la abscisa ϵ_{c0} (deformación de rotura del hormigón a compresión simple) y el vértice extremo del rectángulo en la abscisa ϵ_{cu} (deformación de rotura del hormigón en flexión). La ordenada máxima de este diagrama corresponde a una compresión igual a f_{cd} .

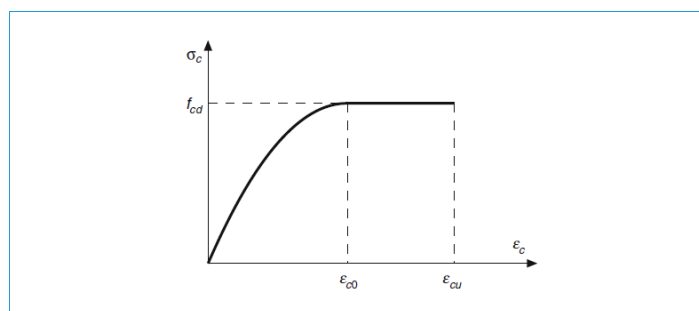


Ilustración 11.- EHE 08 - Figura 39.5.a. Diagrama de cálculo parábola-rectángulo



La ecuación de esta parábola es:

$$\sigma_c = f_{cd} \left[1 - \left(1 - \frac{\varepsilon_c}{\varepsilon_{c0}} \right)^n \right] \quad \text{si } 0 \leq \varepsilon_c \leq \varepsilon_{c0}$$
$$\sigma_c = f_{cd} \quad \text{si } \varepsilon_{c0} \leq \varepsilon_c \leq \varepsilon_{cu}$$

Los valores de la deformación de rotura a compresión simple, ε_{c0} , son los siguientes:

$$\varepsilon_{c0} = 0,002 \quad \text{si } f_{ck} \leq 50 \text{ N/mm}^2$$
$$\varepsilon_{c0} = 0,002 + 0,000085(f_{ck} - 50)^{0,50} \quad \text{si } f_{ck} > 50 \text{ N/mm}^2$$

Los valores de la deformación última, ε_{cu} , vienen dados por:

$$\varepsilon_{cu} = 0,0035 \quad \text{si } f_{ck} \leq 50 \text{ N/mm}^2$$
$$\varepsilon_{cu} = 0,0026 + 0,0144 \left[\frac{(100 - f_{ck})}{100} \right]^4 \quad \text{si } f_{ck} > 50 \text{ N/mm}^2$$

Y el valor n que define el grado de la parábola se obtiene como:

$$n = 2 \quad \text{si } f_{ck} \leq 50 \text{ N/mm}^2$$
$$n = 1,4 + 9,6 \left[\frac{(100 - f_{ck})}{100} \right]^4 \quad \text{si } f_{ck} > 50 \text{ N/mm}^2$$

b) Diagrama rectangular

Está formado por un rectángulo cuya profundidad $\lambda(x) \cdot h$, e intensidad $\eta(x) \cdot f_{cd}$ dependen de la profundidad del eje neutro x (figura 39.5.b), y de la resistencia del hormigón. Sus valores son:

$$\eta(x) = \eta \quad \text{si } 0 < x \leq h$$

$$\eta(x) = 1 - (1 - \eta) \frac{h}{x} \quad \text{si } 0 < x \leq h$$

$$\lambda(x) = \lambda \frac{x}{h} \quad \text{si } 0 < x \leq h$$

$$\lambda(x) = 1 - (1 - \lambda) \frac{h}{x} \quad \text{si } h \leq x < \infty$$

donde:

$$\eta = 1,0 \quad \text{si } f_{ck} \leq 50 \text{ N/mm}^2$$



$$\eta = 1,0 - \frac{(f_{ck} - 50)}{200} \quad \text{si } f_{ck} > 50 \text{ N/mm}^2$$

$$\lambda = 0,8 \quad \text{si } f_{ck} \leq 50 \text{ N/mm}^2$$

$$\lambda = 0,8 - \frac{(f_{ck} - 50)}{400} \quad \text{si } f_{ck} > 50 \text{ N/mm}^2$$

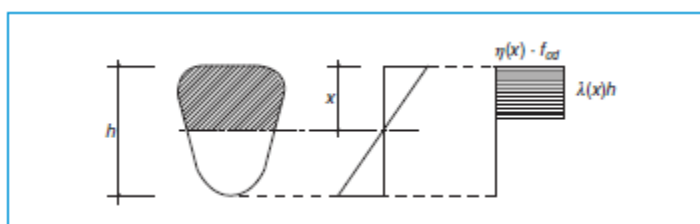


Ilustración 12.- EHE 08 - Figura 39.5.b. Diagrama de cálculo rectangular

c) Otros diagramas de cálculo, como los parabólicos, birrectilíneos, trapezoidales, etc., se aceptarán siempre que los resultados con ellos obtenidos concuerden, de una manera satisfactoria, con los correspondientes a los de la parábola-rectángulo o queden del lado de la seguridad.

3.1.2. Estado Límite Último

[EHE 08 Anejo 14 – 42.1.2 Hipótesis básicas]

El cálculo de la capacidad resistente última de las secciones en las que las fibras desempeñen función estructural se efectuará considerando como diagrama de cálculo del hormigón a tracción alguno de los que se definen en [39.5](#).

[EHE 08 Anejo 14 – 42.1.3 Dominios de deformación]

Se consideran los mismos que para una estructura con hormigón convencional.

Flexión compuesta

[EHE 08 Anejo 14 – 42.3.2 Flexión simple o compuesta]

En aquellos casos en que se utilicen fibras con función estructural, solas o en combinación con armadura tradicional, se deberá cumplir la siguiente limitación:

$$A_p f_{pd} \frac{d_p}{d_s} + A_s f_{yd} + \frac{z_f}{z} A_{ct} f_{ctR,d} > \frac{W_1}{z} f_{ctm} + \frac{P}{z} \left(\frac{W_1}{A} + e \right)$$

donde:

$z_f A_{ct} f_{ctR,d}$ Contribución de las fibras.



z_f	Brazo mecánico de la tracción del hormigón.
A_{ct}	Área traccionada de hormigón.
$f_{ctR,d}$	Resistencia residual a tracción de cálculo en el diagrama rectangular.

En el caso de secciones rectangulares con o sin armadura pasiva puede emplearse la siguiente relación simplificada, en la que no se precisa determinar el área traccionada de hormigón.

$$A_s f_{yd} + 0,4 A_c f_{ctR,d} > 0,04 A_c f_{cd}$$

Esta limitación se justifica como garantía para evitar la rotura frágil del hormigón. La acción de las armaduras tradicionales y de las fibras es complementaria en este aspecto, y por tanto la limitación constituye una exigencia de contenido mínimo en fibras para elementos sin armaduras tradicionales, y la posibilidad de reducir, e incluso eliminar, la exigencia de armaduras tradicionales mínimas en elementos con contenido suficiente de fibras estructurales. Esta limitación no rige para losas apoyadas en el terreno.

Cortante

[EHE 08 Anejo 14 – Artículo 44.º Estado Límite de Agotamiento frente a cortante]

Consideraciones generales

La contribución de las fibras se deberá tener en cuenta en la capacidad resistente de los tirantes.

Piezas de hormigón reforzado con fibras sin y con armadura de cortante

Cuando existan barras longitudinales dobladas que sean tenidas en cuenta en el cálculo como armadura de cortante, al menos un tercio de la resistencia a cortante deberá ser provista por la contribución de las fibras de acero o en su caso por la contribución conjunta de las fibras de acero y estribos verticales. En todo caso, la cuantía mínima de la armadura a cortante está establecida y se dispondrá tal como lo marca el punto 44.2.3.4.1 de la presente Instrucción. El esfuerzo cortante de agotamiento por tracción en el alma vale:

$$V_{u2} = V_{cu} + V_{su} + V_{fu}$$

donde:

V_{cu}	Contribución del hormigón a la resistencia a esfuerzo cortante dado en el punto 44.2.3.2.2
----------	--



V_{su} Contribución de la armadura transversal de alma a la resistencia a esfuerzo cortante. Ídem 44.2.3.2.2.

V_{fu} Contribución de las fibras de acero a la resistencia a esfuerzo cortante.

$$V_{fu} = 0,7\xi\tau_{fd}b_0d$$

donde:

$$\xi = 1 + \sqrt{\frac{200}{d}} \text{ con } d \text{ en (mm) y } \xi \leq 2 \text{ (Ídem 44.2.3.2.1).}$$

τ_{fd} Valor de cálculo del incremento de la resistencia a cortante debido a las fibras, tomando el valor:

$$\tau_{fd} = 0,5f_{ctR,d}\left(\frac{N}{mm^2}\right)$$

En el caso de secciones en T, se podría tener en cuenta la contribución de las alas a través de un coeficiente k_f multiplicador en la expresión de V_{fu} . Este coeficiente puede obtenerse mediante la siguiente expresión. La cuantía mínima de refuerzo a cortante, ya sea en forma de Hormigón Reforzado por Fibras de acero y/o estribos verticales se verifica siempre que se cumpla la relación:

$$k_f = 1 + n\left(\frac{b_f}{b_0}\right)\left(\frac{h_f}{d}\right) \text{ con } k_f < 1,5$$

donde:

h_f Altura de las alas en mm.

b_f Ancho de las alas en mm.

b_0 Ancho del alma en mm.

$$n = \frac{b_f - b_w}{h_f} < 3 \text{ y } n < \frac{3b_w}{h_f}$$

Armaduras longitudinales

En el caso de estructuras de hormigón reforzado con fibras con función estructural, en lugar de V_{su} deberá considerarse ($V_{su} + V_{fu}$) en las expresiones del articulado.

Torsión

El anejo 14 no indica disposiciones concretas para el hormigón con fibras.



Fatiga

El anejo 14 no indica disposiciones concretas para el hormigón con fibras.

3.1.3. Estado Límite de Servicio

Fisuración

El anejo 14 no indica disposiciones concretas para el hormigón con fibras.

Compresión máxima

El anejo 14 no indica disposiciones concretas para el hormigón con fibras.

3.1.4. Cuantías mínimas

Flexión

[EHE 08 Anejo 14 – 42.3.5 Cuantías geométricas mínimas]

Los valores de la tabla 42.3.5 relativos a las cuantías geométricas mínimas que, en cualquier caso, deben disponerse en los diferentes tipos de elementos estructurales, en función del acero utilizado, se podrán reducir, en el caso de hormigones con fibras, en una cuantía mecánica equivalente:

$$A_c f_{ctR,d}$$

donde: A_c y $f_{ctR,d}$ tienen el significado dado anteriormente.

Cortante

[EHE 08 Anejo 14 – 44.2.3.4.1 Armaduras transversales]

Armaduras transversales

La cuantía mínima de refuerzo a cortante, ya sea en forma de Hormigón Reforzado por Fibras de acero y/o estribos verticales se verifica siempre que se cumpla la relación:

$$V_{su} + V_{fu} > \frac{f_{ct,m}}{7,5} b_0 d$$

Torsión

El anejo 14 no indica disposiciones concretas para el hormigón con fibras.



3.2. Model Code 2010

3.2.1. Caracterización mecánica

Structural design of FRC elements is based on the post-cracking residual strength provided by fibre reinforcement. Other cases, like early age crack control or fire resistance, are considered non-structural use of FRC.

For structural use, a minimum mechanical performance of FRC must be guaranteed.

Fibres can be used to improve the behaviour at SLS since they can reduce crack spacing and crack width, thereby improving durability.

Fibres can be used to improve the behaviour at ULS where they can partially or totally substitute conventional reinforcement.

Módulo de elasticidad

[Model Code 2010 – 5.6.1 Introduction]

The mechanical properties of a cementitious matrix are modified when fibres are added. However, elastic properties and compressive strength are not significantly affected by fibres, unless a high percentage of fibres is used.

Coeficiente de Poisson

[Model Code 2010 – 5.6.1 Introduction]

The mechanical properties of a cementitious matrix are modified when fibres are added. However, elastic properties and compressive strength are not significantly affected by fibres, unless a high percentage of fibres is used.

Tracción

[Model Code 2010 – 5.6.2.2 Behaviour in tension]

With regard to the behaviour in tension, which is the most important aspect of FRC, various test methods are possible.

Bending tests can be carried out aiming at determining the load-deflection relation. The results can be used for deriving the stress – crack width relations by inverse analysis, performing equilibrium calculations for numerous crack openings as shown in Figure 5.6-4. A simpler approach can be found in subclause 5.6.4.

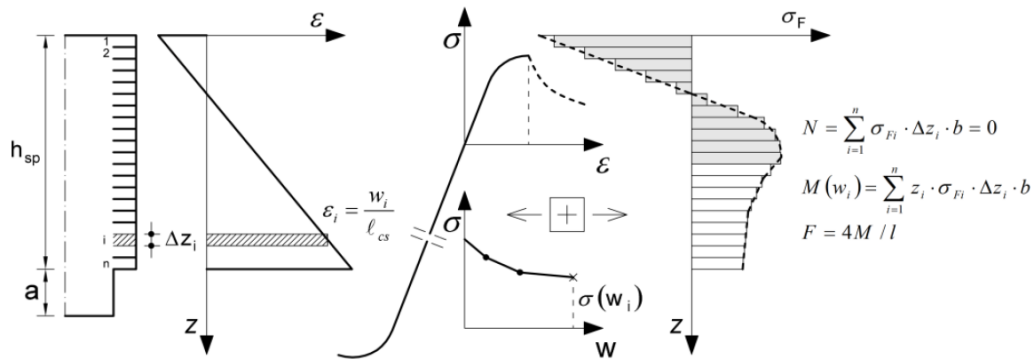


Ilustración 13.- Model Code 2010 - Figure 5.6-4: Inverse analysis of beam in bending performed to obtain stress - crack relation

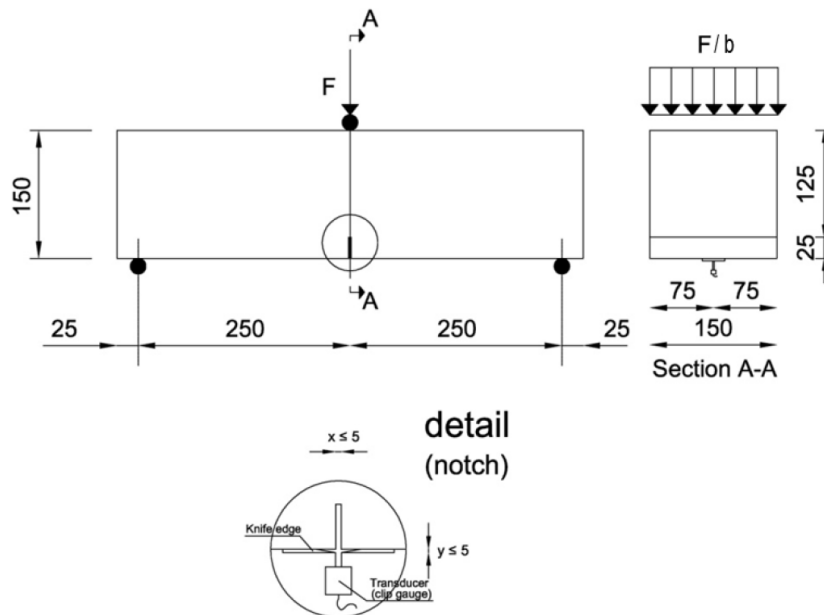


Ilustración 14.- Model Code 2010 - Figure 5.6-5: Test set-up required by EN 14651(dimensions in [mm])

Nominal values of the material properties can be determined by performing a 3-point bending test on a notched beam according to EN 14651 (Figure 5.6-5). The diagram of the applied force (F) versus the deformation shall be produced (Figure 5.6-6). The deformation is generally expressed in terms of Crack Mouth Opening Displacement ($CMOD$)

Parameters, $f_{R,j}$, representing the residual flexural tensile strength, are evaluated from the F - $CMOD$ relationship, as follows:

$$f_{R,j} = \frac{3 F_j l}{2 b h_{sp}^2}$$



where:

f_{Rj} [MPa] is the residual flexural tensile strength corresponding to $CMOD = CMOD_j$

F_j [N] is the load corresponding to $CMOD = CMOD_j$

l [mm] is the span length

b [mm] is the specimen width

h_{sp} [mm] is the distance between the notch tip and the top of the specimen (125 mm).

Other tests can be accepted if correlation factors with the parameters of EN 14651 are proven.

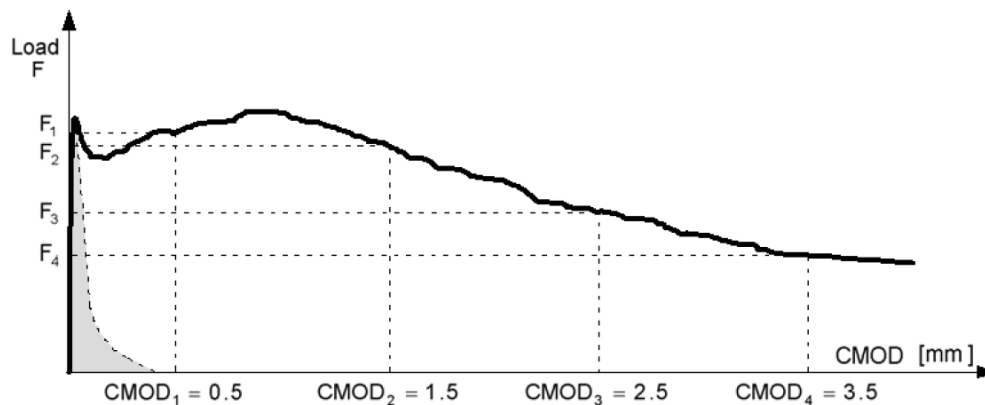


Ilustración 15.- Model Code 2010 - Figure 5.6-6: Typical F-CMOD curve for FRC

In case of organic and natural fibres, post-cracking long term behavior can be affected by an additional creep of the fibres themselves.

For structural applications with normal and high-strength concrete, the material classification is based on the post-cracking residual strength.

For ultra-high strength fibre reinforced concrete special design rules may be adopted.

For instance, a material denoted as “3b” has a strength f_{R1k} ranging between 3 and 4 MPa and the f_{R3k}/f_{R1k} ratio ranging between 0.7 and 0.9.

For high fibre contents, strain hardening materials can be obtained. To guarantee the hardening in tension, the tensile behaviour must be identified by means of uniaxial tension tests carried out on unnotched specimens.

Long term behaviour of cracked FRC under tension has to be properly taken into account for those materials whose long term performance is affected by creep and/or creep rupture (see subclause 5.6.5.).



[Model Code 2010 – 5.6.4 Constitutive laws]

A stress-crack opening law in uniaxial tension is defined for the postcracking behaviour of FRC. Its identification can be obtained by following different procedures as shown in Figure 5.6-4.

Two simplified stress-crack opening constitutive laws may be deduced from the bending test results: a plastic rigid behaviour, or a linear postcracking behaviour (hardening or softening) as schematically shown in

Figure 5.6-7, where f_{fts} represents the serviceability residual strength, defined as the post-cracking strength for serviceability crack openings, and f_{ftu} represents the ultimate residual strength.

The rigid-plastic model takes the static equivalence into account as shown in Figure 5.6-8, i.e. f_{ftu} results from the assumption that the whole compressive force is concentrated in the top fibre of the section:

$$M_u = \frac{f_{R3} b h_{sp}^2}{6} = \frac{f_{Rftu} b h_{sp}^2}{2}$$

$$f_{ftu} = \frac{f_{R3}}{3}$$

Ilustración 16.- Model Code 2010 – Figure 5.6-8 *Simplified model adopted to compute the ultimate residual tensile strength in uniaxial tension f_{ftu} by means of the residual nominal bending strength f_{R3}*

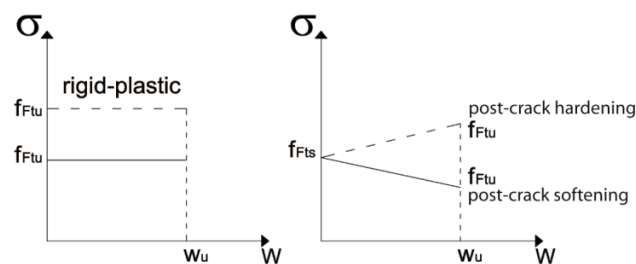


Ilustración 17.- Figure 5.6-8 *Simplified post-cracking constitutive laws: stress-crack opening (continuous and dashed lines refer to softening and hardening post-cracking behaviour, respectively)*



Rigid-plastic model

The rigid-plastic model identifies an unique reference value, f_{Ftu} , based on the ultimate behaviour. Such a value is determined as:

$$f_{Ftu} = \frac{f_{R3}}{3}$$

The equation for f_{Ftu} and $w_u = CMOD_3$ is obtained, from the rotational equilibrium at ULS, when a stress block in tension along the section is taken into account, as shown in Figure 5.6-8.

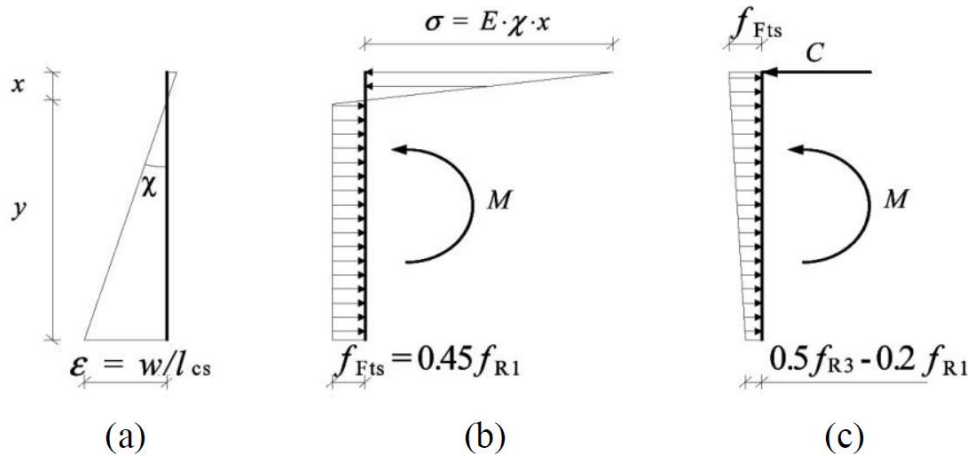


Ilustración 18.- Model Code 2010 – Figure 5.6-9: Stress diagrams for the determination of the residual tensile strength f_{Fts} (b) and f_{Ftu} (c) for the linear model, respectively

The limit value w_u applies particularly for design purposes.

The equation for f_{Ftu} and $w_u \neq CMOD_3$ is obtained by considering a linear constitutive law between points with abscissa $CMOD_1$ and $CMOD_3$, up to the point with abscissa w_u (Figure 5.6-10).

The stress value corresponding to the crack opening $CMOD_1$ is determined from equilibrium, with the assumption that the compressive stress distribution is linear (Figure 5.6-9b) and that the tensile behaviour is elastoplastic until a crack opening displacement corresponding to the serviceability limit state ($CMOD_1$):

$$M(CMOD_1) = \frac{f_{R1} b h_{sp}^2}{6}$$

The variability introduced in the numerical coefficient introduced in Eq. (5.6-5) by the elastic modulus is here neglected and a common value is assumed.



Linear model

The linear model identifies two reference values, namely f_{Fts} and f_{Ftu} .

They have to be defined through residual values of flexural strength using the following equations:

$$f_{Fts} = 0.45f_{R1} \quad (5.6-5)$$

$$f_{Ftu} = f_{Fts} - \frac{w_u}{CMOD_3} (f_{Fts} - 0.5f_{R3} + 0.2f_{R1}) \geq 0 \quad (5.6-6)$$

where w_u is the maximum crack opening accepted in structural design; its value depends on the ductility required.

The stress value corresponding to the crack opening $CMOD_3$ is determined from equilibrium, with the assumption that the compressive stress resultant is applied on the extrados chord (Figure 5.6-9c) and that the tensile behaviour is rigid-linear:

$$M(CMOD_3) = \frac{f_{R3}bh_{sp}^2}{6}$$

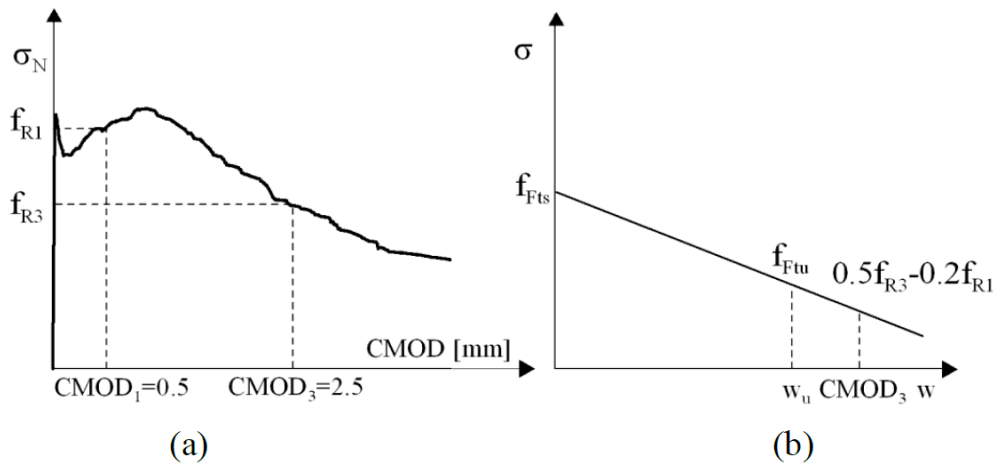


Ilustración 19.- Model Code 2010 - Figure 5.6-10: Typical results from a bending test on a softening material (a); linear post-cracking constitutive law (b)

For numerical analyses, more advanced constitutive laws are recommended, including first crack tensile strength.

When considering softening materials, the definition of the stress-strain law is based on the identification of the crack width and on the corresponding structural characteristic length, l_{cs} , of the structural element. Thus, the strain can be assumed equal to:

$$\varepsilon = w/l_{cs}$$



In elements with conventional reinforcement (rebars), l_{cs} , may be evaluated as:

$$l_{cs} = \min\{s_{rm}, y\}$$

where:

s_{rm} is the mean distance value between cracks;

y is the distance between the neutral axis and the tensile side of the cross section (Figure 5.6-9a), evaluated in the elastic cracked phase by neglecting the residual tensile strength of FRC, and for a load configuration corresponding to the serviceability state of crack opening and crack spacing.

The ultimate tensile strength f_{Ftu} in the linear model depends on the required ductility that is related to the allowed crack width. The ultimate crack width can be calculated as $w_u = l_{cs} \epsilon_{Fu}$, by assuming ϵ_{Fu} equal to 2% for variable strain distribution along the cross section and 1% for constant tensile strain distribution along the cross section. In any case, the maximum crack width may not exceed 2.5 mm.

In sections without traditional reinforcement under bending or under combined tensile-flexural and compressive-flexural forces with resulting force external to the section, $y = h$ is assumed. The same assumption can be taken for slabs.

When considering strain hardening materials, ϵ_{Fu} is equal to 2% for variable strain distribution along the cross section and 1% for constant tensile strain distribution along the cross section.

A material is considered as strain hardening when it shows a hardening behaviour in tension up to a $\epsilon_{Fu} = 1\%$.

Compresión

[Model Code 2010 – 5.6.2.1 Behaviour in compression]

Generally, the compressive relations valid for plain concrete apply to FRC as well.

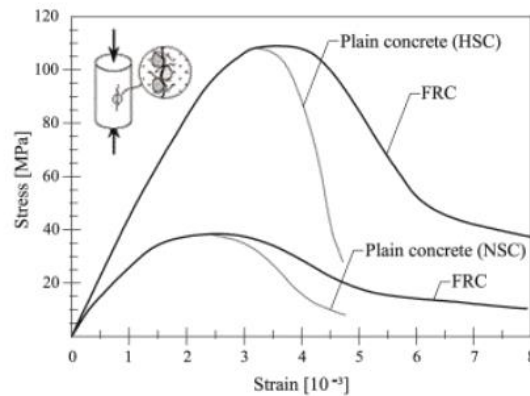


Ilustración 20.- Model Code 2010 - Figure 5.6-3: Main differences between plain and fibre reinforced concrete having both normal and high strength under uniaxial compression.

Uniaxial tensile testing is not advised for standard testing of new mixtures, because tensile tests are difficult to carry out and interpret.

Because the specimens are normally small, the number of fibres in the governing plane will be small and it could present a fibre orientation effect due to the method of manufacturing.

3.2.2. Estado Límite Último

Flexión compuesta

[Model Code 2010 – 7.7.3.1 Bending and/or axial compression in linear members]

The bending failure stage is supposed to be reached when one of the following conditions applies (see Figure 7.7-3): the meaning of the variables is found in subclauses 5.6.4 and 5.6.6):

- attainment of the maximum compressive strain in the FRC, ϵ_{cu} ;
- attainment of the maximum tensile strain in the steel (if present), ϵ_{su} ;
- attainment of the maximum tensile strain in the FRC, ϵ_{Fu} .

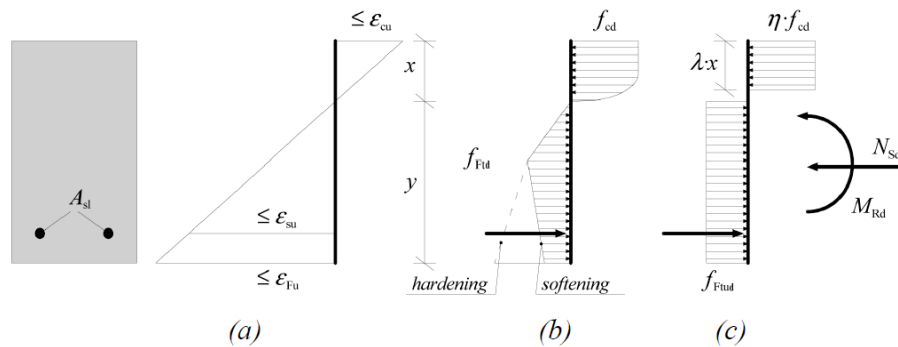


Ilustración 21.- Model Code 2010 – Figure 7.7-3: ULS for bending moment and axial force: use of the simplified stress/strain relationship (λ and η coefficient in accordance Eq. (7.2-15) to (7.2-18) in subclause 7.2.3.1.5).

[Model Code 2010 – 7.2.3.1.5 Stress strain relations for the design of cross-sections]

The factor λ , defining the height of the compression zone and the factor η , defining the effective strength, follow from:

$$\lambda = 0.8 \text{ for } f_{ck} \leq 50 \text{ MPa (7.2-15)}$$

$$\lambda = 0.8 - (f_{ck} - 50) / 400 \text{ for } 50 < f_{ck} \leq 100 \text{ MPa (7.2-16)}$$

and

$$\eta = 1.0 \text{ for } f_{ck} \leq 50 \text{ MPa (7.2-17)}$$

$$\eta = 1.0 - (f_{ck} - 50) / 200 \text{ for } 50 < f_{ck} \leq 100 \text{ MPa (7.2-18)}$$

If the width of the compression zone decreases in the direction of the extreme compression fibre, the value ηf_{cd} should be reduced by 10%.

Cortante

[Model Code 2010 – 7.7.3.2 Shear in beams]

Beams without longitudinal and shear reinforcement

When FRC with tensile-hardening behaviour are used and members without both longitudinal and transverse reinforcement are considered, the principal tensile stress, σ_1 , shall not be higher than the design tensile strength:

$$\sigma_1 \leq \frac{f_{Ftuk}}{\gamma_F}$$

where:

f_{Ftuk} [MPa] is the characteristic value of the ultimate residual tensile strength of FRC determined with [Eq. \(5.6-6\)](#) for $w_u = 1.5 \text{ mm}$ [MPa];



γ_F value found in Table 5.6-1.

Tabla 2.- Model Code 2010 - Table 4.5-7 *Partial safety factors γ_F for loads in the design of structural members not involving geotechnical actions: alternative combination of values*

Actions, γ_F	Unfavourable effect (γ_{sup})	Favourable effect (γ_{inf})
SET1		
Permanent (G), γ_G	1.35	1.0
Prestress (P), γ_P	1.0	1.0
Leading variable action ($Q_{k,1}$), γ_Q	1.5 $\Psi_{0,1}$	Usually neglected
Accompanying variable action ($Q_{k,i}$), γ_Q	1.5 $\Psi_{0,i}$	Usually neglected
SET2		
Permanent (G), γ_G	0.85 · 1.35	1.0
Prestress (P), γ_P	1.0	1.0
Leading variable action ($Q_{k,1}$), γ_Q	1.5	Usually neglected
Accompanying variable action ($Q_{k,i}$), γ_Q	1.5 $\Psi_{0,i}$	Usually neglected

a2. γ_F factors for accidental or seismic situations

The values of γ_F applicable to all actions are equal to 1.

Beams with shear reinforcement

The design value for the shear resistance in members with conventional longitudinal reinforcement and without shear reinforcement is given by (in N):

$$V_{Rd,F} = \left\{ \frac{0.18}{\gamma_c} k \left[100 \rho_l \left(1 + 7.5 \frac{f_{Ftuk}}{f_{ctk}} \right) f_{ck} \right]^{\frac{1}{3}} + 0.15 \sigma_{cp} \right\} b_w d$$

where:

γ_c is the partial safety factor for the concrete without fibres;

k is a factor that takes into account the size effect and it is equal to:

$$1 + \sqrt{\frac{200}{d}} \leq 2.0$$

d [mm] is the effective depth of the cross section

ρ_l is the reinforcement ratio for longitudinal reinforcement equal to:

$$\rho_l = A_{sl} / b_w d$$

A_{sl} [mm²] is the cross sectional area of the reinforcement which extends $\geq l_{bd} + d$ beyond the considered section;



f_{Ftuk} [MPa] is the characteristic value of the ultimate residual tensile strength for FRC, by considering $w_u = 1.5$ mm according to Eq. 5.6-6;

f_{ctk} [MPa] is the characteristic value of the tensile strength for the concrete matrix;

f_{ck} [MPa] is the characteristic value of cylindrical compressive strength;

$\sigma_{cp} = N_{Ed}/A_c < 0.2 f_{cd}$ [MPa] is the average stress acting on the concrete cross section, A_c [mm²], for an axial force N_{Ed} [N], due to loading or prestressing actions ($N_{Ed} > 0$ for compression);

b_w [mm] is the smallest width of the cross-section in the tensile area.

The shear resistance, $V_{Rd,F}$, is assumed to be not smaller than the minimum value, $V_{Rd,Fmin}$, defined as:

$$V_{Rd,Fmin} = (v_{min} + 0.15 \cdot \sigma_{cp}) \cdot b_w \cdot d$$

$$\text{where } v_{min} = 0.035 k^{3/2} f_{ck}^{1/2}$$

A recent model that follows the approach to shear described in subclause 7.3.3.4, computes the term V_{RdF} as follows:

$$V_{Rd,F} = \frac{1}{\gamma_F} (k_v \sqrt{f_{ck}} + k_f f_{Ftuk} \cot \theta) z b_w$$

where:

f_{Ftuk} is the characteristic value of the ultimate tensile strength for FRC, as determined by direct tensile tests, taken at the crack width at ultimate, w_u ;

$$k_f = 0.8$$

and

$$k_v = \frac{0.4}{1 + 1500 \varepsilon_x} \frac{1300}{1000 + k_{dg} z} \text{ for } \rho_w < 0.08 \sqrt{f_{ck}/f_{yk}}$$

$$k_v = \frac{0.4}{1 + 1500 \varepsilon_x} \text{ for } \rho_w \geq 0.08 \sqrt{f_{ck}/f_{yk}}$$

In Eq. (7.7-7) ε_x is the longitudinal strain at the mid-depth of the effective shear depth as determined by either Eqs. (7.3-14) or (7.3-16), as appropriate, z is the internal lever arm (in mm) between the flexural tensile and compressive forces (refer Figure 7.3-9) and k_{dg} , is an aggregate size influence parameter.



The aggregate size influence parameter in Eq. (7.7-7), k_{dg} , is given by:

$$k_{dg} = \frac{32}{16 + d_g} \geq 0.75$$

where d_g is the maximum aggregate size in mm. If the size of the maximum aggregate particles is not less than 16 mm, this parameter may be taken as $k_{dg} = 1.0$.

The limits of the angle of the compressive stress field, θ , relative to the longitudinal axis of the member, as shown in Figure 7.3-11, are:

$$\theta_{min} \leq \theta \leq 45^\circ$$

where the minimum inclination angle is:

$$\theta_{min} = 29^\circ + 7000\varepsilon_x$$

Where for the determination of f_{Ftuk} , the crack width at ultimate (w_u) is taken as:

$$w_u = 0.2 + 1000\varepsilon_x \geq 0.125\text{mm}$$

Beams with shear and longitudinal reinforcement

For the design of members with shear reinforcement the basic relation Eq. (7.3-9) applies, being:

$$V_{Rd} = V_{Rd,c} + V_{Rd,s} \quad (7.7-12)$$

In FRC elements this equation becomes:

$$V_{Rd} = V_{Rd,F} + V_{Rd,s} \quad (7.7-13)$$

where

$V_{Rd,s}$ is to be taken from Eq. (7.3-29).

$V_{Rd,F}$ follows from Eq. [\(7.7-4\)](#).

**The design shear resistance provided by stirrups is:*

$$V_{Rd,s} = \frac{A_{sw}}{s_w} z f_{ywd} \cot \theta \quad (7.3-29)$$

where f_{ywd} denotes the design yield strength of the shear reinforcement.



Torsión

[Model Code 2010 – 7.7.3.3 Torsion in beams]

Beams without longitudinal and transverse reinforcement

When FRC with a hardening tensile behaviour is used in a member without both longitudinal reinforcement and transverse reinforcement, the principal tensile stress shall not exceed the design tensile strength:

$$\sigma_1 \leq \frac{f_{Ftuk}}{\gamma_F}$$

where:

f_{Ftuk} [MPa] is the characteristic value of the ultimate residual tensile strength for FRC at $w_u = 1.5$ mm according to Eq. (5.6.-6) [MPa];

γ_F is the partial safety factor for the FRC, which follows from Table 5.6-1.

Beams with longitudinal and transverse reinforcement

The presence of fibres increases the torsion capacity; however, design models are not currently available. Models should be proven by experiments on real size elements.

Fatiga

No indica recomendaciones específicas para el hormigón con fibras.

3.2.3. Estado Límite de Servicio

Tensión-deformación

[Model Code 2010 – 5.6.5 Stress-strain relationship]

For softening materials at SLS (CASE (I)) the same constitutive relationship adopted for plain concrete in uniaxial tension is used up to the peak strength f_{ct} . In the post-cracking stage, a bilinear relation applies (Figure 5.6-11a).

The post-peak propagation branch (BC) is analytically described as:

$$\frac{\sigma - f_{ct}}{0.2f_{ct} - f_{ct}} = \frac{\varepsilon - \varepsilon_p}{\varepsilon_Q - \varepsilon_p} \text{ for } \varepsilon_p \leq \varepsilon \leq \varepsilon_c$$

$$\text{with } \varepsilon_Q = \frac{G_F}{f_{ct}l_{cs}} + \left(\varepsilon_p - \frac{0.8f_{ct}}{E_c} \right)$$

where G_F represents the fracture energy of plain concrete, see Eq. (5.1-9.)

Point A in the curves of Figure 5.6-11 (a), (b), (c) is defined in Fig. 5.1-4.



For softening materials, the residual strength (fourth branch) is defined by two points corresponding to $(\varepsilon_{SLS}, f_{Fts})$ and $(\varepsilon_{ULS}, f_{Ftu})$ where:

$$\varepsilon_{SLS} = CMOD_1 / l_{cs} \quad (5.6-11)$$

$$\varepsilon_{ULS} = w_u / l_{cs} = \min (\varepsilon_{Fu}, 2.5 / l_{cs})$$

with $\varepsilon_{Fu} = 2\%$ for variable strain distribution along the cross section and 1% for only tensile strain distribution along the cross section, see subclause 5.6.4.

For materials characterized by a stable propagation up to ε_{SLS} with a tensile strength f_{Fts} larger than f_{ct} , two cases can be considered:

CASE (II): the cracking process becomes stable up to the SLS strain and four branches again define the constitutive relationship. The first two branches remain those corresponding to plain concrete, while the third branch (BD) is analytically described as:

$$\frac{\sigma - f_{ct}}{f_{Ftsd} - f_{ct}} = \frac{\varepsilon - \varepsilon_p}{\varepsilon_{SLS} - \varepsilon_p} \quad \text{for } \varepsilon_p \leq \varepsilon \leq \varepsilon_{SLS}$$

CASE (III): the cracking remains stable up to the SLS strain and three branches define the constitutive relationship. The second branch (A'D) is defined as:

$$\frac{\sigma - \sigma_{A'}}{f_{Fts} - \sigma_{A'}} = \frac{\varepsilon - \varepsilon_{A'}}{\varepsilon_{SLS} - \varepsilon_{A'}} \quad \text{for } \varepsilon_{A'} \leq \varepsilon \leq \varepsilon_{SLS}$$

where $\sigma_{A'}$ is on the elastic branch for a stress equal to $0.9 f_{Fts}$.

For both the cases (II) and (III), the material can be softening (DE) or hardening (DE') depending on the slope of the last branch.

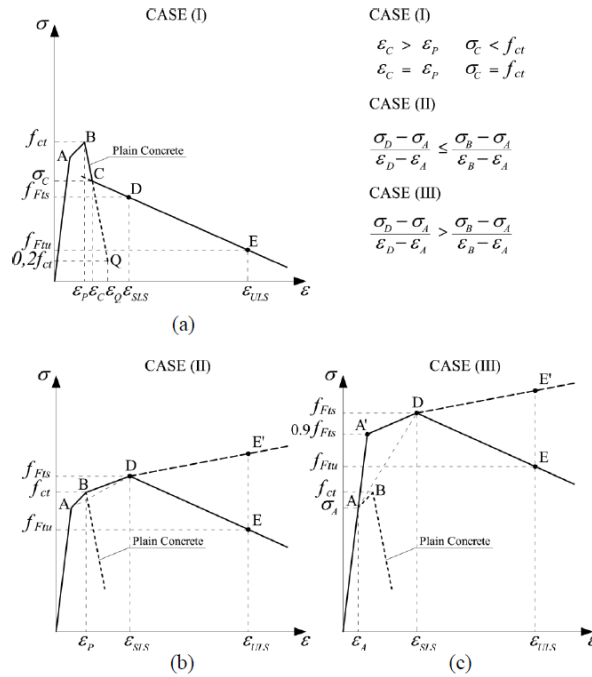


Ilustración 22.-Model Code 2010 - Stress-strain relations at SLS for softening (a) and softening or hardening (b, c) behaviour of FRC

Fisuración

[Model Code 2010 – 7.7.4.2 Crack width in members with conventional reinforcement]

The design crack width w_d in FRC elements can be calculated by:

$$w_d = 2 \left\{ k_c + \frac{1}{4} \frac{\phi_s}{\rho_{s,ef}} \frac{(f_{ctm} - f_{Ftsm})}{\tau_{bm}} \right\} \frac{1}{E_s} (\sigma_s - \beta \sigma_{sr} + \eta_r \varepsilon_r E_s) \quad (7.7-22)$$

where:

f_{Ftsm} follows from Eq. (5.6-5).

For the other symbols reference is made to Eq. (7.6-5).

With $\sigma_{sr} = (f_{ctm} - f_{Ftsm}) \cdot (1 + \alpha_e \rho_s) / \rho_{s,ef}$

In σ_s , the effect of the fibres (f_{Ftsm}) needs to be taken into account.

$$f_{Ftsm} = f_{Ftsk} / 0,7$$

Eq. (7.7-22) is an extension of Eq. (7.6-5). It follows from this equation through the modified value of $l_{s,max}$, the length over which slip between concrete and steel occurs, necessary to reintroduce the cracking-force $A_c(1 + \alpha_e \rho_{s,ef}) f_{ctm}$ back into the concrete by bond.



Because of the action of the fibres, which generate a residual tensile strength f_{Ftsm} , the force to be reintroduced by bond is reduced to $A_c(1+\alpha_e\rho_{s,ef})(f_{ctm} - f_{Ftsm})$.

So, the introduction length $l_{s,max}$ is reduced to:

$$l_{s,max} = kc \frac{1}{4} \frac{(f_{ctm} - f_{Ftsm})}{\tau_{bm}} \frac{\phi_s}{\rho_{s,ef}}$$

[Model Code 2010 – 7.7.4.3 Minimum reinforcement for crack control]

For controlling the cracking in the elements under bending, if needed, a minimum reinforcement should be applied, at least equal to:

$$A_{s,min} = k_c k (f_{ctm} - f_{Ftsm}) \frac{A_{ct}}{\sigma_s}$$

where:

f_{ctm} is the average value of the tensile strength of the concrete matrix;

f_{Ftsm} is the average value of the residual strength of FRC;

A_{ct} is the tensile part of the concrete cross section, evaluated by considering a stress field at elastic limit;

σ_s is the maximum tensile stress in the reinforcement at cracking stage, that can be considered equal to the yielding stress of the steel;

k_c is a coefficient taking account of the stress distribution in the cross section just before cracking and the change of the inner lever arm. For rectangular cross sections $k_c = 1$

k is a coefficient taking into account of non-uniform self-equilibrating stresses, leading to a reduction of the cracking force.

When $A_{s,min}$ is negative, the minimum reinforcement can be due only to the fibre reinforcement.

Compresión máxima

[Model Code 2010 – 7.7.4.1 Stress limitation]

The compressive stresses at the SLS shall be limited in accordance with subclause 7.6.3.3.

Tensile stresses in the rebars shall be limited at the SLS in accordance with subclause 7.6.3.4.



In structural FRC elements having a tension softening behaviour after cracking, the tensile stresses verification is not necessary if the element is verified at ULS.

In structural FRC elements having a tension hardening behaviour after cracking, the tensile stresses verification shall be done by imposing the limitation:

$$\sigma_t \leq 0.6 \cdot f_{Ftsk}$$

* f_{Ftsk} is the characteristic value of the ultimate residual tensile strength of FRC determined with Eq. (5.6-6) for $w_u = 1.5$ mm [MPa];

3.2.4. Cuantías mínimas

Flexión

[Model Code 2010 – 7.7.4.2.4 Minimum shear reinforcement]

For controlling the crack width in the elements under bending, if needed, a minimum reinforcement should be applied, at least equal to:

$$A_{s,min} = k_c k (f_{ctm} - f_{Ftsm}) \frac{A_{ct}}{\sigma_s}$$

where:

f_{ctm} is the average value of the tensile strength of the concrete matrix;

f_{Ftsm} is the average value of the residual strength of FRC;

A_{ct} is the tensile part of the concrete cross section, evaluated by considering a stress field at elastic limit;

σ_s is the maximum tensile stress in the reinforcement in the cracked state, that can be considered equal to the yielding stress of the steel;

k_c is a coefficient taking account of the stress distribution in the cross section just before cracking and the change of the inner lever arm; for rectangular cross sections $k_c = 1$;

k is a coefficient taking into account of non-uniform self-equilibrating stresses, leading to a reduction of the cracking force:

$k = 1.0$ for webs with $h \leq 300$ mm or flanges with width ≤ 300 mm;

$k = 0.65$ for webs with $h \geq 800$ mm or flanges with width ≥ 800 mm;

for intermediate values interpolation can be applied.



When $A_{s,min}$ is negative, the minimum reinforcement can be due only to the fibre reinforcement.

Cortante

[Model Code 2010 – 7.7.3.2.4 Minimum shear reinforcement]

The minimum amount of conventional shear reinforcement (stirrups) is not required if the following condition is fulfilled:

$$f_{Ftuk} \geq 0.08 \sqrt{f_{ck}}$$

where:

f_{Ftuk} [MPa] is the characteristic value of the ultimate residual tensile strength for FRC, by considering $w_u = 1.5$ mm according to Eq. (5.6.-6).

This allows limiting the development and the diffusion of the inclined cracking and, as a consequence, can ensure sufficient member ductility.

When the above-mentioned limitation is not applied, conventional shear reinforcement (stirrups) shall be introduced according to Eq. (7.7-13).

The minimum shear reinforcement should be provided by either stirrups (7.3-13), or fibres.

Eq. (7.7-14) is based on steel fibre concrete research, and should be checked for other types of material.

Torsión

No establece requisitos específicos de cuantías mínimas de torsión para el hormigón reforzado con fibras.



3.3. ACI

3.3.1. Caracterización mecánica

Módulo de elasticidad

[ACI 544.1R – 2.2.3.5 Modulus of elasticity and Poisson's ratio]

In practice, when the volume percentage of fibers is less than 2 percent, the modulus of elasticity and Poisson's ratio of SFRC are generally taken as equal to those of a similar non-fibrous concrete or mortar.

[ACI 544.4R – 1.3.2 Mechanical characteristics and modeling]

It should be noted that the modulus of elasticity of concrete (in the linear ascending precrack region) is not affected by the fibers because they are only effective after concrete has cracked.

Coeficiente de Poisson

[ACI 544.1R – 2.2.3.5 Modulus of elasticity and Poisson's ratio]

In practice, when the volume percentage of fibers is less than 2 percent, the modulus of elasticity and Poisson's ratio of SFRC are generally taken as equal to those of a similar nonfibrous concrete or mortar.

Tracción

[ACI 544.1R – 2.2.3.1.2 Direct tension]

In direct tension, the improvement in strength is significant, with increases of the order of 30 to 40 percent reported for the addition of 1.5 percent by volume of fibers in mortar or concrete [2.38, 2.39].

[ACI 544.4R – 4.2 Tensile stress-strain responde for FRC]

Many studies have been conducted to determine the stress-strain curve of FRC in direct tension (Shah et al. 1978; Gopalaratnam and Shah 1987b); however, there is no standard test method recognized by ASTM. The idealized tensile stress-strain diagram used in this document is the same as one proposed by RILEM TC 162-TDF (2003) shown in Fig. 4.2. The values that define this constitutive model are based on average or characteristic values that are, in turn, used in the design process. The key points of the compression side of the diagram are obtained directly from the standard compressive cylinder test. For the tension side of the diagram, the key points are indirectly obtained from a flexural test.



- a) σ_1 and ϵ_1 —tensile stress and corresponding strain at onset of first cracking
- b) σ_2 and ϵ_2 —stress and strain at the onset of the stable softening branch
- c) σ_3 and ϵ_3 —stress and strain at the end of the softening branch

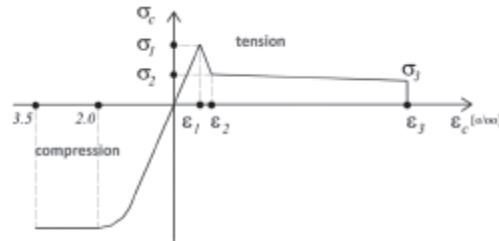


Ilustración 23.- ACI 544.4R - Fig. 4.2 Schematic of a typical stress-strain diagram for FRC in uniaxial tension and compression, according to RILEM TC 162-TDF (2003) and Vandewalle (2003).

Compresión

[ACI 544.1R – 2.2.3.1.1 Compression]

In compression, the ultimate strength is only slightly affected by the presence of fibers, with observed increases ranging from 0 to 15 percent for up to 1.5 percent by volume of fibers [2.34-2.38].

[ACI 544.4R – 4.2 Tensile stress-strain response for FRC]

Many studies have been conducted to determine the stress-strain curve of FRC in direct tension (Shah et al. 1978; Gopalaratnam and Shah 1987b); however, there is no standard test method recognized by ASTM. The idealized tensile stress-strain diagram used in this document is the same as one proposed by RILEM TC 162-TDF (2003) shown in Fig. 4.2. The values that define this constitutive model are based on average or characteristic values that are, in turn, used in the design process. The key points of the compression side of the diagram are obtained directly from the standard compressive cylinder test. For the tension side of the diagram, the key points are indirectly obtained from a flexural test.

- a) σ_1 and ϵ_1 —tensile stress and corresponding strain at onset of first cracking
- b) σ_2 and ϵ_2 —stress and strain at the onset of the stable softening branch
- c) σ_3 and ϵ_3 —stress and strain at the end of the softening branch

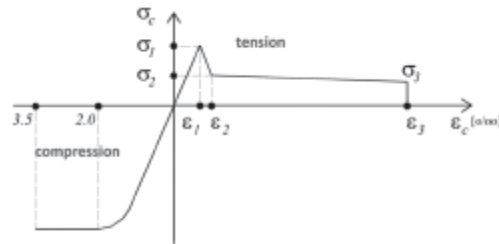


Ilustración 24.- ACI 544.4R - Fig. 4.2 Schematic of a typical stress-strain diagram for FRC in uniaxial tension and compression, according to RILEM TC 162-TDF (2003) and Vandewalle (2003).

3.3.1. Estado Límite Último

Flexión compuesta

[ACI 544.1R – 2.2.3.1.3 Shear and torsion]

Steel fibers generally increase the shear and torsional strength of concrete, although there are little data dealing strictly with the shear and torsional strength of SFRC, as opposed to that of reinforced beams made with a SFRC matrix and conventional reinforcing bars. The increase in strength of SFRC in pure shear has been shown to depend on the shear testing technique and the consequent degree of alignment of the fibers in the shear failure zone [2.40]. For one percent by volume of fibers, the increases range from negligible to 30 percent [2.40]. Research has substantiated increased shear (diagonal tension) capacity of SFRC and mortar beams [2.41-2.44]. Steel fibers have several potential advantages when used to augment or replace vertical stirrups in beams [2.45]. These advantages are: (1) the random distribution of fibers throughout the volume of concrete at much closer spacing than is practical for the smallest reinforcing bars which can lead to distributed cracking with reduced crack size; (2) the first-crack tensile strength and the ultimate tensile strength of the concrete may be increased by the fibers; and (3) the shear-friction strength is increased by resistance to pull-out and by fibers bridging cracks.

Steel fibers in sufficient quantity, depending on the geometric shape of the fiber, can increase the shear strength of the concrete beams enough to prevent catastrophic diagonal tension failure and to force a flexure failure of the beam

[2.44, 2.46-2.48]. Fig. 2.4 shows shear strength as a function of the shear span-to-depth ratio, a/d , for SFRC beams from several published investigations. The bulk of existing test data for shear capacity of SFRC beams are for smaller than prototype-size beams. Limited test data for prototype-size beams indicate that the steel fibers remain effective as shear reinforcement [2.49, 2.50]. The slight decrease in beam shear strength observed in these tests can be explained by the decrease in shear strength with beam size observed for beams without fiber reinforcement.

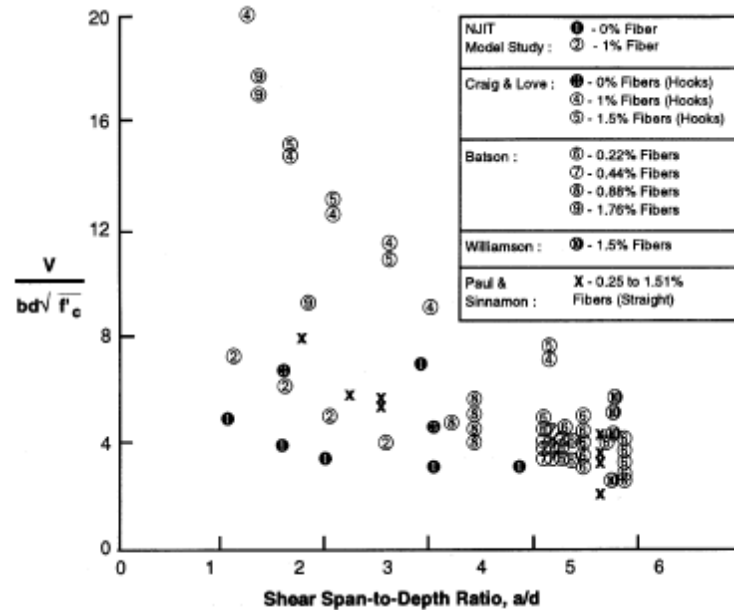


Ilustración 25.- ACI 544.1R - Fig.2.4 - Shear behavior of reinforced SFRC beams.

Design of RC for flexure (stress block)

[ACI 544.4R – 4.4 Design of RC for flexure (stress block)]

The nominal bending moment for a conventional reinforced concrete section without fibers, M_{n-RC} , is calculated according to Eq. (4.4) from the force equilibrium in the cross section as shown in Fig. 4.4. As illustrated schematically, Fig. 4.4(a) is a RC beam section without fibers, Fig. 4.4(b) shows the actual distribution of normal stresses, and Fig. 4.4(c) shows the simplified distribution of normal stresses in the cracked section. After concrete has cracked, the compressive force C is carried by concrete (above the neutral axis) and the tensile force T is carried by reinforcing bar (below the neutral axis). It should be noted that the stress block is only accurate for the calculation of the ultimate moment, not for deriving a moment-curvature relation. The tensile capacity of plain concrete is negligible and is not taken into account in these calculations.

$$M_{n-RC} = A_s f_y \left(d - \frac{a}{2} \right)$$

$$\text{Where } a = \frac{A_s f_y}{0.85 f'_c b}$$

Note that once the flexural strength of concrete is reached, it will crack and all the tensile forces are provided by the steel reinforcement. When designed based on load and resistance factors (LRFD), the design moment capacity of the reinforced concrete section, ϕM_{n-RC} , should be greater than the factored moment M_u applied to the section: $\phi M_{n-RC} > M_u$.



The reduction factor ϕ depends on the type of the member and its failure mode, should be determined based on ACI 318 or other building codes, and is typically between 0.65 and 0.9 for flexural members.

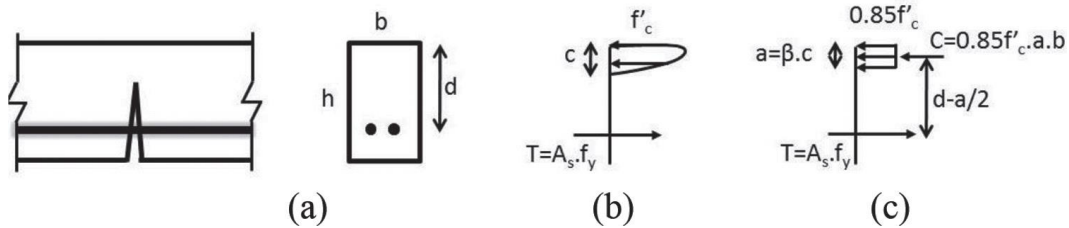


Ilustración 26.- ACI 544.4R - Fig. 4.4—Schematics of stress block for a cracked reinforced concrete flexural member without fibers: (a) reinforced concrete beam section; (b) actual distribution of normal stresses; and (c) simplified distribution of normal stresses.

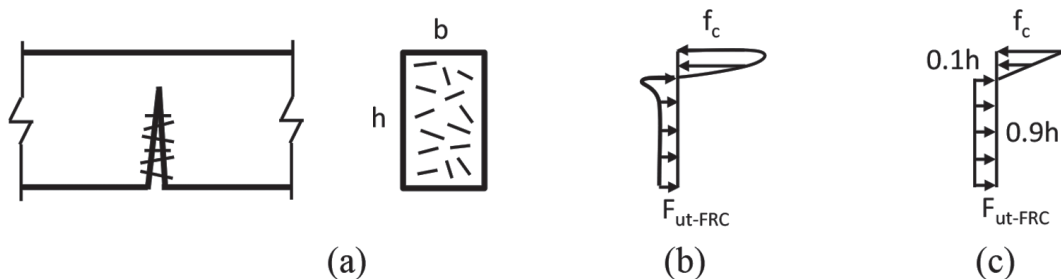


Ilustración 27.- ACI 544.4R - Fig. 4.5—Schematics of stress block for a cracked FRC flexural member. (a) FRC beam section; (b) actual distribution of normal stresses; and (c) simplified distribution of normal stresses.

Design of RC for flexure (ASTM C1609/C1609M, in conjunction with RILEM TC 162-TDF [2003])

[ACI 544.4R – 4.5 Design of RC for flexure (ASTM C1609/C1609M, in conjunction with RILEM TC 162-TDF [2003])]

The same stress block concept can be applied to an FRC section. ASTM C1609/C1609M is performed to obtain the required design parameters. The nominal bending moment for an FRC section, $Mn-FRC$, is calculated according to Eq. (4.5a) and (4.5b) from the force equilibrium in the cross section, as shown in Fig. 4.5. As presented schematically, Fig. 4.5(a) is an FRC beam section reinforced with fibers, Fig. 4.5(b) shows the actual distribution of normal stresses, and Fig. 4.5(c) shows the simplified distribution of normal stresses in the cracked section. The compressive stresses are carried by concrete and the tensile stresses are carried by reinforcing fibers. The distribution of the compressive stresses for FRC is simplified as triangular rather than rectangular because of the composite action of fibers and concrete above the neutral axis. The tensile strength of FRC is much higher than that of plain concrete and therefore is taken into account in these calculations. For ULS, the ultimate tensile strength of cracked FRC, f_{ut-FRC} , can be taken as 0.37 times its flexural residual strength, $f D 150$ (or fe_3), measured from ASTM C1609/ C1609M test as shown in Eq. (4.5a). The moment



capacity of a cracked FRC section is shown in Eq. (4.5b), developed in conjunction with the similar method used by RILEM TC 162-TDF (2003) and Vandewalle (2003). If FRC is designed for smaller crack widths under SLS requirements, other parameters such as f_D 600 can be used that correspond to smaller deflection in the beam test. The choice of the design limit (ULS versus SLS) and the related design parameter depends on the application and serviceability requirements.

$$f_{ut-FRC} = 0.37f_{150}^D$$

$$M_{n-FRC} = f_{150}^D x \frac{bh^2}{6}$$

Sometimes the equivalent residual strength $f_{e,3}$ is used instead of the residual strength f_{150}^D . The former parameter ($f_{e,3}$) is an indication of the total energy absorption (flexural toughness) in a beam test and is usually used for the design of FRC members that are continuously supported such as slabs-on-ground and shotcrete. The latter parameter (f_{150}^D) is the actual value of flexural residual strength at a given deflection or crack width. This parameter is commonly used for FRC members without continuous support, including beams, suspended slabs, and precast segments. The value of f_{150}^D can be slightly smaller than $f_{e,3}$, which results in a more conservative design. The choice between the two parameters depends on the application, design criteria, and safety requirements. The design moment capacity of FRC, ϕM_{n-FRC} , should be greater than the factored moment M_u applied to the section: $\phi M_{n-FRC} > M_u$. Note that compared with conventionally-reinforced concrete, these ϕ factors may require adjustments prior to use for FRC members for compression-controlled and tension-controlled failure modes. More conservative (lower values) of ϕ factors should be used for FRC members without continuous support such as beams, suspended slabs, and precast. For FRC members with continuous support, such as slabs-on-ground and shotcrete, higher values of ϕ factors may be used.

Example: Assume a 6 in. (150 mm) slab-on-ground exposed to tensile shrinkage and temperature stresses. Consider various reinforcement ratios of 0.05, 0.1, and 0.15 percent and find the required flexural residual strength $f_{e,3}$ for FRC to provide the same level of crack control as Grade 60 steel.

$$\text{Tensile force provided by steel: } F_{ts} = \frac{A_s}{bh} F_y = \rho F_y = 60,000\rho$$

The required values of tensile and flexural residual strengths have been calculated for the given steel reinforcement ratios shown in Table 4.5. Note that in this example, the flexural residual strength is 0.37 times the required postcrack tensile strength as described earlier in this section.



Example: Assume an 8 in. (200 mm) precast panel reinforced with No. 4 bars at 16 in. (bar diameter 12.7 mm, spaced at 400 mm) placed in midsection to provide postcrack moment capacity. Find the value of f_{150}^D for FRC to provide the same level of post-crack flexural strength as reinforcing bar. Assume 5000 psi (35 MPa) concrete and

Steel reinforcement ratio ρ	Requires tensile residual strength		FRC flexural residual strength	
	psi	MPa	psi	MPa
0.05	30	0.2	81	0.6
0.10	60	0.4	162	1.1
0.15	90	0.6	243	1.7

Ilustración 28.- ACI 544.4R - Table 4.5 - Typical calculation of FRC residual strength values for crack control

Grade 60 (414 MPa) steel and a moment capacity factor of 0.9 for steel.

Factored moment capacity provided by steel:

$$\phi M_{n-RC} = \phi A_s F_y \left(d - \frac{a}{2} \right) = 0.9 \times 0.147 \times 60,000 \times \left(\frac{8}{2} - \frac{0.17}{2} \right) = 31,120 \text{ lb} - \text{in}$$

$$\text{where } a = \frac{A_s F_y}{0.85 f'_c b} = \frac{0.147 \times 60,000}{0.85 \times 5000 \times 12} = 0.17 \text{ in.}$$

Ultimate moment capacity for FRC:

$$\phi M_{n-FRC} = \phi M_{n-RC} = 31,120 \text{ lb} - \text{in.} = \phi f_{150}^D \frac{b h^2}{6}$$

$$f_{150}^D = \frac{6 M_{n-FRC}}{\phi b h^2} = \frac{6 \times 31,120}{0.9 \times 12 \times 8^2} = 270 \text{ psi (1.86 MPa)}$$

Design of RC for flexure (Model Code 2010 [fib 2013])

[ACI 544.4R – 4.6 Design of RC for flexure (Model Code 2010 [fib 2013])]

The FRC design may be performed using the momentcrack width relationship obtained from BS EN 14651:2005 test on notched beams using Model Code 2010 (fib 2013) design guidelines summarized herein. The nominal moment for an FRC section, M_{n-FRC} , is calculated according Eq. (4.6a) through (4.6d) from the force equilibrium in the cross section, as shown in Fig. 4.6. As presented schematically, Fig. 4.6(a) is an FRC beam section reinforced with fibers; Fig. 4.6(b) shows the distribution of flexural stresses, whereas Fig. 4.5(c) shows the simplified distribution of normal stresses in the cracked section. A constant value of tensile residual strength f_{Ftu} is used for ultimate state design. Two models are proposed for calculating the post-crack tensile strength of FRC in this method. In the first model, called simplified rigid-plastic, the ultimate tensile strength of FRC, $f_{Ftu-FRC}$, is taken as a constant value of one-third times the flexural residual



strength of FRC, $f_{R,3}$, that is measured from the BS EN 14651:2005 beam test. The formulas for calculating the tensile strength and nominal bending moment are shown in Eq. (4.6a) and (4.6b), respectively. The second model assumes a linear relationship between the residual strength and the crack width both for serviceability and ultimate limit design of an FRC section. The formulas for calculating the tensile strength and nominal bending moment are shown in Eq. (4.6c) and (4.6d), respectively. Attention should be paid to the state of design: serviceability limit state (SLS) versus ultimate limit state (ULS) in choosing the correct equations.

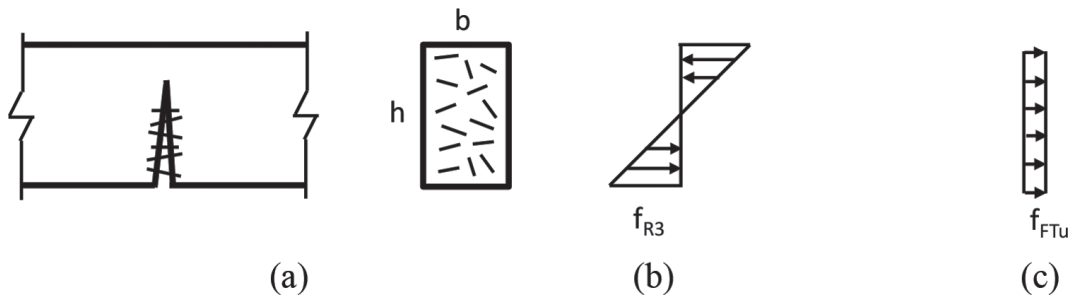


Ilustración 29.- ACI 544.4R - Fig. 4.6—Schematics of stress block for a cracked FRC flexural member: (a) FRC beam section; (b) distribution of flexural stresses; and (c) simplified distribution of normal stresses.

It is noted that design according to Model Code 2010 (*fib* 2013) only covers fiber materials with a Young's modulus not significantly affected by time or temperature, or both. In addition, minimum requirements apply such as $f_{R,1}/f_L > 0.4$ and $f_{R,3}/f_{R,1} > 0.5$, in which f_L is the limit of proportionality (LOP) calculated according to Eq. (3.3.2). The rules given by Model Code 2010 (*fib* 2013) are based on experience with steel fiber-reinforced concrete only.

Using rigid-plastic model (for ULS only):

$$f_{Ftu-FRC} = \frac{f_{R,3}}{3}$$

$$M_{nu-FRC} = f_{R,3} \frac{bh_{sp}^2}{6}$$

Using linear model (for SLS and ULS):

$$f_{Fts-FRC} = 0.45f_{R,1}$$

$$f_{Ftu-FRC} = (0.45f_{R,1}) - \frac{w_u}{CMOD_3} \geq 0$$

$$(0.45f_{R,1} - 0.5f_{R,3} + 0.2f_{R,1})$$

$$M_{ns-FRC} = f_{R,1} \frac{bh_{sp}^2}{6}$$



$$M_{nu-FRC} = f_{R,3} \frac{bh_{sp}^2}{6}$$

Example: BS EN 14651:2005 test has been conducted on FRC beams and the values of $f_{R,1} = 1000$ psi (6.9 MPa) and $f_{R,3} = 800$ psi (5.5 MPa) have been reported. What are the nominal moment capacities of this FRC for SLS and ULS conditions? Assume a maximum crack width $w_u = 0.06$ in. (1.5 mm) and use the linear model approach.

Residual tensile strength of FRC under SLS and ULS:

$$f_{Fts-FRC} = 0.45f_{R,1} = 0.45 \times 100 = 450 \text{ psi (3.1 MPa)}$$

$$\begin{aligned} f_{Ftu-FRC} &= (0.45f_{R,1}) - \frac{w_u}{CMOD_3} (0.45f_{R,1} - 0.5f_{R,3} + 0.2f_{R,1}) \\ &= 450 - \frac{0.05}{0.1} (450 - 0.5 \times 800 + 0.2 \times 1000) \\ &= 325 \text{ psi (2.2 MPa)} \end{aligned}$$

Nominal moment capacity of FRC under SLS and ULS:

$$M_{ns-FRC} = 1000 \frac{6 \times 5^2}{6} = 25,000 \text{ lb-in (9000 N-m)}$$

$$M_{nu-FRC} = 20,000 \text{ lb-in (7200 N-m)}$$



Design of RC for flexure-hybrid reinforcement

[ACI 544.4R – 4.7 Design of RC for flexure-hybrid reinforcement]

Hybrid reinforcement (using bars plus fibers) could be a viable option for the design and construction of concrete members with high levels of reinforcement and steel congestion.

A portion of reinforcing bars may be substituted with fibers to allow for better consolidation of concrete and a faster construction. A recent structural application of hybrid reinforcement was published by Kopczynski and Whiteley (2016), where steel fibers were used to replace diagonal bars in shear wall coupling beams in a high-rise building. Fullscale tests and computer simulations showed an improved strength and ductility in the concrete members with hybrid reinforcement, whereas the total amount of reinforcing bars was reduced by 40 percent. The moment capacity of a hybrid FRC section is calculated taking into account the contribution of both steel bars and fibers, as shown in a general form in Fig. 4.7. As presented schematically, Fig. 4.7(a) is beam section reinforced with bars and fibers, and Fig. 4.7(b) shows the distribution of normal stresses in a cracked section. The compressive stresses are carried by concrete while the tensile stresses/forces are carried by the hybrid action of bars and fibers. Such calculations can be done for serviceability limit state (SLS) and ultimate limit state (ULS) following the general guidelines described in 4.5 and 4.6. The general form of nominal moment capacity of a member with hybrid reinforcement (M_{n-HFRC}) is shown in Eq. (4.7). Various configurations for hybrid reinforcement are possible; more information can be found in Model Code 2010 (*fib* 2013), Vandewalle (2000c), Tiberti et al. (2008), Barros et al. (2015), and Mobasher et al. (2015b).

$$M_{n-HFRC} = M_{n-RC} + M_{n-FRC}$$

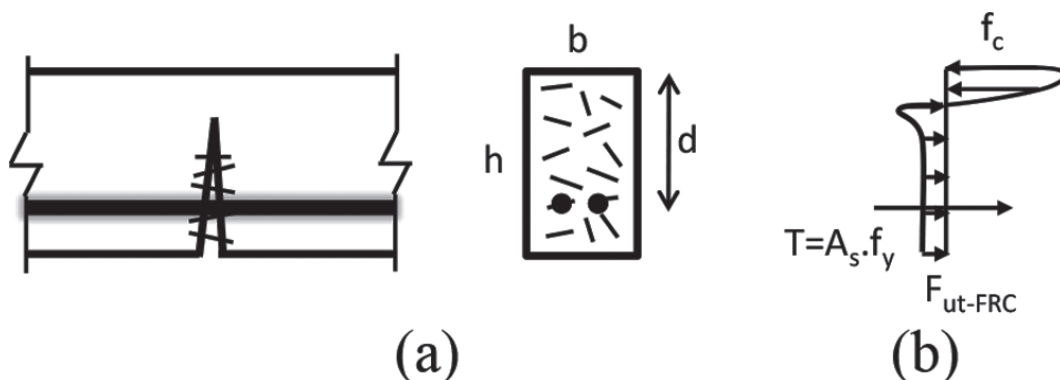


Ilustración 30.- ACI 544.4R - Fig. 4.7—Schematics of stress block for a cracked flexural member with hybrid reinforcement: (a) beam section; and (b) distribution of normal stresses and forces from fibers and reinforcing bar.



Cortante

[ACI 544.4R – 4.8 Design of FRC for shear]

The design aspects of FRC for shear in flexural members where longitudinal bars are used in conjunction with fibers as shear reinforcement are presented herein. The use of fibers as shear reinforcement in reinforced concrete beams has been the focus of several studies, as mentioned in 1.3.7.

Referring to the results of a full-scale study done by Parra-Montesinos (2006), ACI 318 recognizes the use of steel fibers as shear reinforcement in place of stirrups in flexural members with $f'_c < 6000$ psi (40 MPa) and maximum beam height of 24 in. (600 mm). According to ACI 318 Section R26.12.5, steel fibers should have an aspect ratio between 50 and 100 and provide a minimum $R_{T,150}^F$ of 75 percent when tested according to ASTM C1609/C1609M. The lower limit for the shear capacity provided by SFRC is $3.5\sqrt{f'_c}b_wd$ psi ($0.29\sqrt{f'_c}b_wd$ MPa) where b_w is the width and d is the effective height of the beam. Shoaib et al. (2014) showed that concrete beams with higher f'_c and greater overall height than ACI 318 limits and those that did not satisfy the $R_{T,150}^F$ criteria were able to provide a shear capacity of at least $2.0\sqrt{f'_c}b_wd$ psi ($0.17\sqrt{f'_c}b_wd$ MPa).

Model Code 2010 (fib 2013) Section 7.7.3.2 has summarized the shear design considerations for SFRC. For concrete members with conventional longitudinal reinforcement but without shear reinforcement, Eq. (4.8) may be used for calculating the shear capacity. According to this code, it is possible to eliminate minimum amount of conventional shear reinforcement (stirrups) if the ultimate tensile residual strength of FRC is sufficiently high—that is, $f_{ut-FRC} > (0.6) f_c^{(1/2)}$ psi ($f_c^{(1/2)}/20$ MPa). where $V_{FRC} > (\gamma_{min} + 0.15 \sigma_{cp})bd$, where $\gamma_{min} = 0.035ks^{(3/2)}f_c^{(1.2)}$.

In this equation, γ_c is concrete partial safety factor without fibers; ks is size effect factor and is equal to $1 + (8/d)^{(1/2)} \leq 2.0$ (in.-lb units) ($1 + (200/d)^{(1/2)} \leq 2.0$ [SI units]); ρ is longitudinal reinforcement ratio and is equal to $A_s/(b \cdot d)$; f_{tu-FRC} is the ultimate tensile residual strength of FRC; f_t and f_c are tensile and compressive strength values of plain concrete, respectively, and σ_{cp} is average normal stress acting on concrete cross section due to loading or prestressing. Note that ACI 318 has a more conservative approach and higher safety factors than Model Code 2010 (fib 2013) for these shear calculations.

$$V_{FRC} = 26.8x \left\{ \frac{0.18}{\gamma_c} k_s \left[100\rho \left(1 + 7.5 \frac{f_{ut-FRC}}{f_t} \right) f_c \right]^{\frac{1}{3}} + 0.15\sigma_{cp} \right\} bd \text{ (in - lb units)}$$



$$V_{FRC} = \left\{ \frac{0.18}{\gamma_c} k_s \left[100\rho \left(1 + 7.5 \frac{f_{ut-FRC}}{f_t} \right) f_c \right]^{\frac{1}{3}} + 0.15\sigma_{cp} \right\} bd \text{ (SI units)}$$

Altoubat et al. (2009) have shown that synthetic macrofibers can also provide the required shear capacity in flexural members when used at the proper dosage. More recently, Altoubat et al. (2016) investigated the use of synthetic macrofibers as the shear reinforcement in flexural members, showing that some of the existing empirical formulas (developed for steel fibers) overestimate the shear strength of FRC with synthetic fibers; however, the equations in Model Code 2010 (*fib* 2013) could be safely used for such a prediction.

Other shear capacity models have been proposed that may be suitable when the mechanical properties of FRC are available. Shoaib et al. (2012) developed a shear capacity model for members with hooked-end steel fibers that can account for the observed size effect in shear. Dinh et al. (2010) and others have also validated various shear capacity models.

For FRC members with both flexural and shear reinforcement, the contribution of fibers can be added (that is, $V_{HFRC} = V_s + V_{FRC}$).

Torsión

El código ACI no presenta recomendaciones específicas para el hormigón reforzado con fibras.

Fatiga

[ACI 544.1R – 2.2.3.3 Fatigue behaviour]

Experimental studies show that, for a given type of fiber, there is a significant increase in flexural fatigue strength with increasing percentage of steel fibers [2.31, 2.69-2.72]. The specific mix proportion, fiber type, and fiber percentage for an application in question should be compared to the referenced reports. Depending on the fiber type and concentration, a properly designed SFRC mixture will have a fatigue strength of about 65 to 90 percent of the static flexural strength at 2 million cycles when nonreversed loading is used [2.72, 2.73], with slightly less fatigue strength when full reversal of load is used [2.71].

It has been shown that the addition of fibers to conventionally reinforced beams increases the fatigue life and decreases the crack width under fatigue loading [2.70]. It has also been shown that the fatigue strength of conventionally reinforced beams made with SFRC increases. The resulting deflection changes accompanying fatigue loading also decrease [2.74]. In some cases, residual static flexural strength has been 10 to 30



percent greater than for similar beams with no fatigue history. One explanation for this increase is that the cyclic loading reduces initial residual tensile stresses caused by shrinkage of the matrix [2.75].

3.3.2. Estado Límite de Servicio

Fisuración

[ACI 544.4R – 5.7 Crack control and durability]

In many areas, the durability of concrete can be significantly improved by the use of fiber reinforcement (ACI 544.5R). Examples include plastic and restrained shrinkage cracking, which are primary problems that occur in concrete structures with a relatively large surface area such as walls, bridge decks, slabs, and overlays. These applications are susceptible to rapid changes in temperature and humidity, resulting in high water evaporation and high potential for shrinkage cracking. Fiber reinforcement has also been shown to improve the resistance of concrete in exposure to freezing-and-thawing cycles (Balaguru and Ramakrishnan 1986). Using macrofibers in concrete alters the crack widths and spacing that can positively affect the long-term durability.

Thin bridge deck overlays, marine and environmental structures, and tunnel linings are some of the applications where fiber reinforcement has successfully been used for improved crack control and enhanced durability (Zollo 1975). Cracks in properly designed fiber-reinforced concrete are typically much thinner than those in concrete reinforced with bars. Therefore, the rate of ingress for water and chemicals into concrete becomes much slower, resulting in a longer life span. Moreover, there exists a lot of research and practical experience showing significant reduction in crack width in environmental structures using hybrid reinforcement (bars plus fibers).

For concrete structures retaining water or exposed to external water, cracking is a major cause for reduction in serviceability due to the corrosion of steel reinforcement.

In particular, cracking has a significant effect on the durability in an environment with frequent freezing-and-thawing cycles. To ensure proper serviceability, cracking should be examined so that the flexural crack width is not greater than the allowable crack width. ACI 224R limits the allowable crack width to 0.012 in. (0.3 mm) for concrete structures exposed to soil. This value may vary for different applications in various environments. Serviceability limit state design has been discussed in detail for segmental tunnel lining by Bakhshi and Nasri (2015) using both fiber reinforcement and conventional reinforcement. Model Code 2010 (*fib* 2013), CNR-DT 204/2006 (National Research Council 2007), RILEM TC 162-TDF (2003), and DAfStb (2012) are among available references to calculate crack width in concrete sections reinforced by fibers without conventional reinforcement.



Compresión máxima

No se indican requisitos específicos para el hormigón con fibras.

3.3.3. Cuantías mínimas

Flexión

[ACI 544.4R – 4.9 Parametric-based design for FRC]

Equations to determine the moment-curvature relationship, ultimate moment capacity, and minimum flexural reinforcement ratio were explicitly derived (Mobasher et al. 2015b).

Figure 4.9b presents all three distinct material models used in the derivation of analytical expressions of moment-curvature and load-deflection of HRC beams, which include the interaction of compression and tension failure of FRC as well as failure by tension yielding of steel. The ultimate moment capacity as a function of residual tensile strength and reinforcement can be used as a convenient design tool for combinations of reinforcement, calculated as shown in

Eq. (4.9j). Using this equation, an analytical expression for minimum reinforcement ratio $\rho_{g,min}$ for conventional reinforced concrete is also obtained. For example, using parameters $\mu = 0$, $\gamma = 3/4$, and $\omega = 6$, Eq. (4.9k) is obtained with represents the minimum reinforcement as a function of depth location and its stiffness (steel or FRP).

$$M_n \approx m_{\infty} M_{cr} = \frac{6\rho_g n k (\mu\alpha - \mu + \alpha\omega) + 3\omega\mu - 3(\rho_g n k)^2}{\omega + \mu} M_{cr} \quad (4.9j)$$

$$\rho_{min} = \frac{9\alpha - \sqrt{81\alpha^2 - 6}}{2\alpha n k} \quad (4.9k)$$

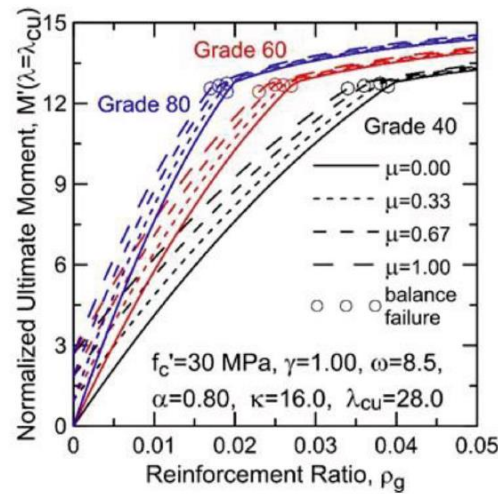


Ilustración 31.- ACI 544.4 - Fig. 4.9c Design chart for normalized ultimate moment capacity (determined at $\lambda = \lambda_{cu}$) for different levels of postcrack tensile strength μ and reinforcement ratio.

Figure 4.9c shows a design chart for the parametric design model with various grades of steel. Flexural design using this chart requires ultimate moment M_u due to factored loads normalized with respect to cross-sectional geometry.

For any combination of normalized residual tensile strength μ , grade of steel, and reinforcement ratio ρ_g , the allowable demand ultimate moment capacity M_u' is obtained from this chart. Results are then scaled to numerical values using the section cracking moment M_{cr} . An excel spreadsheet has been developed by Mobasher et. al (2015a) as a design guide for both the FRC and HRC. Several examples are presented in the following section.

Cortante

[ACI 544.4R – Design of FRC for shear]

According to this code, it is possible to eliminate minimum amount of conventional shear reinforcement (stirrups) if the ultimate tensile residual strength of FRC is sufficiently high—that is, $f_{ut-FRC} > (0.6) f_c (1/2)$ psi ($f_c (1/2)/20$ MPa).

Torsión

El código ACI no incluye indicaciones específicas de cuantías mínimas a torsión para el hormigón reforzado con fibras.



3.4. RILEM

3.4.1. Caracterización mecánica

[RILEM TC 162-TDF – σ - ϵ - DESIGN METHOD 1.Scope]

The design principles described in the following are based on the fracture mechanical approach known as the fictitious crack model, which relies on the so-called stress-crack opening relationship $\sigma_w(w)$ as the basic material input.

The design method is applicable for Steel Fibre Reinforced Concretes (SFRC) that exhibit *tension softening behaviour*. The method can also be used for other Fibre Reinforced Cementitious Composites (FRCC) that exhibit tension softening behaviour as well as plain concrete (which is assumed always to exhibit tension softening behaviour).

Módulo de elasticidad

[RILEM TC 162-TDF – σ - ϵ - DESIGN METHOD 2. Material Properties]

The compressive strength of steel fibre reinforced concrete (= SFR-concrete) should be determined by means of standard tests, either on concrete cylinders ($O = 150 \text{ mm}$, $h = 300 \text{ mm}$) or concrete cubes (side = 150 mm).

The design principles are based on the characteristic 28-day strength, defined as that value of strength below which more than 5% of the population of all possible strength determinations of the volume of the concrete under consideration, are expected to fall. Hardened SFR-concrete is classified in respect to its compressive strength by SFR-concrete strength classes which relate to the cylinder strength f_{ck} or the cube strength $f_{ck,cube}$ (Table 1). Those strength classes are the same as for plain concrete.

Table 1 – Steel fibre reinforced concrete strength classes: characteristic compressive strength f_{ck} (cylinders), mean $f_{ctm,fl}$ and characteristic $f_{ctk,fl}$ flexural tensile strength in N/mm^2 ; mean secant modulus of elasticity in kN/mm^2							
Strength class of SFR-concrete	C20/25	C25/30	C30/37	C35/45	C40/50	C45/55	C50/60
f_{ck}	20	25	30	35	40	45	50
$f_{ctm,fl}$	3.7	4.3	4.8	5.3	5.8	6.3	6.8
$f_{ctk,fl}$	2.9	3.4	3.9	4.3	4.7	5.1	5.5
E_{fcm}	29	30.5	32	33.5	35	36	37

Ilustración 32.- RILEM TC 162 - Modulus of elasticity

Coeficiente de Poisson

No recoge disposiciones específicas.



Tracción

[RILEM TC 162-TDF – σ - ϵ - DESIGN METHOD 3. Ultimate limit states]

The stresses in the steel fibre reinforced concrete in tension as well as in compression are derived from the stress-strain diagram shown in Fig. 2; and explained in appendix 1;

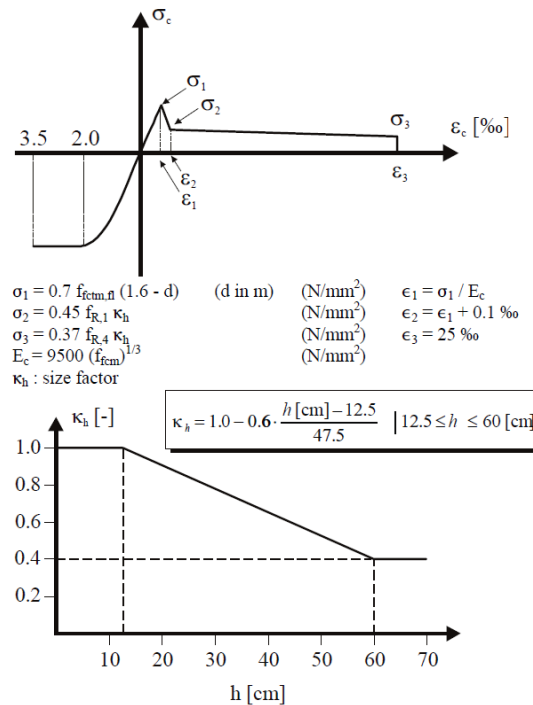


Ilustración 33.- RILEM TC 162 - Fig 2 Stress-strain diagram and size factor κ_h .

[RILEM TC 162-TDF – σ - ϵ - DESIGN METHOD Appendix 1]

The stresses σ_2 and σ_3 in the σ - ϵ -diagram are derived from the residual flexural tensile strength as explained below.

The residual flexural tensile strengths $f_{R,1}$ and $f_{R,4}$ are calculated considering a linear elastic stress distribution in the section [3] (Fig. 1.1a). However, in reality, the stress distribution will be different. To calculate a more realistic stress σ_f in the cracked part of the section, the following assumptions have been made (Fig. 1.1b): the tensile stress σ_f in the cracked part of the steel fibre concrete section is constant;

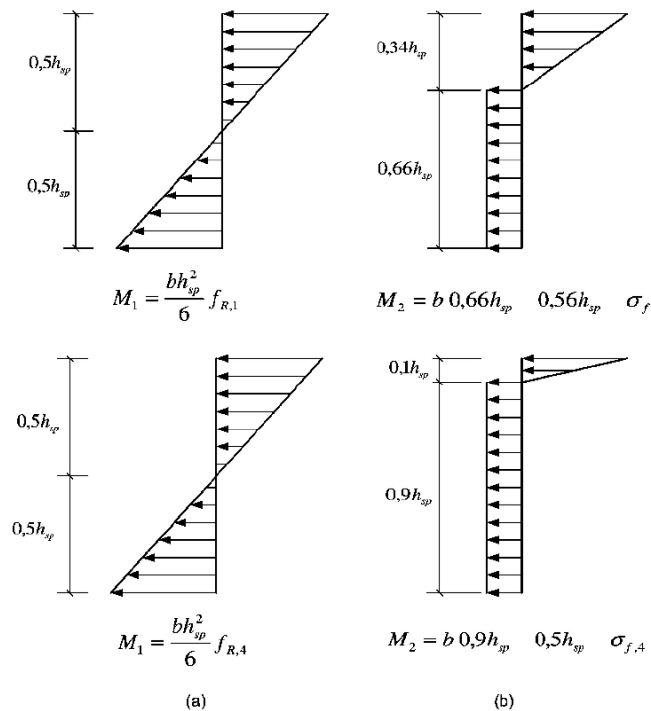


Ilustración 34.- RILEM TC 162 – Fig 1.1 Stress distribution

- the crack height is equal to $\pm 0.66 h_{sp}$ at $F_{R,1}$, to $\pm 0.90 h_{sp}$ at $F_{R,4}$ respectively.

Requiring $M_1 = M_2$, σ_f can then be expressed as:

$$\sigma_{f,1} = 0.45 f_{R,1}$$

$$\sigma_{f,4} = 0.37 f_{R,4}$$

[RILEM TC 162-TDF – Test and design methods for Steel fibre reinforced concrete – Bending Test]

This test method evaluates the tensile behaviour of steel fibre-reinforced concrete in terms of areas under the load-deflection curve obtained by testing a simply supported notched beam under three-point loading.

This test method is used for the determination of:

- the limit of proportionality (LOP), *i.e.* the stress which corresponds to the point on the load-deflection curve ($\Rightarrow F_u$) defined in point 5 as limit of proportionality;
- two equivalent flexural tensile strengths which identify the material behaviour up to the selected deflection. These equivalent flexural tensile strengths are determined according to point 5.



Besides the necessary measurement of the mid-span deflection (δ), opening displacement of the mouth of the notch (CMOD) is optional. The purpose of both measurements is to formulate in a later phase:

- a relation between crack mouth opening displacement and mid-span deflection;
- a relation between the stress-crack mouth opening displacement relationship, recorded during the bending test, on the one hand and the stress-crack width relationship, measured during a uniaxial tensile test, on the other.

The span length of the three-point loading test is 500 mm (Fig. 4).

The testing machine should be operated so that the measured net-deflection of the specimen at mid-span increases at a constant rate of 0.2 mm/min until the specified end-point deflection is reached. During testing the value of the load and net-deflection at mid-span ($\delta = (\delta_I + \delta_{II}) / 2$) are recorded continuously. The measurement of the crack mouth opening displacement is optional.

At least 3 specimens should be tested.

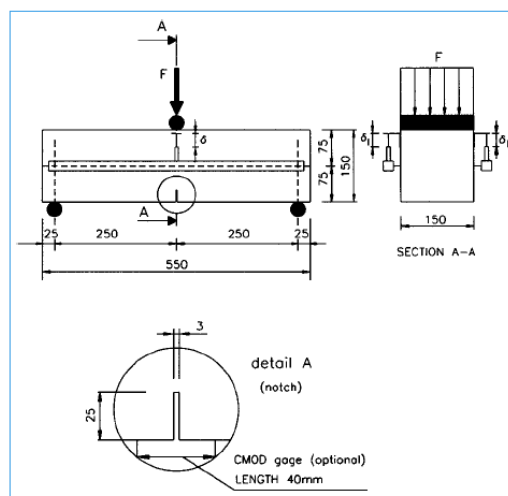


Ilustración 35.- RILEM TC 162-TDF – Fig. 4 Arrangement of displacement monitoring gauges

Compresión

Indicada en el apartado anterior.

3.4.2. Estado Límite Último

[RILEM TC 162-TDF – Design of steel fibre reinforced concrete using the σ -w method: principles and applications 4.5 Limit states (Ultimate limit state)]



In case of cross sections without conventional reinforcement the ultimate limit state in bending is determined simply by the ultimate load carrying capacity calculated according to the above-mentioned methods.

In the case of under-reinforced cross-section, the ultimate load carrying capacity is usually reached at onset of reinforcement yielding. Beyond that point, the member exhibits a softening that is governed by the amount of reinforcement and the fibre concrete properties. At yielding of the reinforcement the concrete in compression can be first assumed to behave linear elastically which enables the use of the methods presented in Section 4.3. The maximum stress level in the concrete can then be checked. If the assumption is shown to be appropriate, the ultimate strength of the cross section determined with the methods presented above is adequate. In cases where the assumption of a linear behaviour in compression is not valid, the non-linearity of the concrete in compression should be taken into account as specified by codes for normal reinforced concrete members.

[RILEM TC 162-TDF – σ - ϵ - DESIGN METHOD 3. Design at ultimate limit states]

In assessing the ultimate resistance of a cross section, the assumptions given below are used:

- plane sections remain plane (Bernoulli);
- the stresses in the steel fibre reinforced concrete in tension as well as in compression are derived from the stress-strain diagram shown in Fig. 2 and explained in appendix 1;
- the stresses in the reinforcement (bars) are derived from an idealised bi-linear stress-strain diagram;
- for cross sections subjected to pure axial compression, the compressive strain in the SFR-concrete is limited to -2‰. For cross sections not fully in compression, the limiting compressive strain is taken as -3.5‰. In intermediate situations, the strain diagram is defined by assuming that the strain is -2‰ at a level $\frac{3}{7}$ of the height of the compressed zone, measured from the most compressed face;
- for steel fibre reinforced concrete which is additionally reinforced with bars, the strain is limited to 25‰ at the position of the reinforcement (Fig. 3);

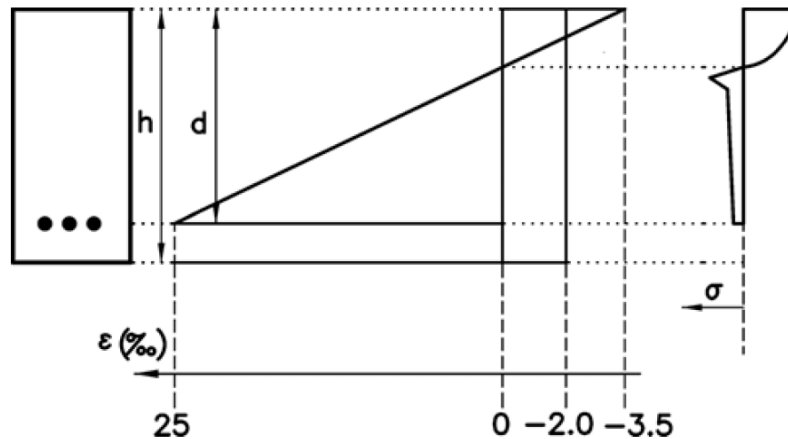


Ilustración 36.- RILEM TC 162 – Fig 3 Stress and strain distribution

- to ensure enough anchorage capacity for the Steel fibres, the maximum deformation in the ultimate limit state is restricted to 3.5 mm. If crack widths larger than 3.5 mm are used, the residual flexural tensile strength corresponding to that crack width and measured during the bending test has to be used to calculate σ_3 . It is recommended that this value, which replaces $f_{R,4}$, should not be lower than 1 N/mm²;
- in some cases, as mentioned below, the contribution of the steel fibres near the surface has to be reduced. For this reason the steel fibres should not be taken into account in a layer near the surface:
 - *for exposure class 2 (appendix 2):* if crack width is larger than 0.2 mm (serviceability limit states: see 4), the height of the cracked zone has to be reduced by 10 mm. This rule is only applicable in the ultimate limit state.
 - *for exposure classes 3 and higher:* special provisions have to be taken.

Flexión compuesta

No indica recomendaciones particulares para el hormigón con fibras.

Cortante

[RILEM TC 162-TDF – σ - ϵ - DESIGN METHOD – 3.2 Shear]

The calculation for shear shown here applies to beams and plates containing traditional flexural reinforcement (bar and mesh). It also applies to prestressed elements and columns in which axial compression forces are present. The approach proposed is the best possible until further evidence becomes available.

When no longitudinal reinforcement or compression zone is available, no generally accepted calculation method for taking into account the effect of the steel fibres can be formulated.



Bent-up bars shall not be used as shear reinforcement in beams except in combination with steel fibres and/or stirrups. In this case at least 50 % of the necessary shear reinforcement shall be provided by steel fibres and/or stirrups.

For shear design of members with constant depth, the member is assumed to consist of compressive and tensile zones of which the centres are separated by a distance equal to the internal lever arm z (Fig. 6). The shear zone has a depth equal to z and width b_w . The internal lever arm is calculated perpendicular to the longitudinal reinforcement by ignoring the effect of any bent-up longitudinal reinforcement.

The parameters given in Fig. 6 are:

α : the angle of the shear reinforcement in relation to the longitudinal axis ($45^\circ \leq \alpha \leq 90^\circ$)

θ : the angle of the concrete struts in relation to the longitudinal axis

F_s : tensile force in the longitudinal reinforcement (N)

F_c : compressive force in the concrete in the direction of the longitudinal axis (N)

b_w : minimum width of the web (mm)

d : effective depth (mm)

s : spacing of stirrups (mm)

z : the internal lever arm corresponding to the maximum bending moment in the element under consideration (mm) in a member with constant depth. In the shear analysis, an approximate value $z = 0.9 d$ can normally be used.

An example of the standard method, *i.e.*: $\theta = 45^\circ$, will be used for the shear analysis.

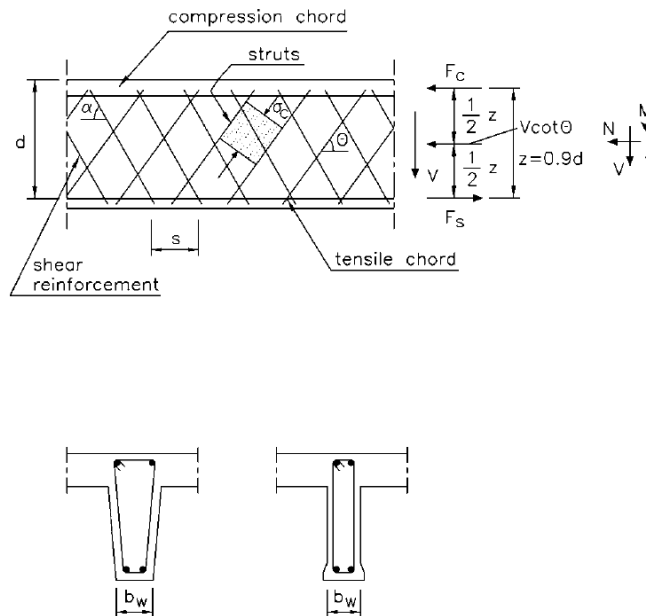


Ilustración 37.- RILEM TC 162 – Fig 6 Strut and tie model

Standard method

The design shear resistance of a section of a beam with shear reinforcement and containing steel fibres is given by the equation:

$$V_{Rd3} = V_{c,d} + V_{w,d} + V_{f,d}$$

With:

V_{cd} : the shear resistance of the member without shear reinforcement, given by:

$$V_{cd} = \left[0.12k(100\rho_l f_{ck})^{\frac{1}{3}} + 0.15\sigma_{cp} \right] b_w d \text{ (N)}$$

Where:

$$k = 1 + \sqrt{\frac{200}{d}} \text{ (d in mm) and } k \leq 2$$

$$\rho_l = \frac{A_s}{b_w d} \leq 2\%$$

A_s = area of tension reinforcement extending not less than "d + anchorage length" beyond the section considered (Fig. 7) (mm²).

b_w = minimum width of the section over the effective depth d (mm).



$$\sigma_{cp} = \frac{N_{sd}}{A_c} \text{ (N/mm}^2\text{)}$$

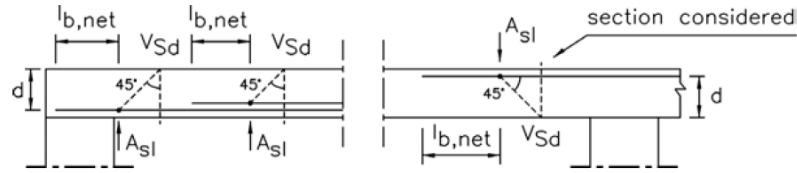


Ilustración 38.- RILEM TC 162 – Fig.7 ρ_l for V_{cd}

N_{sd} = longitudinal force in section due to loading or prestressing (compression: positive) (N). In the case of prestressing, “h” should be used instead of “d” in formula (11).

V_{fd} : contribution of the steel fibre shear reinforcement, given by:

$$V_{fd} = 0.7 k_f k_l \tau_{fd} b_w d$$

where:

k_f = factor for taking into account the contribution of the flanges in a T-section :

$$k_f = 1 + n \left(\frac{h_f}{b_w} \right) \left(\frac{h_f}{d} \right) \text{ and } k_f \leq 1.5$$

with

h_f = height of the flanges (mm)

b_f = width of the flanges (mm)

b_w = width of the web (mm)

$$n = \frac{b_f - b_w}{h_f} \leq 3 \text{ and } n \leq \frac{3b_w}{h_f}$$

$$k = 1 + \sqrt{\frac{200}{d}} \text{ (d in mm) and } k \leq 2$$

τ_{fd} = design value of the increase in shear strength due to steel fibres:

$$\tau_{fd} = 0.12 f_{Rk,4} \text{ (N/mm}^2\text{)}$$

V_{wd} : contribution of the shear reinforcement due to stirrups and/or inclined bars, given by:



$$V_{wd} = \frac{A_{sw}}{s} 0.9 d f_{ywd} (1 + \cot \alpha) \sin \alpha \quad (N)$$

s = spacing between the shear reinforcement measured along the longitudinal axis (mm)

α = angle of the shear reinforcement with the longitudinal axis

f_{ywd} = design yield strength of the shear reinforcement (N/mm²).

When checking against crushing at the compression struts, V_{Rd2} is given by the equation:

$$V_{Rd,2} = \frac{1}{2} v f_{cd} 0.9 d b_w (1 + \cot \alpha) \sin \alpha \quad (N)$$

With:

$$v = 0.7 - \frac{f_{fck}}{200} \geq 0.5 \quad (f_{fck} \text{ in N/mm}^2)$$

For vertical stirrups, or for vertical stirrups combined with inclined shear reinforcement, $\cot \alpha$ is taken as zero.

[RILEM TC 162-TDF – 6. SHEAR CAPACITY: ULTIMATE LIMIT STATE]

The shear capacity of FRC beams with conventional longitudinal reinforcing bars has been analyzed extensively in the literature [7] by considering the failure to occur due to crack propagation along known planes.

Only such cases will be considered in this section since there is no generally accepted method for the determination of the shear capacity of FRC elements without conventional reinforcement. The approach of [7] to calculate the contribution from the fibres is described in the following.

Following Eurocode 2, [10], the ultimate shear load carrying capacity V_{Rd3} is taken to be the sum of the contributions of the member without shear reinforcement $V_{c,d}$, of the stirrups and/or inclined bars, $V_{w,d}$, and the steel fibres $V_{f,d}$:

$$V_{Rd3} = V_{c,d} + V_{w,d} + V_{f,d}$$

The contributions of the member without shear reinforcement and the stirrups and/or inclined bars can be calculated according to Eurocode 2. See also [2].

Considering a rectangular cross-section with width b , effective depth d (distance from the top of the beam to the reinforcing bars) and inner lever arm $z = 0.9d$, see Fig. 17, the



fibre contribution $V_{f,d}$ is calculated from the design stress-crack opening relationship $\sigma_{w,d}(w)$ in the following way:

$$V_{f,d} = bz\sigma_{p,d}(w_m)$$

with:

$$\sigma_{p,d}(w_m) = \frac{1}{w_m} \int_0^{w_m} \sigma_{w,d}(u) du$$

The quantity is called the mean design residual stress at the crack width w_m and represents the mean value of the post-cracking stress between zero and w_m .

A definition of w_m is necessary to quantify the ultimate load-carrying capacity of the beam failing in shear. Experimental studies carried out with different geometries of steel FRC beams, reinforced with conventional longitudinal re-bars, have analyzed the onset of inclined cracks and the formation of concrete struts in compression [6]. According to the results, the spacing of these cracks is roughly equal to the inner lever arm of the beam and the ultimate crack opening is proportional to the height of the beam. Since the crack opening is controlled by the longitudinal reinforcement, it is proposed that the maximum crack opening be taken as:

$$w_m = \varepsilon_s Z$$

where ε_s is the strain of the longitudinal reinforcement. Since $V_{f,d}$ typically decreases with an increase in the maximum crack opening, the fibre contribution should be determined for a maximum allowable crack width. If the maximum strain in the longitudinal steel re-bar is taken to be 1%, then w_m should be taken as $0.009d$.

In order to obtain an equivalence relationship between conventional transverse reinforcement and fibres, we equate the contribution of $V_{w,d}$ to $V_{f,d}$ given in

Equation (61) to obtain an equivalent mean design residual stress, $\sigma_{p,d}^*(w_m)$:

$$\sigma_{p,d}^*(w_m) = \frac{V_{w,d}}{bz}$$

This implies that the equivalent mean residual stress of $\sigma_{p,d}^*(w_m)$ would yield the same load-carrying capacity as stirrups and/or inclined bars giving rise to $V_{w,d}$.

Furthermore, the equivalence in Equation (64) can be used to extend the definition of the minimum shear stirrup reinforcement given in the Eurocode 2 by:

$$\sigma_{p,d}^* + \rho_t f_{y,d} \geq 0.02 f_{c,d}$$



Where $f_{c,d}$ is the design compressive strength of the concrete, $f_{y,d}$ is the design yield strength of the stirrups and ρ_t is the area of stirrup reinforcement per unit length.

Torsión

No indica recomendaciones particulares para el hormigón con fibras.

Fatiga

No indica recomendaciones particulares para el hormigón con fibras.

3.4.3. Estado Límite de Servicio

[RILEM TC 162-TDF – σ - ϵ - DESIGN METHOD 4. Design at serviceability limit states]

When an uncracked section is used, the full steel fibre reinforced concrete section is assumed to be active and both concrete and steel are assumed to be elastic in tension as well as in compression.

When a cracked section is used, the steel fibre reinforced concrete is assumed to be elastic in compression, and capable of sustaining a tensile stress equal to $0.45 f_{R,1}$.

Fisuración

[RILEM TC 162-TDF – 4.5 Limit states (Serviceability limit state)]

The serviceability limit state defines a maximum crack opening depending on the exposure class of the construction. Limiting crack openings are suggested in [2]. Both the case of steel fibre reinforced concrete with and without conventional reinforcement are covered.

Code values may be adopted. Crack openings follow directly for the cross-sectional analysis described above.

[RILEM TC 162-TDF – σ - ϵ - DESIGN METHOD 4.2 Limit states of cracking]

In the absence of specific requirements (*e.g.* watertightness), the criteria for the maximum design crack width (w_d) under the quasi-permanent combination (***) of loads, which are mentioned in Table 3 for different exposure classes (see Appendix 2), may be assumed.



Tabla 3.- RILEM TC 162 – Table 3 Criteria for crack with

Table 3 - Criteria for crack width				
Exposure class (*)	Steel fibres	Steel fibres + ordinary reinforcement	steel fibres +	
			post-tensioning	pre-tensioning
1	(****)	(****)	0.2 mm	0.2 mm
2	0.3 mm	0.3 mm	0.2 mm	decompression (**)
3	Special crack limitations dependent upon the nature of the aggressive environment involved have to be taken.			
4				
5				

(*): see Appendix 2

(**): the decompression limit requires that, under the frequent combination (***) of loads, all parts of the tendons or ducts lie at least 25 mm within concrete in compression

(***): see ENV 1992-1-1 [1]

(****): for exposure class 1, crack width has no influence on durability and the limit could be relaxed or deleted unless there are other reasons for its inclusion.

[RILEM TC 162-TDF – σ - ϵ - DESIGN METHOD 4.4 Calculation of crack width]

Crack control is only possible if at least one of the conditions mentioned in 3.1.2 is satisfied. The calculation of the design crack width in steel fibre reinforced concrete is similar to that in normal reinforced concrete. However, it has to be taken into account that the tensile stress in steel fibre reinforced concrete after cracking is not equal to zero but equal to $0.45 f_{Rm,1}$ (constant over the cracked part of the cross section).

Formula (22) can be used to calculate the reinforcement A_{sr} (mm²) which satisfies the crack width limit.

With $\gamma_R = f_{yk} / \sigma_s = 1.4$ the crack width is approximately limited to 0.25 mm:

$$\frac{A_{sr}}{A_{ct}} = \frac{k_c k_p k f_{fct,ef} - \frac{0.45}{1.4} f_{Rm,1}}{\frac{f_{yk}}{1.4}}$$

In ordinary reinforced concrete, the following formula is used:

$$w_k = \beta s_{rm} \epsilon_{sm}$$

where:

w_k = the design crack width (mm)

s_{rm} = the average final crack spacing (mm)

ϵ_{sm} = the mean steel strain in the reinforcement allowed under the relevant combination of loads for the effects of tension stiffening, shrinkage, etc.



β = a coefficient relating the average crack width to the design value.

= 1.7 for load induced cracking and for restrained cracking in sections with a minimum dimension in excess of 800 mm.

= 1.3 for restrained cracking in sections with a minimum depth, breadth or thickness (whichever is the lesser) of 300 mm or below. Values for intermediate section sizes may be interpolated.

ε_{sm} may be calculated from the relation:

$$\varepsilon_{sm} = \frac{\sigma_s}{E_s} \left[1 - \beta_1 \beta_2 \left(\frac{\sigma_{sr}}{\sigma_s} \right)^2 \right]$$

where:

σ_s = the stress in the tensile reinforcement calculated on the basis of a cracked section (N/mm²).

σ_{sr} = the stress in the tensile reinforcement calculated on the basis of a cracked section under loading conditions causing first cracking (N/mm²).

β_1 = coefficient which takes account of the bond properties of the bars

= 1.0 for high bond bars

= 0.5 for plain bars

β_2 = a coefficient which takes account of the duration of the loading or of repeated loading

= 1.0 for single, short term loading

= 0.5 for a sustained load or for many cycles of repeated loading.

For members subjected only to intrinsic imposed deformations, σ_s may be taken as equal to σ_{sr} .

The average final crack spacing for members subjected principally to flexure or tension can be calculated from the equation:

$$s_{rm} = \left(50 + 0.25 k_1 k_2 \frac{\phi_b}{\rho_r} \right) \left(\frac{50}{L/\phi} \right) (\text{mm})$$

where:

$$50 / (L / \phi) \leq 1$$



ϕ_b = the bar size in mm. Where a mixture of bar sizes is used in a section, an average bar size may be used

k_1 = a coefficient which takes account of the bond properties of the bars;

$k_1 = 0.8$ for high bond bars and 1.6 for plain bars. In the case of imposed deformations, k_1 should be replaced by $k_1 \cdot k$, with k being defined in 4.3. Minimum reinforcement.

k_2 = a coefficient which takes account of the form of the strain distribution.

= 0.5 for bending and 1.0 for pure tension.

ρ_r = the effective reinforcement ratio, $A_s/A_{c,eff}$ where A_s is the area of reinforcement contained within the effective tension area $A_{c,eff}$. The effective tension area is generally the area of concrete surrounding the tension reinforcement of depth equal to 2.5 times the distance from the tension face of the section to the centroid of reinforcement [1].

L = length of steel fibre (mm)

ϕ = diameter of steel fibre (mm)

For steel fibre reinforced concrete, σ_s and σ_{sr} in (31) are calculated taking into account the postcracking tensile strength of the steel fibre reinforced concrete, i.e. $0.45 f_{Rm,1}$, in the cracked part of the section.

Compresión máxima

No indica recomendaciones particulares para el hormigón con fibras.

3.4.4. Cuantías mínimas

Flexión

[RILEM TC 162-TDF – σ - ϵ - DESIGN METHOD 4.3 Minimum reinforcement]

The following formula is proposed for calculating the minimum reinforcement A_s in order to obtain controlled crack formation:

$$A_s = (k_c k_k k_p f_{fct,ef} - 0.45 f_{Rm,1}) \frac{A_{ct}}{\sigma_s}$$

where:

$f_{Rm,1}$ = the average residual flexural tensile strength of the steel fibre reinforced concrete at the moment when a crack is expected to occur (N/mm²),



- A_s = area of reinforcement within tensile zone (mm²). If A_s is smaller than zero only steel fibres are necessary.
- A_{ct} = area of concrete within tensile zone (mm²). The tensile zone is that part of the section which is calculated to be in tension just before formation of the first crack.
- σ_s = the maximum stress permitted in the reinforcement immediately after formation of the crack (N/mm²). This may be taken equal to the yield strength of the reinforcement (f_{yk}). However, a lower value may be needed to satisfy the crack width limits.
- $f_{ct,ef}$ = the tensile strength of the concrete effective at the time when the cracks may first be expected to occur (N/mm²). In some cases, depending on the ambient conditions, this may be within 3 - 5 days from casting. Values of $f_{ct,ef}$ may be obtained from formula (1) by taking as f_{ck} the strength at the time cracking is expected to occur. When the time of cracking cannot be established with confidence as being less than 28 days, it is recommended that a minimum tensile strength of 3 N/mm² be adopted.
- k_c = a coefficient which takes account of the nature of the stress distribution within the section immediately prior to cracking. The relevant stress distribution is that resulting from the combination of effects of loading and restrained imposed deformations.

$k_c = 1$ for pure tension ($e = M/N = 0$)

$k_c = 0.4$ for bending without normal compressive force ($e = \infty$).

In the range between $e = 0$ and $e = \infty$:

* $e/h < 0.4$

$$k_c = \frac{1 + \frac{e}{0.4h}}{1 + \frac{6e}{h}}$$

* $e/h \geq 0.4$

$$k_c = \frac{1 + \frac{0.4h}{e}}{2.5(1 + \frac{h}{6e})}$$



k = a coefficient which allows for the effect of nonuniform self-equilibrating stresses. The value can be taken as 0.8 as a first approximation. For further details, see ENV 1992-1-1 [1].

k_p = a coefficient which takes account of the prestressing effect:

$$k_p = 1 - \frac{\alpha}{k_c} \left(1 - k_c + 2.4 \frac{e_v}{h} - 6 \frac{e_v k_c}{h} \right)$$

where:

α = the ratio of prestressing = $\frac{\sigma_{cp}}{k f_{ct,ef}}$

$$\sigma_{cp} = \frac{N_{sd}}{A_c} \text{ (N/mm}^2\text{)}$$

N_{sd} = prestressing force (N)

A_c = cross section of concrete (mm²)

e_v = the eccentricity of the prestressing force (mm)

if $e_v = 0$

$$k_p = 1 - \frac{\alpha}{k_c} (1 - k_c)$$

for pure bending ($k_c = 0.4$), it follows that:

$$k_p = 1 - 1.5\alpha$$

Cortante

No indica recomendaciones particulares para el hormigón con fibras.

Torsión

No indica recomendaciones particulares para el hormigón con fibras.



3.5. CNR

3.5.1. Caracterización mecánica

Módulo de elasticidad

[CNR-DT 204/2006 - 2.5 FIBER REINFORCED CONCRETE]

(1)P The physical and mechanical properties of the composite material depend on the proportions of the components as well as the properties of each component (cementitious matrix and fibers)

(2) The addition of fibers can improve the toughness, durability, impact resistance (resiliency), fatigue and abrasion resistance of the cementitious matrix.

(3) The mechanical properties of the fiber reinforced must be directly determined on specimens through standardized tests.

(2)P The minimum volume fraction of the fibers for structural applications must not be less than 0.3%

(4) Without specific tests, all the mechanical properties, not specified, can be assumed as those of ordinary concrete.

[CNR-DT 204/2006 - 2.5.2.4 Modulus of elasticity]

Modulus of elasticity is not generally affected by fibers, so it may be assumed equal to that of the matrix.

Coefficiente de Poisson

[CNR-DT 204/2006 - 2.5 FIBER REINFORCED CONCRETE]

(1)P The physical and mechanical properties of the composite material depend on the proportions of the components as well as the properties of each component (cementitious matrix and fibers)

(2) The addition of fibers can improve the toughness, durability, impact resistance (resiliency), fatigue and abrasion resistance of the cementitious matrix.

(3) The mechanical properties of the fiber reinforced must be directly determined on specimens through standardized tests.

(2)P The minimum volume fraction of the fibers for structural applications must not be less than 0.3%



(4) Without specific tests, all the mechanical properties, not specified, can be assumed as those of ordinary concrete.

Tracción

[CNR-DT 204/2006 – 2.5.2.2 Tensile behaviour]

(1)P Fibers improve the tensile behaviour of the cracked matrix, as schematically shown in Figure 2-1:

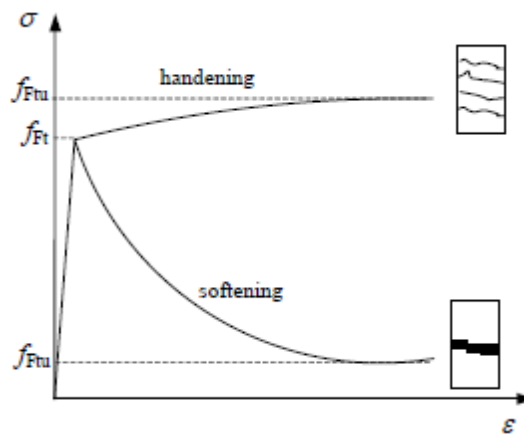


Ilustración 39.- CNR-DT 204/2006 - Figure 2-1-Tensile behaviour.

(2) For low fiber content (with volume fractions approx. lower than 2%), the behaviour is softening.

(3) For large fiber content (with volume fractions higher than 2%), the strength can be higher than the matrix one, since a hardening behaviour connected to multi-cracking phenomenon may occur (Figure 2-1).

(4) The uniaxial first crack tensile strength of fiber reinforced concrete, f_{Ft} , may be assumed equal to that of the matrix, f_{ct} . For softening behaviour material, the strength, f_{Ft} , may be assumed equal to the maximum stress (Figure 2-1).

(5) The residual uniaxial tensile strength of the material, f_{Ftu} (Figure 2-1), is significantly affected by the volume fraction of fibers, V_f , by the aspect ratio, l_f/d_f , as well as the bond between concrete and steel, for both the cases (softening and hardening behaviour).

This statement may be easily deduced from the equilibrium in the direction at right angle with the fracture surface, assuming fibers parallel to this direction and evaluating the pull-out specific force (Q) as:



$$Q = n_f \pi d_f l_b \tau_m = \omega \frac{V_f}{A_f} \pi d_f l_b \tau_m = \omega V_f \frac{l_f}{d_f} \tau_m$$

where:

- n_f is the number of fibers in the unit of fracture area;
- d_f is the equivalent diameter of the fiber;
- $l_b = l_f/4$ is the conventional bond length of every fiber;
- τ_m is the mean tangential bond stress
- ω is a coefficient taking into account the real orientation of the fibers;
- V_f is the volume fraction of the fibers;
- A_f is the area of the cross section of a single fiber.

The equation (1.1) provides an approximate value, since it does not take into account other factors, e.g. fiber shape, fiber-matrix interface, casting direction, mixing and compaction technique of the fresh concrete that affects fiber distribution and orientation in the matrix.

(6) As a result, a performance approach, able to experimentally identify the constitutive tensile curve by means of appropriate tests on fiber reinforced concrete specimens is suggested.

The nominal stress - crack opening law, σ_N - w , may be determined through uniaxial tension or bending tests.

The uniaxial tension test directly provides the σ - w law and may be performed in accordance to UNI 11188.

For softening behaviour material, the execution of this test is not simple. Thus, the bending test may be performed in accordance to UNI 11039 (Figure 2-2).

In this case, the nominal stress is evaluated assuming an elastic behaviour of the specimen (with reference to Figure 2-2: $\sigma_N = 6 \cdot P \cdot l / (b \cdot h^2)$).

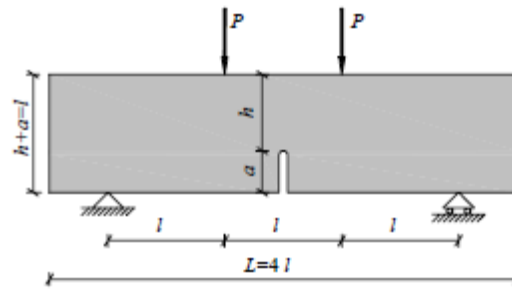


Ilustración 40.- CNR-DT 204/2006 - Figure 2-2 - Four point bending test as suggested in UNI 11039.

(7) The σ - w law, deduced from a bending test and carried out using the procedures reported in Appendix A, may be directly used to analyse structural elements subjected to bending.

For elements subjected to simple tension, the strength must be reduced through a coefficient equal to 0.7.

When a notched specimen has a hardening behaviour resulting from a bending test, the test must be repeated on an un-notched specimen in order to verify the real ductility.

The bending test on an un-notched specimen should also be performed on thin walled elements subjected to bending in order to take into account significant variables such as the casting direction, the mixing technique and the wall effect (Appendix A).

(8) The post-cracking strength may be defined on the basis of point values, f_i , corresponding to specified nominal value of crack opening, or on mean values, f_{eqi} , calculated for assigned intervals of crack opening (Figure 2-3). When a notched specimen is considered, the crack opening may be conventionally assumed equal to the displacement between two points at the notch tip, CTOD.

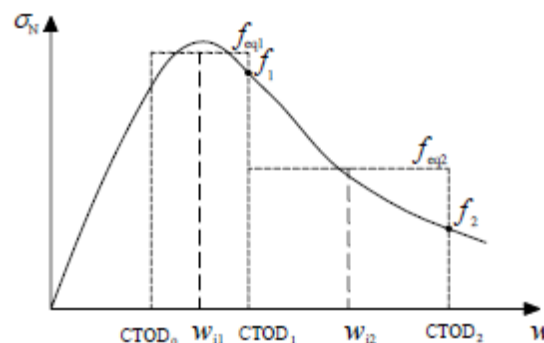


Ilustración 41.- CNR-DT 204/2006 - Figure 2-3 – Definition of point and mean residual strength

(9) Two simplified stress-crack opening constitutive laws may be deduced on the basis of the bending test results: a linear post-cracking behaviour (hardening or softening) or



a plastic rigid behaviour, as schematically shown in Figure 2-4. In the latter, f_{Fts} represents the serviceability residual strength, defined as the post-cracking strength for serviceability crack openings, whereas f_{Ftu} represents the ultimate residual strength.

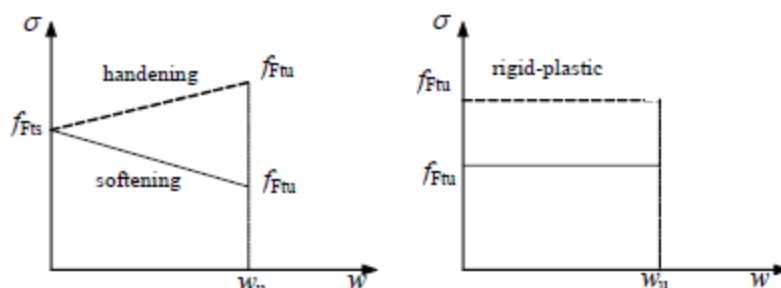


Ilustración 42.- CNR-DT 204/2006 - Figure 2-4 - Simplified constitutive laws: tension-crack opening.

(10) The stresses, f_{Fts} e f_{Ftu} , characterizing these two models may be evaluated through the procedure reported in Appendix A.

(11) When considering a softening behaviour materials, the ultimate crack opening value, w_u , of the constitutive law cannot be greater than the maximum value of 3 mm for elements subjected to bending, and 1.5 mm, for elements subjected to tension.

(12) When hardening behaviour materials are considered, and multi-cracking occurs, the identification of crack openings is not necessary because a stress-strain law may be directly used, as specified later.

(13) More complex alternative methods, suggested in literature, may be used provided that they are validated.

Compresión

[CNR-DT 204/2006 – 2.5.2.1 Compressive behaviour]

(1)P Fibers generally reduce the brittleness of the matrix, but they do not have significant effect on the compressive behaviour.

(2) In practice, the constitutive law of fiber reinforced concrete can be assumed equal to that of ordinary concrete.



3.5.1. Estado Límite Último

[CNR-DT 204/2006 – 3 DESIGN BASIC CONCEPTS AND SPECIAL PROBLEMS]

(1)P This chapter deals with fiber reinforced concrete (FRC) structures, either in the presence or without traditional reinforcement.

(2)P The design must fulfill resistance and serviceability requirements for the working life of the fiber reinforced concrete structures.

(3) For structural applications of FRC with softening behaviour, the following relationship must be fulfilled:

$$f_{Ftsk}/f_{ctk} > 0.2. (3.1)$$

(4) In all FRC structures the following condition has to be satisfied:

$$\alpha_u \geq 1.2 \cdot \alpha_1$$

where α_u is the maximum load and α_1 is the first cracking load (typical values of α_u and α_1 are shown in Annex D).

(5) Structural elements made of FRC can be cast without any traditional reinforcement. In the case of mono-dimensional elements, in addition to the limitations (3) and (4), the FRC adopted must have a hardening behaviour under tension, with the following restrictions:

- $(f_{Ftu}/f_{Fts})_k > 1.05$;
- $(f_{Ftu}/f_{Fts}) \geq 1$, with reference to the single test.

[CNR-DT 204/2006 – 3.5 CHARACTERISTIC VALUES OF MATERIAL STRENGTH]

(1) The characteristic value of the compressive strength of FRC (f_F) is to be determined in the same way as for the concrete matrix.

(2)P The characteristic value of the tensile strength of FRC (f_{Ftk}) is related, beyond to the results of tests on suitable specimens, to the structure.

(3) The characteristic value of the tensile strength of FRC (f_{Ftk}) can be determined from the mean value (f_{Ftm}) as follows:

$$f_{Ftk} = f_{Ftm} - \alpha \cdot k \cdot s,$$

where s is the standard deviation and k is a function of the number of specimens.



The α coefficient considers the effects of structural statical indeterminacy, as shown in Appendix D.

A typical value of α and k is shown in Appendix D.

[CNR-DT 204/2006 – 4.1 ULS FOR MONO-DIMENSIONAL ELEMENTS]

(1)P The ULS design requires the evaluation of the ultimate bending moment resistance as well as the comparison with the design value of the applied bending moment.

(2)P The fundamental hypotheses for the ULS analysis of FRC sections are:

- sections remain plane up to the ultimate state (to linear strain distribution);
- perfect bond between the rebars and the surrounding FRC;
- the stresses in the FRC are derived from the design stress/strain relationship given in §§ 2.5.2.2 and 2.5.2.3;
- the stress/strain relationships reinforcing or prestressing steel, if present, are derived from the current Codes.

(3)P The bending failure is considered when one of the following conditions is obtained:

- attainment of the maximum compressive strength, ϵ_{cu} , in FRC;
- attainment of the maximum tensile strength ϵ_{su} , in steel (if present);
- attainment of the maximum tensile strength, ϵ_{Fu} , in FRC.

When a FRC with a softening behaviour is considered, the maximum tensile strain, ϵ_{Fu} , shall be considered equal to 2%. The ultimate value of the crack opening, w_u , shall satisfy in all cases the limitation: $w_u = \epsilon_u \cdot l_{cs} \leq 3 \text{ mm}$.

The corresponding tensile stress value (in the post peak branch) shall be considered as the ultimate value of the residual tensile stress.

When a FRC with a hardening behaviour is considered, the maximum tensile strain, ϵ_{Fu} , shall be considered equal to 1%.



Flexión compuesta

[CNR-DT 204/2006 – 4.1.2 Bending with axial force]

(1) For a fixed value of the applied design axial force, N_{sd} , the ultimate bending moment, M_{Rd} , can be evaluated by means of the translation and rotation equilibrium equations.

(2) The evaluation of the ultimate moment can be carried out in reference to the strain and stress distributions shown in Figure 4-1, corresponding to the FRC stress/strain relationship reported in §§ 2.5.2.2 and 2.5.2.3 and reinforcement steel laws (if present) in accordance to the current Codes.

(3) With reference to the condition shown in Figure 4-1 and in accordance to Eurocode 2 (EC2) the evaluation of the ultimate moment for a given axial force can be made by adopting the simplified stress/strain relationship (that corresponds to the maximum compressive and post-peak tensile stress, see § 2.5.2.3), by verifying *a posteriori* so that the ultimate strains ϵ_{cu} , ϵ_{su} and ϵ_{Fu} are not violated and the collapse mechanism respected.

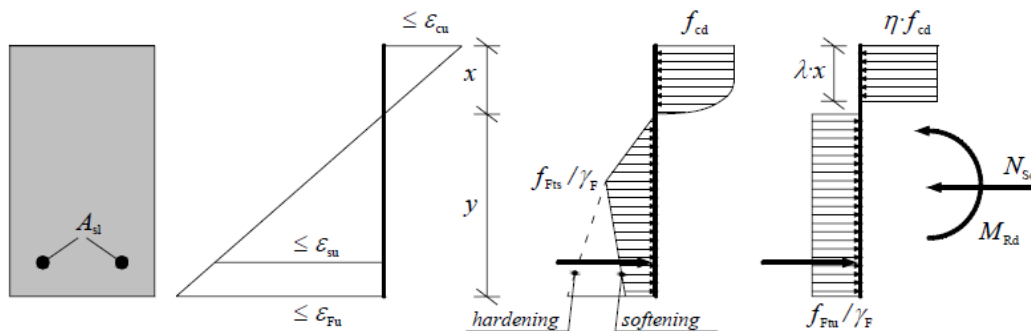


Ilustración 43.- CNR-DT 204/2006 - Figure 4-1 – ULS for bending moment and axial force: use of the simplified stress/strain relationship (stress-block with η e λ coefficient in accordance with EC2).

Cortante

[CNR-DT 204/2006 – 4.1.3 Shear]

General

For the ULS verification of the shear resistance, the mono-dimensional members (beams) shall satisfy the prescriptions given in the following.

Members without design shear and conventional longitudinal reinforcement

(1)P When FRCs with hardening tensile behaviour are used and members without both longitudinal and transverse reinforcement are considered, the principal tensile stress, σ_1 , shall not be greater than the design tensile strength:



$$\sigma_1 \leq \frac{f_{Ftuk}}{\gamma_F}$$

(2)P In members without either longitudinal or transverse reinforcement, FRCs with softening behaviour shall not be used.

Members without design shear reinforcement, with conventional longitudinal reinforcement

(1)P The design value for the shear resistance in members with conventional longitudinal reinforcement and without shear reinforcement is given by:

$$V_{Rd,F} = \left\{ \frac{0.18}{\gamma_c} k \left[100 \rho_l \left(1 + 7.5 \frac{f_{Ftuk}}{f_{ctk}} \right) f_{ck} \right]^{\frac{1}{3}} + 0.15 \sigma_{cp} \right\} b_w d \text{ (stresses in MPa)}$$

where:

- γ_c is the partial safety factor for the concrete matrix without fibers;
- k is a factor that takes into account the size effect and equal to $1 + \sqrt{\frac{200}{d}} \leq 2.0$
- d is the effective depth of the cross section;
- ρ_l is the reinforcement ratio for longitudinal reinforcement and equal to $\rho_l = A_{sl}/b_w d \leq 0.02$;
- A_{sl} is the cross sectional area of the reinforcement which is bonded beyond the considered section;
- f_{Ftuk} is the characteristic value of the ultimate residual tensile strength for the FRC, by considering $w_u = 1.5$ mm (see Appendix A);
- f_{ctk} is the characteristic value of the tensile strength for the concrete matrix in accordance to the current Codes;
- f_{ck} is the characteristic value of cylindrical compressive strength in accordance to the current Codes;
- $\sigma_{cp} = N_{Ed}/A_c$ is the average stress acting on the concrete cross section, A_c , for an axial force N_{Ed} due to loading or prestressing actions (shall be considered positive compression stresses);
- b_w is the smallest width of the cross-section in the tensile area.



The shear resistance $V_{Rd,F}$, is assumed not to be less than the minimum value, $V_{Rd,Fmin}$, defined as:

$$V_{Rd,Fmin} = (v_{min} + 0.15 \cdot \sigma_{cp}) \cdot b_w \cdot d$$

where v_{min} is a coefficient equal to $0.035k^{3/2}f_{ck}^{1/2}$.

(2) For members with loads applied on the upper side within a distance $0.5d \leq a \leq 2d$ from the edge of a support (or centre of bearing where flexible bearings are used), the acting shear force may be reduced by $\beta = a/(2 \cdot d)$. This is only valid provided that the longitudinal reinforcement is fully anchored at the support. For $a \leq 0.5d$ the value $a = 0.5d$ should be used.

(3) When point loads close to the support or in diffusive regions are present, the verification can be carried out with *strut-and-tie* models.

The maximum shear resistance shall not be greater than the maximum shear force which can be sustained by the member, limited by the crushing of the compression struts., $V_{Rd,max}$, defined in the following § 4.1.3.4 in Eq. 3.15.

Members with shear and longitudinal conventional reinforcement

(1) The ultimate shear resistance, V_{Rd} , for FRC members with transverse reinforcement can be evaluated as the sum of a contribution due to the web reinforcement, $V_{Rd,s}$, and a contribution due to the fiber reinforcement, $V_{Rd,F}$:

$$V_{Rd,s} = V_{Rd,s} + V_{Rd,F}$$

$V_{Rd,s}$ can be evaluated as:

$$V_{Rd,s} = \frac{A_{sw}}{s} z f_{ywd} (\cot \varphi + \cot \theta) \sin \varphi$$

where:

- θ is the angle between the concrete compression strut and the beam axis perpendicular to the shear force, equal to 45° if prestressing action is not present;

- ψ is the angle between shear reinforcement and the beam axis perpendicular to the shear force

- z is the inner lever arm, for a member with constant depth, corresponding to the bending moment in the element under consideration. In the shear analysis of reinforced concrete without axial force, the approximate value $z = 0.9d$ may be used;

- A_{sw} is the cross-sectional area of the conventional shear reinforcement;



- s is the spacing of the conventional shear reinforcement;
- f_{ywd} is the design yield strength of the shear reinforcement.

In Equation (4.5), the cross-sectional area of the conventional shear reinforcement, A_{sw} , shall not be greater than:

$$A_{sw,max} \leq \frac{0.5v f_{cd} \sin \varphi}{1 - \cos \varphi} \frac{b_w s}{f_{ywd}}$$

where v a strength reduction factor for concrete cracked in shear, that can be assumed equal to:

$$v = 0.6 \left(1 - \frac{f_{ck}}{250} \right) [f_{ck} \text{ in MPa}]$$

In all cases, the maximum shear resistance shall not be greater than the maximum shear force which can be sustained by the member, limited by the crushing of the compression struts., $V_{Rd,max}$, defined as:

$$V_{Rd,max} = \frac{b_w z v f_{cd} (\cot \varphi + \cot \theta)}{(1 + \cot^2 \theta)}$$

Torsión

[CNR-DT 204/2006 – 4.1.4 Torsion]

Members without torsional longitudinal and transverse conventional reinforcement

(1)P When FRCs with hardening tensile behaviour are used and members without longitudinal rebars and transverse reinforcement are considered, the principal tensile stress, σ_1 , shall not be greater than the design tensile strength:

$$\sigma_1 \leq \frac{f_{Ftuk}}{\gamma_F}$$

Members with torsional longitudinal and transverse conventional reinforcement

(1) When members with longitudinal rebars and transverse reinforcement are considered, the contribution of fiber reinforcement can be taken into account based on adequate models.



Fatiga

[CNR-DT 204/2006 – 2.5 FIBER REINFORCED CONCRETE]

The addition of fibers can improve the toughness, durability, impact resistance (resiliency), fatigue and abrasion resistance of the cementitious matrix.

3.5.2. Estado Límite de Servicio

Fisuración

[CNR-DT 204/2006 – 5.2 CRACK WIDTH]

(1) The characteristic crack width w_k , in FRC elements can be evaluated by using the following relationship:

$$w_k = \beta \cdot s_{rm} \cdot \epsilon_{sm}$$

where:

- s_{rm} is the average crack spacing, evaluated with equation (2.4);
- ϵ_{sm} is the mean strain in the reinforcement under the relevant combination of loads, including the effect of imposed deformations, taking into account the effects of tension stiffening (in accordance with the current Codes);
- β is a coefficient that correlates the average crack width with the value calculated according to the current Codes for the concrete matrix (without fiber reinforcement).

(2) For the evaluation of ϵ_{sm} , FRC tensile strength can take into account and a constant stress distribution over the cross section equal to f_{Ftsk} can be rounded.

Compresión máxima

[CNR-DT 204/2006 – 5.1 STRESS VERIFICATION]

5.1 STRESS VERIFICATION

(1) The compressive stresses at SLS shall be limited in accordance to the current Codes.

(2) When structural elements with softening FRCs are considered, the verification of the tensile stresses is satisfied if the element is verified at ULS.

(3) When structural elements with hardening FRCs are considered, the tensile stresses verification shall be done by imposing the limitation:

$$\sigma_t \leq 0.6 \cdot f_{Ftuk}.$$



$*f_{Ftuk}$ is the characteristic value of the ultimate residual tensile strength for the FRC by considering $w_u = 1.5 \text{ mm}$

3.5.3. Cuantías mínimas

Flexión

[CNR-DT 204/2006 – 5.3 MINIMUM REINFORCEMENT FOR CRACK CONTROL]

(1) For cracking control in the elements under bending, a minimum reinforcement should be present, its area should be present and greater than:

$$A_{s,min} = (k_c k_s k_p f_{ctm} - f_{Ftsm}) \frac{A_{ct}}{\sigma_s}$$

where:

- f_{ctm} is the average value of the tensile strength of the concrete matrix;
- f_{Ftsm} is the average value of the residual strength of the FRC;
- A_{ct} is the tensile part of the concrete cross section, evaluated by considering a stress field at the elastic limit;
- σ_s is the maximum tensile stress in the reinforcement after cracking, that can be considered equal to the yielding stress of the steel;
- k_c, k_s, k_p are correction coefficients in accordance to EC2.

(2) When the value of $A_{s,min}$ obtained by Eq. 4.27 is negative, the minimum reinforcement can be provided by fibers only.

Cortante

[CNR-DT 204/2006 – 4.1.3.5 Minimum shear reinforcement]

(1) It is possible to avoid the presence of conventional shear reinforcement (stirrups) if the following limitation is respected:

$$f_{Ftuk} \geq \frac{\sqrt{f_{ck}}}{20} [f_{ck} \text{ in MPa}]$$

This limitation allows limiting the development and the diffusion of the inclined cracking and, as a consequence, can ensure a sufficient member ductility.

(2) When the above-mentioned limitation is violated, a conventional shear reinforcement (stirrups) shall be introduced, sufficient to ensure an ultimate shear resistance greater than the first cracking one, V_{cr} :



$$V_{cr} = 0.67 \cdot f_{ctk} \cdot b_w \cdot d.$$

The part of the shear resistance due to the shear reinforcement is equal to the difference:

$$V_{Rds,min} = V_{cr} - V_{Rd,F}.$$

(3) The longitudinal spacing between the shear reinforcements (stirrups), s , shall not exceed the value $0.8 \cdot d$.

(4) When a great amount of longitudinal reinforcement in the compressive zone is present, adequate stirrups reinforcement shall be applied in order to prevent rebar instability.

Torsión

No se proporcionan indicaciones específicas para la cuantía mínima de torsión en hormigón con fibras.



3.6. JSCE

The name “High Performance Fiber Reinforced Cement Composites” comes from the excellent performance under tensile loading conditions. It is also known as “Strain Hardening Cement-based Composites” (SHCC) due to the tensile strain-hardening properties. “Engineered Cementitious Composites” (ECC) are typical examples of the same type of material. [10]

HPFRCC is a composite material comprising a cement-based matrix and short reinforcing fibers and is a highly ductile material exhibiting multiple fine cracks and pseudo strain-hardening characteristics under uniaxial tensile stress. [10]

3.6.1. Caracterización mecánica

Módulo de elasticidad

[JSCE – 3.4 Young’s modulus]

In principle, Young’s modulus of HPFRCC shall be derived from JIS A 1149 “Method of Test for static modulus of elasticity of concrete”.

[Commentary] Young’s modulus of HPFRCC can be obtained by adopting the testing method used for ordinary concrete. The Young’s modulus thus obtained takes a smaller value, i.e. between 1/2 and 2/3 or so of that for ordinary concrete. Fig. 3.4.1 shows an example of relationship between Young’s modulus and compressive strength expressed in measured values.

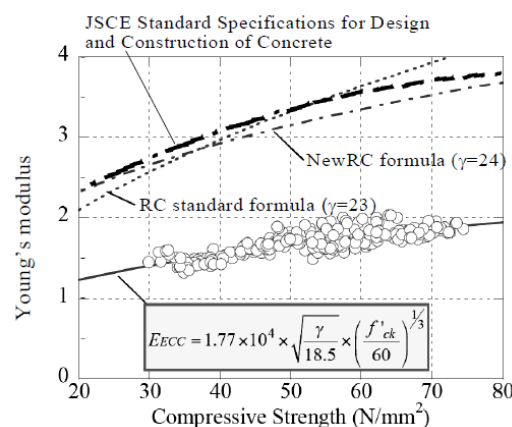


Ilustración 44.- JSCE - Fig 3.5.1 Example of determination of Young's modulus

Coeficiente de Poisson

[JSCE – 3.5 Poisson’s ratio]



Poisson's ratio of HPFRCC shall be determined based on experiments or on existing data.

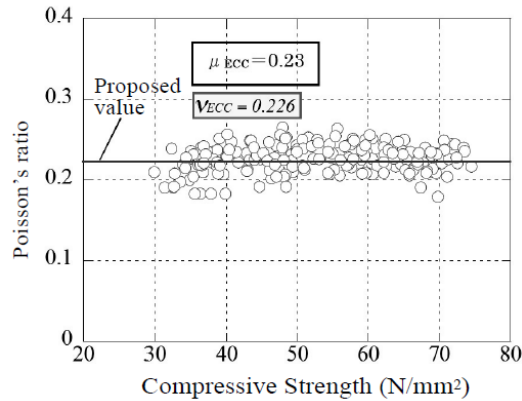


Ilustración 45.- JSCE - Fig 3.5.1 Example of determination of Poisson's ratio

[Commentary] Fig. 3.5.1 is an example of the measured Poisson's ratio of HPFRCC. As shown in the figure, the Poisson's ratio of HPFRCC is slightly higher than that of ordinary concrete, yielding an average value of 0.226. Values listed in the *List of Characteristics Values for HPFRCC Products* of appendix I-1 can also be used.

Tracción

[JSCE – 3.3.1 Tensile stress-strain curve]

(1) Tensile stress-strain curve of HPFRCC shall be determined through an appropriate test method. According to the limit state in question, an appropriate shape can be assumed based on the reliable past data.

(2) The tensile stress-strain curve shown in Fig. 3.3.1 can be used when studying the ultimate limit state of section fracture for members subjected to a bending moment or a bending moment and axial forces.

(3) The tensile stress-strain curve shown in Fig. 3.3.1 can be used for serviceability verification.

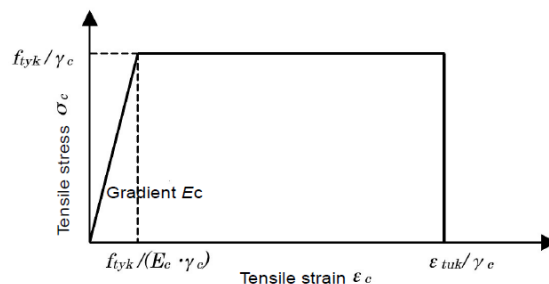


Ilustración 46.- JSCE - Fig 3.3.1 Tensile stress-strain relationship



[Commentary] When representing the tensile stress-strain curve of HPFRCC with a simple approximation, it was possible to achieve the same level of conformity as that for ordinary RC members through the use of a perfect elastoplastic model that has the tensile yield strength at the peak as illustrated by the broken line in Fig. 3.3.1. For this reason, this “Recommendations” document adopts a perfect elastoplastic model that uses the characteristic values of tensile yield strength divided by the material safety factor, as denoted by a solid line in the figure.

The ultimate strain of HPFRCC is normally greater than the yield strain of the reinforcing bar and the strain of the tensile steel bar reaches yield strain before HPFRCC reaches its ultimate strain. Thus the effect of the ultimate strain value of HPFRCC on the cross-sectional strength is estimated negligible. In the analytical result mentioned above, a model that assumes the tensile yield strength can be maintained even if it exceeds the ultimate strain of 1.3 percent (0.0013) obtained from a material test gives a HPFRCC’s tensile strain of 1.7 percent (0.017) showing good agreement with that of experiments. Therefore, the characteristic value of ultimate tensile strain as shown in 3.2.4 of this “Recommendations” document can be regarded as the ultimate strain. When the design cross-sectional strength is underestimated in analysis, the tensile stress-strain relation should be appropriately reevaluated. Also the failure mode needs to be confirmed with a model that appropriately reflects the stress-strain relation of HPFRCC.

Compresión

[JSCE – 3.3.2 Compressive stress-strain curve]

(1) The compressive stress-strain curve of HPFRCC shall in principle be determined through an appropriate test. An appropriate shape of compressive stress-strain curve can be assumed according to the nature of the ultimate state based on the reliable past data.

(2) The compressive stress-strain curve like the one shown in Fig. 3.3.2 may be used when studying the ultimate limit state of section failure for the members subjected to a bending moment or a bending moment and axial compressive forces. ϵ'_m and ϵ'_{cu} can be determined based on appropriate tests. The following stress-strain equation can be applied for the initial curved zone.

$$\sigma'_c = 0.85 f'_{ck} / \gamma_c \times \epsilon'_c / \epsilon'_m \times (2 - \epsilon'_c / \epsilon'_m)$$

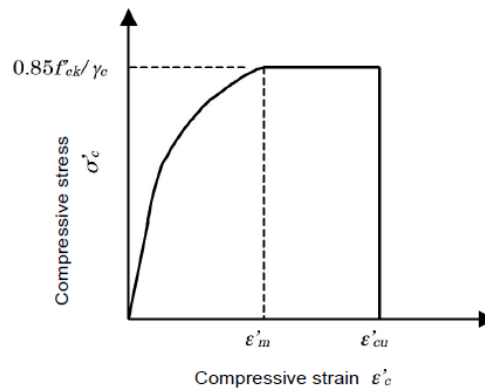


Ilustración 47.- JSCE - Fig 3.3.2 Compressive stress-strain relationship

(3) The compressive stress-strain relationship can be regarded as linear when serviceability performance is verified. Young's modulus can be determined according to section 3.4.

(4) Evaluation of the compressive stress-strain relationship under biaxial or triaxial stresses shall take into account the effects of multi-axial stress conditions where necessary when verifying safety or serviceability performance. The material shall be assumed as linear-elastic for examination of the serviceability limit state, and Young's modulus and Poisson's ratio can be set at values specified in sections 3.4 and 3.5, respectively.

[Commentary] (2) An example of compressive stress-strain relationship, which is derived from the results of tests on cylinder specimens of 100 mm in diameter and 200 mm in height, is shown in Fig. 3.3.2. As shown in the figure, the strain value at the maximum load is 0.4% (0.004) approximately. In the compressive stress-strain relationship shown in Fig. 3.3.2, the strain ϵ'_m at the peak stress is greater than 0.002, i.e. that of ordinary concrete. This shows one of the characteristics of HPFRCC; the stress decreases slowly with increasing strain after the maximum load thanks to the confinement effect by fiber bridging.

To take into account these HPFRCC material characteristics in structural design, it is necessary to determine the stress-strain relation on the basis of flexural tests of HPFRCC. However, when appropriate test data are not available, ϵ'_m can be the strain at the maximum compressive stress, and ϵ'_{cu} can be set equal to ϵ'_m .

(4) ϵ'_m and ϵ'_{cu} in the compressive stress-strain relation of HPFRCC are subjected to the surrounding restraint as in normal concrete and hence should be determined taking into account the restraint at working positions.



3.6.2. Estado Límite Último

Flexión compuesta

(1) For a member subjected to axial compressive force, the upper limit for axial compressive capacity N'_{oud} shall be calculated by Eq.(6.2.1) .

$$N'_{oud} = (k_1 f'_{cd} A_c + f'_{yd} A_{st}) / \gamma_b \quad (6.2.1)$$

where

A_c : cross-sectional area of HPFRCC,

f'_{cd} : design compressive strength of HPFRCC

A_{st} : total cross-sectional area of longitudinal reinforcing steel

f'_{yd} : design compressive yield strength of longitudinal reinforcing steel

k_1 : strength reduction factor ($1 - 0.003 f'_{ck} \leq 0.85$ with $f'_{ck} \leq 80$ N/mm²)

f'_{ck} : characteristic value of compressive strength of HPFRCC (N/mm²)

γ_b : member factor; which may generally be taken as 1.3.

(2) Assumptions set out in (i), (ii) and (iii) below shall be followed when calculating the design capacity of a member subjected to bending moment and axial force, with regard to either the member's cross-section or unit width depending on the direction or the stress resultant. In such a case, the member factor γ_b may generally be taken as 1.1.

(i) Fiber strain is proportional to the distance from the neutral axis.

(ii) Stress-strain curve of HPFRCC follows that given in section 3.3 when the design tensile yield strength f'_{tyd} is greater than 1.5 N/mm². Tensile stress of HPFRCC is neglected if f'_{tyd} is smaller than 1.5 N/mm².

(iii) Stress-strain curve of steel reinforcement follows that given in section 3.3.3 "Stress-strain relationship" of Standard Specifications for Concrete Structures – *Structural Performance Verification*.

[Commentary] (1) Where a member subjected to axial compressive force has a small M_d/N'_d , the load-bearing capacity is considerably decreased by a slight increase in bending moment, due to the resulting increase in eccentricity, which might be caused



during the construction process for example. To exclude such cases, the design compressive capacity is given an upper limit, where the member factor is taken as 1.3.

(2) HPFRCC is a highly ductile material exhibiting pseudo-strain hardening characteristics under uniaxial tensile stress and can bear part of the tensile forces in a stable manner. The contribution of tensile stress of HPFRCC to the capacity of member cross section is taken account in the verification of safety. However, when the tensile yield strength of HPFRCC is small, the contribution to the capacity of member cross section is found to be small by experiment. Thus, tensile stress of HPFRCC can be considered only in the case that the design tensile yield strength f_{tyd} is greater than 1.5 N/mm². The strain and stress distributions are schematically represented by Fig. 6.2.1.

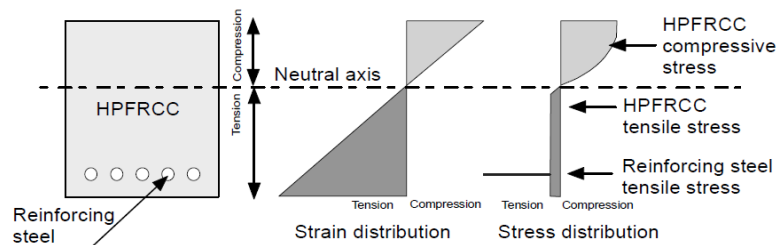


Ilustración 48.- JSCE - Fig. 6.2.1 Schematic representations of strain and stress distributions

Derived from Standard Specifications, the bending capacity calculation method described here has already been verified. Thus, member coefficient ϕ_b is taken as 1.1 as prescribed in the Standard Specifications.

Figure 6.2.3 shows the results of a verification study on the bending capacity calculation method, applying HPFRCC to the 70-mm tensile-side portion of the member with a total thickness of 180mm, tied with truss reinforcements (Fig. 6.2.2). It has been confirmed that the test results (“ECC-measured” in Fig. 6.2.3) can be evaluated by analysis based on assumptions (i), (ii) and

(iii) (“HPFRCC-analysis” in the same figure). The same figure also shows the results of a reinforced concrete structure made solely of ordinary concrete, i.e. without HPFRCC (“RC-measured” in the same figure). It shows that the HPFRCC specimens exert greater bending capacity thereby confirming the reinforcement effects of HPFRCC.

Cortante

[JSCE – 6.3 Examination of safety against shear forces]

Except otherwise specified in this Chapter, follow section 6.3 “Shear” of Standard Specifications for Concrete Structures–*Structural Performance Verification*.



The design shear capacity of a linear member consisting solely of HPFRCC and reinforcing steels V_{yd} may be obtained by Equation (6.3.1) below.

$$V_{yd} = V_{cd} + V_{sd} + V_{fd} + V_{ped}$$

where V_{cd} : design shear capacity of a linear member without any shear reinforcing steels, excluding the strength exerted by reinforcing fiber, which is given by Equation (6.3.2) below.

$$V_{cd} = \beta_d \beta_p \beta_n f_{vcd} b_w d / \gamma_b$$

where

$$f_{vcd} = 0.7 \times 0.20 \sqrt[3]{f'_{cd}} (N/mm^2), \text{ where } f_{vcd} \leq 0.50 N/mm^2$$

$$\beta_d = \sqrt[4]{1/d} (d: m); \quad \text{when } \beta_d > 1.5, \beta_p \text{ is taken as } 1.5$$

$$\beta_p = \sqrt[3]{100 p_w}; \quad \text{when } \beta_p > 1.5, \beta_p \text{ is taken as } 1.5$$

$$\beta_n = 1 + \frac{M_0}{M_d}; (N'_d \geq 0) \quad \text{when } \beta_n > 2, \beta_n \text{ is taken as } 2$$

$$\beta_n = 1 + 2 \frac{M_0}{M_d}; (N'_d < 0) \quad \text{when } \beta_n < 0, \beta_n \text{ is taken as } 0$$

N'_d : design axial compressive force

M_d : design bending moment

M_0 : bending moment necessary to cancel stress due to axial force at extreme tension fiber corresponding to design bending moment M_d .

b_w : width of web

d : effective depth

$$p_w = A_s / (b_w d)$$

A_s : cross-sectional area of tensile reinforcement

f'_{cd} : design compressive strength of concrete, in units of N/mm^2

γ_b : generally = 1.3 d

V_{sd} : design shear capacity of shear reinforcement, given by Equation (6.3.4) below.



$$V_s = \left[\frac{A_w f_{wyd} (\sin \alpha_s + \cos \alpha_s)}{s_s} \right] \frac{z}{\gamma_b}$$

A_w : total cross-sectional area of the shear reinforcing steel placed at spacing s_s

f_{wyd} : design yield strength of the shear reinforcing steel, 400N/mm² or less

α_s : angle of the shear reinforcing steel to the member axis

s_s : spacing of shear reinforcing steel

z : distance from location of compressive stress resultant to centroid of tensile steel, may generally be taken as $d/1.15$

γ_b : 1.10 in general

V_{fd} : design shear capacity of reinforcing fiber, given by Equation (6.3.5)

$$V_{fd} = (f_{vd} / \tan \beta_u) \cdot b_w \cdot z / \gamma_b \quad (6.3.5)$$

f_{vd} : design tensile yield strength of HPFRCC, $f_{vd} = 0$ when f_{vd} is smaller than 1.5N/mm².

β_u : angle of the diagonal crack surface to the member axis. $\beta_u = 45^\circ$.

γ_b : 1.3 in general

V_{ped} : component of effective tensile force in longitudinal prestressing steel parallel to the shear force, given by Equation (6.3.6).

$$V_{ped} = P_{ed} \cdot \sin \alpha_p / \gamma_b \quad (6.3.6)$$

P_{ed} : effective tensile force in longitudinal prestressing steel

α_p : angle of longitudinal prestressing to the member axis

γ_b : 1.1 in general

(2) Design shear capacity of a steel reinforced concrete member partly reinforced by HPFRCC shall be determined with appropriate methods such as tests. However, design shear capacity of a member combined with HPFRCC and normal concrete by appropriate technology may be determined according to section 6.3.3 “Design shear capacity of linear members” of Standard Specifications for Concrete Structures –*Structural Performance Verification* replacing HPFRCC with normal concrete.



(3) Design diagonal compressive capacity V_{wcd} of web-concrete in resisting shear force may be calculated using Equation (6.3.7).

$$V_{wcd} = f_{wcd} \cdot b_w \cdot d / \gamma_b \quad (6.3.7)$$

where $f_{wcd}: 1.25 \sqrt{f'_{cd}}$ (N/mm²) with $f_{wcd} \leq 7.8$ (N/mm²) and γ_b ; 1.3 in general.

[Commentary] As shown in Equation (6.3.1), the design shear strength V_{yd} is given as the sum of the capacity exerted by HPFRCC's matrix V_{cd} , capacity exerted by HPFRCC's reinforcing fiber V_{fd} , and capacity exerted by shear reinforcing steels V_{sd} . It is possible to take advantages of HPFRCC in design by making use of the strong resistance offered by the reinforcing fiber. The method of considering the effects of reinforcing fiber in design formula is derived from *Recommendations for Design and Construction of Ultra High-Strength Fiber Reinforced Concrete Structures (Draft)*.

The capacity exerted by matrix is derived from Standard Specifications for Concrete Structures – *Structural Performance Verification*. However, V_{yd} is assumed to be reduced by a factor of 0.7 because HPFRCC allows cracks in service.

Figure 6.3.2 shows the verification results for the shear capacity equation using the specimens outlined in Fig. 6.3.1. Specimens A had a fiber content of 1.5% or 2.0% and shear reinforcement ratio of 0% or 0.15% or 0.3%, and specimen B had a fiber content of 2.0% and shear reinforcement ratio of 0%. Figure 6.3.2 indicates the shear capacity equation (6.3.1) generally allows a conservative evaluation of the shear capacity. It should be noted, however, that given the limited test data, an appropriate confirmation process such as by testing should be followed for cases where the cross-sectional height or reinforcement ratio is considerably different.

According to Recommendations for Design and Construction of Ultra High-Strength Fiber Reinforced Concrete Structures (Draft), a value of 40° is recommended for β_u when there is no axial force. If β_u is also set at 40° for HPFRCC not subjected to axial force, it means that the test values have been conservatively evaluated. Still, β_u is given as 45° here, due to the shortage of test data available.

(2) When a steel reinforced concrete member is partly reinforced by HPFRCC, a rational evaluation of shear capacity of such member is difficult because the sections of the member are governed by different reinforcing mechanisms according to the applied part. Thus this "Recommendations" document proposes other appropriate methods such as testing, while the design shear capacity of member combined with HPFRCC and normal concrete by appropriate technology may be determined by replacing HPFRCC with normal concrete. This estimation is sufficiently on the safety side because the fiber shares major part of the shear capacity of the HPFRCC and V_{yd} shows to be sufficiently



larger than the concrete-equivalent shear capacity, even V_{cd} is reduced by a factor of 0.7.

Torsión

[JSCE – 6.4 TORSION SAFETY]

(1) In principle, follow section 6.4 “Torsion” of Standard Specifications Concrete Structures –*Structural Performance Verification*.

(2) The torsional capacity of HPFRCC after initiating torsional cracking shall be calculated by an appropriate method such as testing.

[Commentary] Due to the shortage of data on the torsional capacity of HPFRCC after initiating torsional cracks, the safety should be examined by an appropriate method such as testing.

Fatiga

[JSCE – 3.9 Fatigue]

(1) The characteristic value of HPFRCC’s fatigue strength shall be determined from the results of fatigue strength tests that are performed in consideration for the exposed condition of the structure and other relevant conditions.

(2) In general, material factor of HPFRCC γ_c is set at 1.3 in the fatigue limit state.

(3) In general, the design compressive/flexural compressive fatigue strength of HPFRCC f_{rd} can be obtained by Equation (3.9.1), assuming it is a function of fatigue life N and permanent-load-induced stress σ_p . It shall be noted, however, that the fatigue strength shall be experimentally determined where HPFRCC is continuously or often saturated with water.

$$f_{rd} = 0.85 f_d (1 - \sigma_p / f_d) (1 - \log N / 17) \text{ (N/mm}^2\text{)} \quad (3.9.1)$$

where, $N \leq 2 \times 10^6$, f_d : design compressive strength of HPFRCC, and material factor γ_c is given as 1.3 here.

(4) The design compressive/flexural compressive fatigue strength of HPFRCC f_{rd} shall be experimentally determined, assuming it is a function of fatigue life N and stress σ_p .

[Commentary] (3) Because compressive fatigue characteristics are known to be improved greatly by reinforcement with fiber, the values used in the design of ordinary concrete are also used here as a conservative design value for HPFRCC.



(4) Fig. 3.9.1 is presented as an example of flexural tensile fatigue strength of HPFRCC. As shown in the figure, a bilinear approximation can be adopted for HPFRCC's flexural tensile fatigue strength when the number of fatigue cycle N_u is logarithmically represented. This can be given by the following equations where S is the ratio of flexural tensile stress to the statistic flexural strength under fatigue loading. When S is 0.5 or lower, no fatigue failure occurs upon 2 million times of fatigue cycles.

$$\begin{aligned} S &= 1.000 - 0.0098 \times \log(N_u) & 1 \leq N_u < 1 \times 10^4 \\ S &= 1.595 - 0.0761 \times \log(N_u) & 1 \times 10^4 \leq N_u \leq 2 \times 10^6 \end{aligned}$$

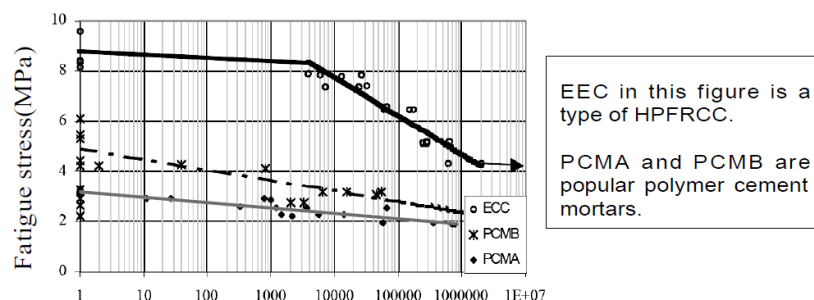


Ilustración 49.- JSCE - Fig. 3.9.1 Example of flexural fatigue test of HPFRCC

[JSCE – 6.5 Examination of safety against fatigue]

In principle, follow chapter 8 of Standard Specifications for Concrete Structures – *Structural Performance Verification*.

[Commentary] In HPFRCC, reinforcing fibers randomly distributed over the crack plane exhibit a bridging effect and control crack initiation and development. Formation of multiple fine cracks may enable a high energy absorption performance and may contribute to a higher fatigue resistance by the prevention of crack localization.

Verification of safety against fatigue

In principle, follow section 8.2 of Standard Specifications for Concrete Structures – *Structural Performance Verification*.

[Commentary] A flow diagram of the safety verification for fatigue on the basis of materials fatigue strength is shown in Fig. 6.5.1, where design variable stress σ_d may be given by the method shown in 6.5.4 of this “Recommendations” document. Using fatigue life N and the minimum stress or design stress at permanent load, design fatigue strength f_{rd} may be obtained according to the design fatigue strength formula in Standard Specifications for Concrete Structures – *Structural Performance Verification* for steel and according to section 3.9 of this “Recommendations” document for HPFRCC.



Design variable force and equivalent number of cycles

In principle, follow section 8.3 “Design variable force and equivalent number of cycles” in Standard Specifications for Concrete Structures –*Structural Performance Verification*.

Stress calculation due to variable loads

In principle, follow section 8.4 “Computation of stress due to variable load” in *Standard Specifications for Concrete Structures –Structural Performance Verification*

Design shear fatigue capacity of members

Design shear fatigue capacity of members shall in principle be estimated with appropriate methods such as testing where necessary.

[Commentary] Sufficient data are not accumulated to determine the design shear fatigue capacity of members, hence appropriate methods such as testing should be used where necessary.

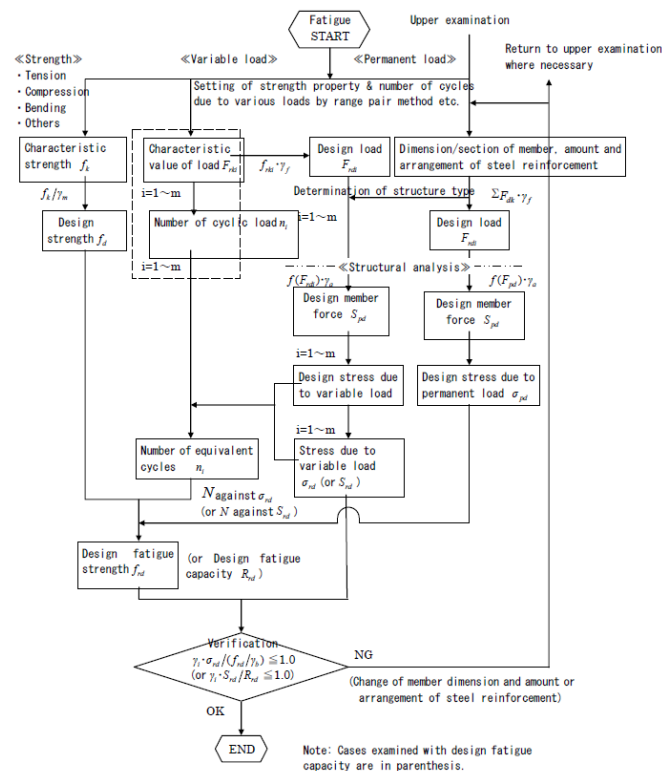


Ilustración 50.- JSCE - Fig. 6.5.1 Flow diagram for wxamining the limit state fatigue

3.6.3. Estado Límite de Servicio

Fisuración

[JSCE – 7.6 Examination of cracking]



General

(1) Cracks in HPFRCC due to bending moments, shear forces, torsional moments and axial forces shall be examined with appropriate methods determining whether safety and serviceability of structure are impaired.

(2) Examination of cracks in terms of resistance to environmental actions is essentially a control of crack width in HPFRCC surfaces under specified environmental conditions and not to allow Steel corrosion associated with ingress of chloride ions and carbon dioxide and resulting degradation of required performance of structures during design service life. Examination may be accomplished by confirming the following (i) and (ii) with the method specified in Chapter 9.

(i) Crack width of HPFRCC is less than the permissible width for steel corrosion determined under specified environmental conditions, cover thickness, design service life and other factors.

(ii) Predicted chloride ion concentration at steel reinforcement in HPFRCC under specified environmental conditions, cover thickness, HPFRCC quality level and crack width is lower than the permissible concentration for initiation of steel corrosion during service life. Evaluation of cracks is not necessary for temporary structures, structures with very short design service life and structures with surface protection.

(3) When water tightness is an important factor, an appropriate permissible crack width may be specified, and then be confirmed that crack widths are less than the permissible value.

(4) When appearance is an important factor, an appropriate permissible crack width may be specified, and then be confirmed that any crack widths are less than the permissible value.

[Commentary] (1) Cracks in a structure may cause degradation of performance such as safety and serviceability due to steel corrosion. Thus the crack in HPFRCC should be evaluated with appropriate methods in terms of safety, serviceability and resistance to environmental actions.

Among various causes for cracking in HPFRCC structures, this section essentially addresses cracks due to load, especially bending moments, shear forces, torsional moments and axial forces. When a structural system changes during construction and the service life, the stress resultant should be evaluate taking into account of these changes.

(2) When verifying the resistance to environmental actions in terms of cracks, protection of Steel from corrosion due to chloride ion ingress can be accomplished not



only by the crack width control capability but also by cover thickness and HPFRCC quality. Based on this fact, examination of limit state of cracks for resistance to environmental actions shall be made, in principle, by confirming both that crack width is less than the permissible width and that predicted chloride ion concentration at the steel reinforcement is lower than the permissible concentration for initiation of steel corrosion during service life. HPFRCC material has a capability of controlling crack width to be sufficiently fine and chloride ion permeability to HPFRCC with distributed cracks shall be estimated by a formula shown in equation (3.3.2) in appendix II-3 using maximum crack width and strain in HPFRCC. Thus the unified examination of tensile strain, cracking and the resistance to environmental actions (Chapter 9 of this “Recommendations” document) shall be possible provided that the relation between crack width – tensile strain – chloride ion permeability is determined experimentally beforehand.

(3) When water tightness is an important factor, examination of cracking should be made in terms of crack initiation or crack width control.

(4) When appearance is an important factor, a permissible crack width should be specified when necessary, and examination of cracking shall be made by a method similar to that for durability.

Permissible crack width

In principle, follow section 7.4.2 “Permissible crack width” of Standard Specifications of Concrete structures –*Structural Performance Verification*.

[Commentary] The capability of controlling crack width is a major characteristic of structural members using HPFRCC. Previous studies show that the crack width of HPFRCC can be regarded as a material property rather than structural property under given cross sectional dimensions or loading conditions. Hence, for the design of structural members using HPFRCC, the resistance to environmental actions such as chloride ion ingress should be examined by using the crack control property of the HPFRCC as specified in Chapter 9 of this “Recommendations” document. However, use of HPFRCC over the range of crack width greater than that allowed for the normal reinforced concrete members is not of significance and the data covering the range of the crack width are not sufficient, thereby this “Recommendations” document is in principle based on the permissible crack width range of the normal reinforced concrete.

Classification of environmental conditions

In principle, follow section 7.4.3 “Classification of environmental conditions” of Standard Specifications for Concrete structures –*Structural Performance Verification*.



Examination of bending cracks

(1) Examination of crack width is not necessary when the tensile stress of HPFRCC due to bending moments is lower than the cracking strength of HPFRCC.

(2) Crack width shall be examined by confirming that the maximum crack width obtained from tensile strain in HPFRCC is lower than the permissible crack width specified in section 7.6.2

(3) Relationship between maximum crack width and tensile strain shall be determined, in principle, by uniaxial tensile test.

[Commentary] (1) Examination of bending crack is not necessary when the bending crack does not occur at the limit state of serviceability. However, in cases when there is a high risk of cracking, such as thermal cracking, which are normally excluded in the examination of the serviceability limit state, an examination using appropriate method shall be carried out to prevent such racking.

Tensile stress due to autogenous shrinkage may become significant in a HPFRCC with high volume powder component. This factor shall be taken into consideration.

(2), (3) Unlike ordinary concrete, HPFRCC has the capability of controlling crack width. The stress-strain relationship of HPFRCC obtained by uniaxial tensile test (see Testing Method 2, 3 and 4) and the crack width-strain relationship are shown in Fig. 7.6.1. The comparison of crack widths between steel reinforced HPFRCC and monolithic HPFRCC under the tensile test is shown in Fig. 7.6.3. Crack width of HPFRCC reinforced with steel bar was equivalent to or smaller than that without steel reinforcement. Thus the relation between crack width of HPFRCC and tensile strain can be designed conservatively by using a design formula derived from material tests without steel reinforcement. Thereby for the materials with a formulated crack width-tensile strain relation in appendix II-1, verification of crack width can be made first by estimating the maximum crack width from the tensile strain of HPFRCC, and next by comparison with the permissible crack width.

Examination of shear cracks

In principle, follow section 7.4.6 “Examination of shear cracks” of Standard Specifications for Concrete structures –*Structural Performance Verification*.

Examination of torsional cracks

In principle, follow section 7.4.7 “Examination of torsional cracks” of Standard Specifications for Concrete structures –*Structural Performance Verification*.



Structural details

Additional reinforcements to control cracks due to temperature changes and shrinkage are not necessary provided that the characteristic value of the maximum crack width of HPFRCC is less than the crack width shown in section 7.6.2.

[Commentary] HPFRCC has a crack width control capability. Hence, additional reinforcement is not necessary provided that the characteristic value of the maximum crack width of HPFRCC is less than the permissible crack width.

Compresión máxima

[JSCE – 7.3 Stress limit value]

Compressive stress of HPFRCC due to bending moments and axial forces and tensile stress of steel shall not exceed the limit values given in (1) and (2).

(1) Limit value of compressive stress due to bending moment and axial forces of HPFRCC are $0.4f'_{ck}$ under permanent load where f'_{ck} is a characteristic value of compressive strength of HPFRCC.

(2) Limit value of steel tensile stress is f_{yk} , where f_{yk} is a characteristic value of tensile yield strength of steel.

[Commentary] When HPFRCC is permanently subjected to multi-axial constraints, the limit value may be mitigated with an appropriate evaluation method.

The tensile stress of the steel may be limited by the yield stress, because the assumptions for structural analysis and stress computation in section 7.2 of the “Recommendations” document are no longer valid due to the tensile stress of steel exceeding the elastic limit. When cracking is examined for normal concrete, stress in reinforcing steel is sufficiently smaller than the characteristic value of tensile yielding strength. However for HPFRCC members, stress in reinforcing steel is not smaller than the characteristic value of tensile yielding strength due to the large deformation capability of HPFRCC, hence a verification taking into account the influence of creep deformation of HPFRCC is necessary whether the stress in reinforcing steel in the long term is not larger than the characteristic value of tensile yielding strength.

3.6.4. Cuantías mínimas

Flexión

[JSCE – 6.2.2 Structural details]



In principle, structural details shall be determined based on section 6.2.2 “Structural details” of Standard Specifications for Concrete Structures –*Structural Performance Verification*.

[Commentary] When the tension reinforcement ratio becomes extremely small in a reinforced concrete member, the yielding load becomes smaller than the cracking load, and steel bars may yield or fracture immediately after cracking and the bending member shows brittle failure mode. Only one crack may occur and it may show a failure mode like unreinforced concrete. This requires the tension reinforcement ratio of a rectangular member, where flexural moment is dominant, should be larger than 0.2 percent as specified in Standard Specifications for Concrete Structures –*Structural Performance Verification*. HPFRCC on the other hand is a highly ductile material showing pseudo strain-hardening characteristics and can bear tensile stress in a stable manner. Experimental results showed that cracking did not result in a brittle failure even though tension reinforcement ratio is smaller than 0.2 percent. However, this “Recommendations” document follows Standard Specifications for Concrete Structures –*Structural Performance Verification* because sufficient data is not yet available.

Cortante

[JSCE – 6.3.8 Structural details]

(1) No particular specifications are prescribed for the minimum number of stirrups when the design tensile yielding strength of HPFRCC is larger than 1.5 N/mm². However in the other case, amount of shear reinforcement greater than 0.15% shall be arranged throughout the length of the linear member. The stirrup spacing shall in principle be less than 3/4 of the effective depth of the member and less than 400mm. This rule is not applicable to planar members

(2) Where the calculation results show that the linear member needs shear steel reinforcement, the stirrup spacing shall be less than 1/2 of the effective depth and less than 300 mm. In addition, the same amount of shear steel reinforcement shall be provided over a distance equal to the effective depth of member from the end of the region that is found to be in need of shear Steel reinforcement in calculation.

(3) When stirrups are anchored in a tension region, an appropriate confirmation process such as testing shall be followed.

[Commentary] (1) In the case of a HPFRCC beam specimen with a HPFRCC’s tensile yield strength of 3 N/mm² as shown in Fig. 6.3.3, the level of shear force exerted by 0.15% reinforcing fiber is more than 5 times that of the shear force exerted by shear reinforcing bars at a shear reinforcement ratio of 0.15%. HPFRCC beams do not exhibit brittle failure even after developing diagonal cracking because the reinforcing fiber



shares tensile stress in a direction orthogonal to the crack plane. Thus, no particular specifications are prescribed for the minimum amount of steel shear reinforcement here.

(2) Where there is a need to provide shear steel reinforcement, the stirrups should be arranged according to Standard Specifications for Concrete Structures –*Structural Performance Verification*.

(3) Being a highly ductile material that develops a number of dense micro-cracks, HPFRCC is expected to provide adequate bonding even when anchored in a tensile region. However, because the bond strength of HPFRCC anchored in a tensile region has yet to be clarified, an appropriate confirmation process such as testing should be adopted.

Torsión

No se recogen requisitos específicos para el hormigón con fibras.



3.7. COMPARATIVA

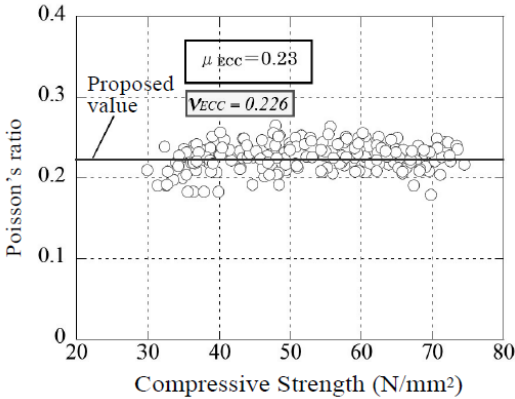
Tras analizar la normativa existente a nivel internacional, recopilando los apartados más relevantes para el diseño y cálculo de una torre eólica, se han realizado las siguientes tablas resumen, que recogen por apartados analizados, el planteamiento de cada normativa.

De este modo, podemos comparar rápidamente los distintos aspectos de diseño del hormigón reforzado con fibras de los diferentes países identificando el estado de desarrollo de la normativa, comprendiendo las particularidades de cálculo para este material e identificando las limitaciones de la normativa para algunos aspectos.



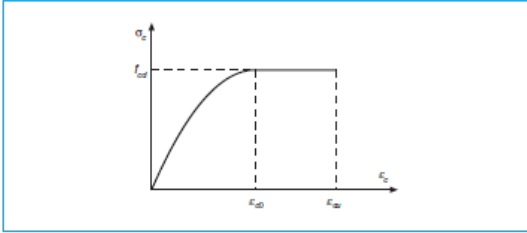
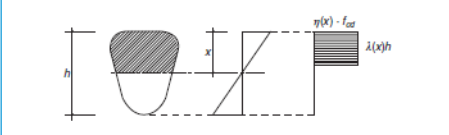
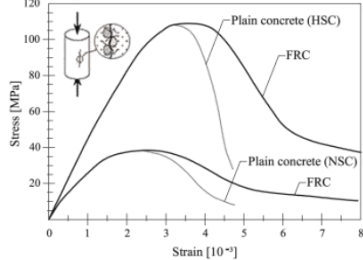
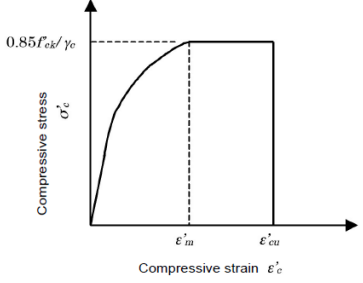
Módulo de Elasticidad																																													
EHE 08	Model Code 2010	ACI	RILEM	CNR	JSCE																																								
<p>*No propone modificaciones para el hormigón con fibras</p>	<p>Elastic properties and compressive strength are not significantly affected by fibers, unless a high percentage of fibers is used.</p>	<p>In practice, when the volume percentage of fibers is less than 2 percent, the modulus of elasticity and Poisson’s ratio of SFRC are generally taken as equal to those of a similar non-fibrous concrete or mortar.</p>	<div>Table 1 – Steel fibre reinforced concrete strength classes: characteristic compressive strength f_{ck} (cylinders), mean $f_{ctm,fl}$ and characteristic $f_{ctk,fl}$ flexural tensile strength in N/mm²; mean secant modulus of elasticity in kN/mm²</div> <table><tr><th>Strength class of SFR-concrete</th><th>C20/25</th><th>C25/30</th><th>C30/37</th><th>C35/45</th><th>C40/50</th><th>C45/55</th><th>C50/60</th></tr><tr><td>f_{ck}</td><td>20</td><td>25</td><td>30</td><td>35</td><td>40</td><td>45</td><td>50</td></tr><tr><td>$f_{ctm,fl}$</td><td>3.7</td><td>4.3</td><td>4.8</td><td>5.3</td><td>5.8</td><td>6.3</td><td>6.8</td></tr><tr><td>$f_{ctk,fl}$</td><td>2.9</td><td>3.4</td><td>3.9</td><td>4.3</td><td>4.7</td><td>5.1</td><td>5.5</td></tr><tr><td>E_{cem}</td><td>29</td><td>30.5</td><td>32</td><td>33.5</td><td>35</td><td>36</td><td>37</td></tr></table>	Strength class of SFR-concrete	C20/25	C25/30	C30/37	C35/45	C40/50	C45/55	C50/60	f_{ck}	20	25	30	35	40	45	50	$f_{ctm,fl}$	3.7	4.3	4.8	5.3	5.8	6.3	6.8	$f_{ctk,fl}$	2.9	3.4	3.9	4.3	4.7	5.1	5.5	E_{cem}	29	30.5	32	33.5	35	36	37	<p>Modulus of elasticity is not generally affected by fibers, so it may be assumed equal to that of the matrix.</p>	<p>In principle, Young’s modulus of HPFRCC shall be derived from JIS A 1149 “Method of Test for static modulus of elasticity of concrete”.</p> <p>[Commentary] Young’s modulus of HPFRCC can be obtained by adopting the testing method used for ordinary concrete. The Young’s modulus thus obtained takes a smaller value, i.e. between 1/2 and 2/3 or so of that for ordinary concrete. Fig. 3.4.1 shows an example of relationship between Young’s modulus and compressive strength expressed in measured values.</p> <div><p>JSCE Standard Specifications for Design and Construction of Concrete</p><p>Young's modulus</p><p>Compressive Strength (N/mm²)</p><p>RC standard formula ($\gamma=23$)</p><p>NewRC formula ($\gamma=24$)</p><p>$E_{ECC} = 1.77 \times 10^4 \times \sqrt{\frac{\gamma}{18.5 \times \left(\frac{f'_{ck}}{60}\right)^{\frac{1}{3}}}}$</p></div>
Strength class of SFR-concrete	C20/25	C25/30	C30/37	C35/45	C40/50	C45/55	C50/60																																						
f_{ck}	20	25	30	35	40	45	50																																						
$f_{ctm,fl}$	3.7	4.3	4.8	5.3	5.8	6.3	6.8																																						
$f_{ctk,fl}$	2.9	3.4	3.9	4.3	4.7	5.1	5.5																																						
E_{cem}	29	30.5	32	33.5	35	36	37																																						



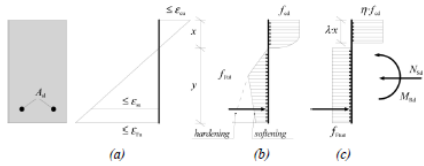
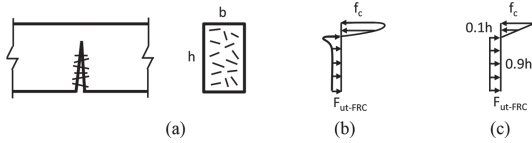
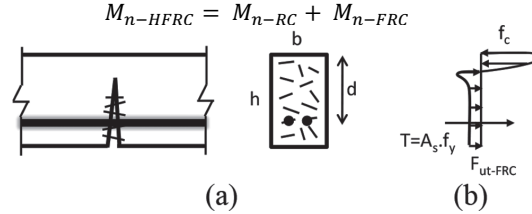
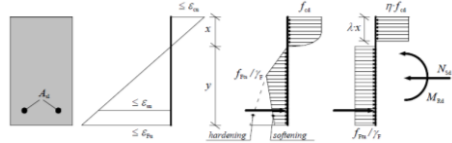
Coeficiente de Poisson					
EHE 08	Model Code 2010	ACI	RILEM	CNR	JSCE
Las fibras individualmente, o como grupo, deberán tener un coeficiente de Poisson similar al del hormigón si se quiere tener en cuenta el efecto red a nivel estructural.	The mechanical properties of a cementitious matrix are modified when fibres are added. However, elastic properties and compressive strength are not significantly affected by fibres, unless a high percentage of fibres is used.	In practice, when the volume percentage of fibers is less than 2 percent, the modulus of elasticity and Poisson’s ratio of SFRC are generally taken as equal to those of a similar nonfibrous concrete or mortar.	-	Without specific tests, all the mechanical properties, not specified, can be assumed as those of ordinary concrete	<p>Poisson’s ratio of HPFRCC shall be determined based on experiments or on existing data.</p>  <p>[Commentary] Fig. 3.5.1 is an example of the measured Poisson’s ratio of HPFRCC. As shown in the figure, the Poisson’s ratio of HPFRCC is slightly higher than that of ordinary concrete, yielding an average value of 0.226.</p>

Tracción					
EHE 08	Model Code 2010	ACI	RILEM	CNR	JSCE
<p>Del ensayo propuesto en UNE-EN 14651 se obtiene el diagrama carga-abertura de fisura del hormigón</p> <p>A partir de estos valores se determinará el diagrama de cálculo a tracción según lo indicado en el Artículo 39°.</p> <p>- Diagrama rectangular:</p> <p>- Diagrama multilinear:</p>	<p>Nominal values of the material properties can be determined by performing a 3-point bending test on a notched beam according to EN 14651 (Figure 5.6-5). The diagram of the applied force (F) versus the deformation shall be produced (Figure 5.6-6).</p> $f_{R,j} = \frac{3 F_j l}{2 b h_{sp}^2}$	<p>a) σ_1 and ϵ_1—tensile stress and corresponding strain at onset of first cracking</p> <p>b) σ_2 and ϵ_2—stress and strain at the onset of the stable softening branch</p> <p>c) σ_3 and ϵ_3—stress and strain at the end of the softening branch</p>	<p>$\sigma_1 = 0.7 f_{t,cm,0} (1.6 \cdot d)$ (d in m) (N/mm²) $\epsilon_1 = \sigma_1 / E_c$</p> <p>$\sigma_2 = 0.45 f_{t,cm,0} \kappa_s$ (N/mm²) $\epsilon_2 = \epsilon_1 + 0.1 \text{ ‰}$</p> <p>$\sigma_3 = 0.37 f_{t,cm,0} \kappa_s$ (N/mm²) $\epsilon_3 = 25 \text{ ‰}$</p> <p>$E_c = 9500 (f_{t,cm,0})^{1/3}$ (N/mm²)</p> <p>κ_s: size factor</p> <p>$\kappa_s = 1.0 - 0.6 \cdot \frac{h [\text{cm}] - 12.5}{47.5} \quad 12.5 \leq h \leq 60 [\text{cm}]$</p>	<p>handening</p> <p>softening</p>	<p>(1) Tensile stress-strain curve of HPFRCC shall be determined through an appropriate test method. According to the limit state in question, an appropriate shape can be assumed based on the reliable past data.</p> <p>(2) The tensile stress-strain curve shown in Fig. 3.3.1 can be used when studying the ultimate limit state of section fracture for members subjected to a bending moment or a bending moment and axial forces.</p> <p>(3) The tensile stress-strain curve shown in Fig. 3.3.1 can be used for serviceability verification.</p> <p>Tensile stress σ_c</p> <p>Tensile strain ϵ_c</p> <p>Gradient E_c</p> <p>$f_{tyk} / (E_c \cdot \gamma_c)$</p> <p>$\epsilon_{tuk} / \gamma_c$</p>



Compresión					
EHE 08	Model Code 2010	ACI	RILEM	CNR	JSCE
<p>a)Diagrama parábola rectángulo</p>  $\sigma_c = f_{cd} \left[1 - \left(1 - \frac{\varepsilon_c}{\varepsilon_{c0}} \right)^n \right] \quad \text{si } 0 \leq \varepsilon_c \leq \varepsilon_{c0}$ $\sigma_c = f_{cd} \quad \text{si } \varepsilon_{c0} \leq \varepsilon_c \leq \varepsilon_{cu}$ $\varepsilon_{c0} = 0,002 \quad \text{si } f_{ck} \leq 50 \text{ N/mm}^2$ $\varepsilon_{c0} = 0,002 + 0,000085(f_{ck} - 50)^{0,50} \quad \text{si } f_{ck} > 50 \text{ N/mm}^2$ $\varepsilon_{cu} = 0,0035 \quad \text{si } f_{ck} \leq 50 \text{ N/mm}^2$ $\varepsilon_{cu} = 0,0026 + 0,0144 \left[\frac{(100 - f_{ck})}{100} \right]^4 \quad \text{si } f_{ck} > 50 \text{ N/mm}^2$ $n = 2 \quad \text{si } f_{ck} \leq 50 \text{ N/mm}^2$ $n = 1,4 + 9,6 \left[\frac{(100 - f_{ck})}{100} \right]^4 \quad \text{si } f_{ck} > 50 \text{ N/mm}^2$ <p>b) Diagrama rectangular</p> $\eta(x) = \eta \quad \text{si } 0 < x \leq h$ $\eta(x) = 1 - (1 - \eta) \frac{h}{x} \quad \text{si } 0 < x \leq h$ $\lambda(x) = \lambda \frac{x}{h} \quad \text{si } 0 < x \leq h$ $\lambda(x) = 1 - (1 - \lambda) \frac{h}{x} \quad \text{si } h \leq x < \infty$ <p>donde:</p> $\eta = 1,0 \quad \text{si } f_{ck} \leq 50 \text{ N/mm}^2$ $\eta = 1,0 - \frac{(f_{ck} - 50)}{200} \quad \text{si } f_{ck} > 50 \text{ N/mm}^2$ $\lambda = 0,8 \quad \text{si } f_{ck} \leq 50 \text{ N/mm}^2$ $\lambda = 0,8 - \frac{(f_{ck} - 50)}{400} \quad \text{si } f_{ck} > 50 \text{ N/mm}^2$  <p>Ilustración 51.- EHE 08 - Figura 39.5.b. Diagrama de cálculo rectangular</p> <p>c) Otros diagramas de cálculo, como los parabólicos, birrectilíneos, trapezoidales,etc., se aceptarán siempre queden del lado de la seguridad.</p>	<p>Generally, the compressive relations valid for plain concrete apply to FRC as well.</p>  <p>Figure 5.6-3: Main differences between plain and fibre reinforced concrete having both normal and high strength under uniaxial compression.</p>	<p>In compression, the ultimate strength is only slightly affected by the presence of fibers, with observed increases ranging from 0 to 15 percent for up to 1.5 percent by volume of fibers</p>	<p>-</p>	<p>Fibers generally reduce the brittleness of the matrix, but they do not have significant effect on the compressive behaviour.</p> <p>In practice, the constitutive law of fiber reinforced concrete can be assumed equal to that of ordinary concrete</p>	<p>(1) The compressive stress-strain curve of HPFRCC shall in principle be determined through an appropriate test. An appropriate shape of compressive stress-strain curve can be assumed according to the nature of the ultimate state based on the reliable past data.</p> <p>(2) The compressive stress-strain curve like the one shown in Fig. 3.3.2 may be used when studying the ultimate limit state of section failure for the members subjected to a bending moment or a bending moment and axial compressive forces. ε'_m and ε'_{cu} can be determined based on appropriate tests. The following stress-strain equation can be applied for the initial curved zone.</p> $\sigma'_c = 0.85 f'_{ck} \gamma_c \times \varepsilon'_c / \varepsilon'_m \times (2 - \varepsilon'_c / \varepsilon'_m)$  <p>(3) The compressive stress-strain relationship can be regarded as linear when serviceability performance is verified. Young's modulus can be determined according to section 3.4.</p> <p>(4) Evaluation of the compressive stress-strain relationship under biaxial or triaxial stresses shall take into account the effects of multi-axial stress conditions where necessary when verifying safety or serviceability performance. The material shall be assumed as linear-elastic for examination of the serviceability limit state, and Young's modulus and Poisson's ratio can be set at values specified in sections 3.4 and 3.5, respectively.</p>



ELU – Flexión compuesta					
EHE 08	Model Code 2010	ACI	RILEM	CNR	JSCE
<p>En aquellos casos en que se utilicen fibras con función estructural, solas o en combinación con armadura tradicional, se deberá cumplir la siguiente limitación:</p> $A_p f_{pd} \frac{d_p}{d_s} + A_s f_{yd} + \frac{z_f}{z} A_{ct} f_{ctR,d} > \frac{W_1}{z} f_{ctm} + \frac{P}{z} \left(\frac{W_1}{A} + e \right)$ <p>donde:</p> <p>$z_f A_{ct} f_{ctR,d}$ Contribución de las fibras. z_f Brazo mecánico de la tracción del hormigón. A_{ct} Área traccionada de hormigón. $f_{ctR,d}$ Resistencia residual a tracción de cálculo en el diagrama rectangular.</p> <p>En el caso de secciones rectangulares con o sin armadura pasiva puede emplearse la siguiente relación simplificada, en la que no se precisa determinar el área traccionada de hormigón.</p> $A_s f_{yd} + 0,4 A_c f_{ctR,d} > 0,04 A_c f_{cd}$	<p>The bending failure stage is supposed to be reached when one of the following conditions applies:</p> <ul style="list-style-type: none">- attainment of the maximum compressive strain in the FRC, ε_{cu};- attainment of the maximum tensile strain in the steel (if present), ε_{su};- attainment of the maximum tensile strain in the FRC, ε_{Fu}. 	<p>Design of RC for flexure (stress block)</p> $M_{n-RC} = A_s f_y \left(d - \frac{a}{2} \right)$ $a = \frac{A_s f_y}{0.85 f'_c b}$ <p>Design of RC for flexure (ASTM C1609/C1609M, in conjunction with RILEM TC 162-TDF [2003])</p>  $f_{ut-FRC} = 0.37 f_{150}^D$ $M_{n-FRC} = f_{150}^D \frac{b h^2}{6}$ <p>Design of RC for flexure (Model Code 2010 [fib 2013])</p> <p>Using rigid-plastic model (for ULS only):</p> $f_{Ftu-FRC} = \frac{f_{R,3}}{3}$ $M_{nu-FRC} = f_{R,3} \frac{b h_{sp}^2}{6}$ <p>Using linear model (for SLS and ULS):</p> $f_{Fts-FRC} = 0.45 f_{R,1}$ $f_{Ftu-FRC} = (0.45 f_{R,1}) - \frac{w_u}{CMOD_3} \geq 0$ $(0.45 f_{R,1} - 0.5 f_{R,3} + 0.2 f_{R,1})$ $M_{ns-FRC} = f_{R,1} \frac{b h_{sp}^2}{6}$ $M_{nu-FRC} = f_{R,3} \frac{b h_{sp}^2}{6}$ <p>Design of RC for flexure-hybrid reinforcement</p>  $M_{n-HFRC} = M_{n-RC} + M_{n-FRC}$		<p>(1) For a fixed value of the applied design axial force, NS_d, the ultimate bending moment, MR_d, can be evaluated by means of the translation and rotation equilibrium equations.</p> <p>(2) The evaluation of the ultimate moment can be carried out in reference to the strain and stress distributions shown in Figure 4-1, corresponding to the FRC stress/strain relationship reported in §§ 2.5.2.2 and 2.5.2.3 and reinforcement steel laws (if present) in accordance to the current Codes.</p> <p>(3) With reference to the condition shown in Figure 4-1 and in accordance to Eurocode 2 (EC2) the evaluation of the ultimate moment for a given axial force can be made by adopting the simplified stress/strain relationship (that corresponds to the maximum compressive and post-peak tensile stress, see § 2.5.2.3), by verifying <i>a posteriori</i> so that the ultimate strains ε_{cu}, ε_{su} and ε_{Fu} are not violated and the collapse mechanism respected.</p> 	<p>(1) For a member subjected to axial compressive force, the upper limit for axial compressive capacity N'_{oud} shall be calculated by Eq.(6.2.1)</p> $N'_{oud} = (k_1 f'_{cd} A_c + f'_{yd} A_{st}) / \gamma_b$ <p>where</p> <p>A_c: cross-sectional area of HPFRCC, f'_{cd}: design compressive strength of HPFRCC A_{st}: total cross-sectional area of longitudinal reinforcing steel f'_{yd}: design compressive yield strength of longitudinal reinforcing steel k_1: strength reduction factor ($1 - 0.003 f'_{ck} \leq 0.85$ with $f'_{ck} \leq 80$ N/mm²) f'_{ck}: characteristic value of compressive strength of HPFRCC (N/mm²) γ_b: member factor; which may generally be taken as 1.3.</p> <p>(2) Assumptions set out in (i), (ii) and (iii) below shall be followed when calculating the design capacity of a member subjected to bending moment and axial force, with regard to either the member's cross-section or unit width depending on the direction or the stress resultant. In such a case, the member factor γ_b may generally be taken as 1.1.</p> <p>(i) Fiber strain is proportional to the distance from the neutral axis.</p> <p>(ii) Stress-strain curve of HPFRCC follows that given in section 3.3 when the design tensile yield strength f'_{tyd} is greater than 1.5 N/mm². Tensile stress of HPFRCC is neglected if f'_{tyd} is smaller than 1.5 N/mm².</p> <p>(iii) Stress-strain curve of steel reinforcement follows that given in section 3.3.3 "Stress-strain relationship" of Standard Specifications for Concrete Structures – Structural Performance Verification.</p>



ELU - Cortante					
EHE 08	Model Code 2010	ACI	RILEM	CNR	JSCE
$V_{u2} = V_{cu} + V_{su} + V_{fu}$ donde: $V_{cu} = \left[\frac{0.15}{\gamma_c} \xi (100 \rho_l f_{cv})^{1/3} + 0.15 \sigma'_{cd} \right] \beta b_0 d$ $V_{su} = z \cdot \text{sen} \alpha (\cot \alpha + \cot \theta) \sum A_a f_{ya,d}$ $V_{fu} = 0.7 \xi \tau_{fd} b_0 d$ $\xi = 1 + \sqrt{\frac{200}{d}} \text{ d en mm}$ $\xi \leq 2$ $\tau_{fd} = 0.5 f_{ctR,d} \left(\frac{N}{mm^2} \right)$ *En el caso de estructuras de hormigón reforzado con fibras con función estructural, en lugar de V_{su} deberá considerarse ($V_{su} + V_{fu}$) en las expresiones del articulado.	<p>Beams without longitudinal and shear reinforcement</p> $\sigma_1 \leq \frac{f_{Ftuk}}{\gamma_F}$ <p>Beams without shear reinforcement</p> $V_{Rd,F} = \left\{ \frac{0.18}{\gamma_c} k \left[100 \rho_l \left(1 + 7.5 \frac{f_{Ftuk}}{f_{ctk}} \right) f_{ck} \right] + 0.15 \sigma_{cp} \right\} b_w d$ $k = 1 + \sqrt{\frac{200}{d}} \leq 2.0$ $\rho_l = A_{sl} / b_w d$ $\sigma_{cp} = N_{Ed} / A_c < 0.2 f_{cd}$ $V_{Rd,Fmin} = (v_{min} + 0.15 \cdot \sigma_{cp}) \cdot b_w \cdot d$ <p>where $v_{min} = 0.035 k^{3/2} f_{ck}^{1/2}$</p> <p>Beams with shear and longitudinal reinforcement</p> <p>For the design of members with shear reinforcement the basic relation Eq. (7.3-9) applies, being:</p> $V_{Rd} = V_{Rd,c} + V_{Rd,s}$ <p>In FRC elements this equation becomes:</p> $V_{Rd} = V_{Rd,F} + V_{Rd,s}$	$V_{FRC} = 26.8 x \left\{ \frac{0.18}{\gamma_c} k_s \left[100 \rho \left(1 + 7.5 \frac{f_{ut-FRC}}{f_t} \right) f_c \right] + 0.15 \sigma_{cp} \right\} b d \text{ (in lb units)}$ $V_{FRC} = \left\{ \frac{0.18}{\gamma_c} k_s \left[100 \rho \left(1 + 7.5 \frac{f_{ut-FRC}}{f_t} \right) f_c \right] + 0.15 \sigma_{cp} \right\} b d \text{ (SI units)}$	$V_{Rd3} = V_{c,d} + V_{w,d} + V_{f,d}$ $V_{cd} = \left[0.12 k (100 \rho_l f_{ck})^{1/3} + 0.15 \sigma_{cp} \right] b_w d \text{ (N)}$ $k = 1 + \sqrt{\frac{200}{d}} \text{ (d in mm) and } k \leq 2$ $\rho_l = \frac{A_s}{b_w d} \leq 2\%$ $V_{fd} = 0.7 k_f k_l \tau_{fd} b_w d$ $V_{wd} = \frac{A_{sw}}{s} 0.9 d f_{ywd} (1 + \cot \alpha) \sin \alpha \text{ (N)}$	<p>Members without design shear reinforcement, with conventional longitudinal reinforcement</p> $V_{Rd,F} = \left\{ \frac{0.18}{\gamma_c} k \left[100 \rho_l \left(1 + 7.5 \frac{f_{Ftuk}}{f_{ctk}} \right) f_{ck} \right] + 0.15 \sigma_{cp} \right\} b_w d \text{ (stresses in MPa)}$ $k = 1 + \sqrt{\frac{200}{d}} \leq 2.0$ $\rho_l = A_s / b_w d \leq 0.02;$ $\sigma_{cp} = N_{Ed} / A_c$ $V_{Rd,Fmin} = (v_{min} + 0.15 \cdot \sigma_{cp}) \cdot b_w \cdot d$ $v_{min} = 0.035 k^{3/2} f_{ck}^{1/2}$ <p>Members with shear and longitudinal reinforcement</p> $V_{Rd,s} = V_{Rd,s} + V_{Rd,F}$ $V_{Rd,s} = \frac{A_{sw}}{s} z f_{ywd} (\cot \varphi + \cot \theta) \sin \varphi$ $A_{sw,max} \leq \frac{0.5 v f_{cd} \sin \varphi b_w s}{1 - \cos \varphi f_{ywd}}$ $v = 0.6 \left(1 - \frac{f_{ck}}{250} \right) [f_{ck} \text{ in MPa}]$ $V_{Rd,max} = \frac{b_w z v f_{cd} (\cot \varphi + \cot \theta)}{(1 + \cot^2 \theta)}$	<p>Except otherwise specified in this Chapter, follow section 6.3 “Shear” of Standard Specifications for Concrete Structures—Structural Performance Verification.</p> <p>The design shear capacity of a linear member consisting solely of HPFRCC and reinforcing steels V_{yd} may be obtained by Equation (6.3.1) below.</p> $V_{yd} = V_{cd} + V_{sd} + V_{fd} + V_{ped}$ <p>where V_{cd}: design shear capacity of a linear member without any shear reinforcing steels, excluding the strength exerted by reinforcing fiber, which is given by Equation (6.3.2) below.</p> $V_{cd} = \beta_d \beta_p \beta_n f_{vcd} b_w d / \gamma_b$



ELU - Torsión					
EHE 08	Model Code 2010	ACI	RILEM	CNR	JSCE
-	<p>Beams without longitudinal and transverse reinforcement</p> <p>When FRC with a hardening tensile behaviour is used in a member without both longitudinal reinforcement and transverse reinforcement, the principal tensile stress shall not exceed the design tensile strength:</p> $\sigma_1 \leq \frac{f_{Ftuk}}{\gamma_F}$ <p>where: f_{Ftuk} [MPa] is the characteristic value of the ultimate residual tensile strength for FRC at $w_u = 1.5$ mm according to Eq. (5.6.-6).</p> <p>Beams with longitudinal and transverse reinforcement</p> <p>The presence of fibres increases the torsion capacity; however, design models are not currently available. Models should be proven by experiments on real size elements.</p>	-	-	<p>Members without torsional longitudinal and transverse conventional reinforcement</p> $\sigma_1 \leq \frac{f_{Ftuk}}{\gamma_F}$ <p>Members with torsional longitudinal and transverse conventional reinforcement</p> <p>When members with longitudinal rebars and transverse reinforcement are considered, the contribution of fiber reinforcement can be taken into account based on adequate models.</p>	<p>(1) In principle, follow section 6.4 “Torsion” of Standard Specifications Concrete Structures –<i>Structural Performance Verification</i>.</p> <p>(2) The torsional capacity of HPFRCC after initiating torsional cracking shall be calculated by an appropriate method such as testing.</p> <p>[Commentary] Due to the shortage of data on the torsional capacity of HPFRCC after initiating torsional cracks, the safety should be examined by an appropriate method such as testing.</p>



ELU - Fatiga					
EHE 08	Model Code 2010	ACI	RILEM	CNR	JSCE
-	-	<p>Experimental studies show that, for a given type of fiber, there is a significant increase in flexural fatigue strength with increasing percentage of steel fibers [2.31, 2.69-2.72]. The specific mix proportion, fiber type, and fiber percentage for an application in question should be compared to the referenced reports. Depending on the fiber type and concentration, a properly designed SFRC mixture will have a fatigue strength of about 65 to 90 percent of the static flexural strength at 2 million cycles when nonreversed loading is used [2.72, 2.73], with slightly less fatigue strength when full reversal of load is used [2.71].</p> <p>It has been shown that the addition of fibers to conventionally reinforced beams increases the fatigue life and decreases the crack width under fatigue loading [2.70]. It has also been shown that the fatigue strength of conventionally reinforced beams made with SFRC increases. The resulting deflection changes accompanying fatigue loading also decrease [2.74]. In some cases, residual static flexural strength has been 10 to 30 percent greater than for similar beams with no fatigue history. One explanation for this increase is that the cyclic loading reduces initial residual tensile stresses caused by shrinkage of the matrix [2.75].</p>	-	<p>The addition of fibers can improve the toughness, durability, impact resistance (resiliency), fatigue and abrasion resistance of the cementitious matrix.</p>	<p>(1) The characteristic value of HPFRCC's fatigue strength shall be determined from the results of fatigue strength tests that are performed in consideration for the exposed condition of the structure and other relevant conditions.</p> <p>(2) In general, material factor of HPFRCC γ_c is set at 1.3 in the fatigue limit state.</p> <p>(3) In general, the design compressive/flexural compressive fatigue strength of HPFRCC f_{rd} can be obtained by Equation (3.9.1), assuming it is a function of fatigue life N and permanent-load-induced stress σ_p. It shall be noted, however, that the fatigue strength shall be experimentally determined where HPFRCC is continuously or often saturated with water.</p> <p>$f_{rd} = 0.85 f_d (1 - \sigma_p / f_d) (1 - \log N / 17)$ (N/mm²) (3.9.1) where, $N \leq 2 \times 10^6$, f_d: design compressive strength of HPFRCC, and material factor γ_c is given as 1.3 here.</p> <p>(4) The design compressive/flexural compressive fatigue strength of HPFRCC f_{rd} shall be experimentally determined, assuming it is a function of fatigue life N and stress σ_p.</p>

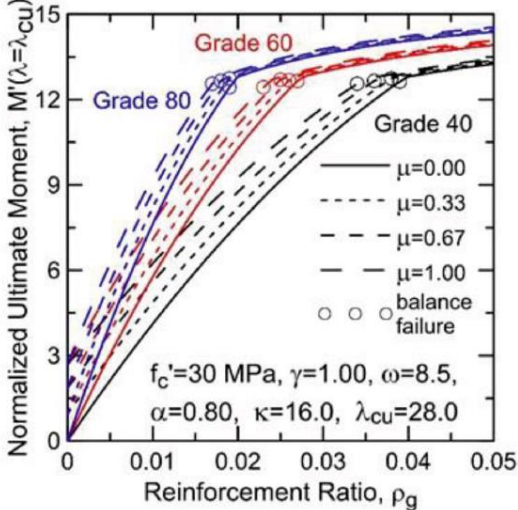


ELS - Fisuración																																		
EHE 08	Model Code 2010	ACI	RILEM	CNR	JSCE																													
-	<div>$w_d = 2\{kc + \frac{1}{4}\frac{\phi_s}{\rho_{s,ef}}\frac{(f_{ctm} - f_{Ftms})}{\tau_{bm}}\}\frac{1}{E_s}(\sigma_s - \beta\sigma_{sr} + \eta_r\varepsilon_rE_s)$$\sigma_{sr} = (f_{ctm} - f_{Ftms}) \cdot (1 + \alpha_e.\rho_s) / \rho_{s,eff}$$f_{Ftms} = f_{Ftsk} / 0,7$</div> <div>Minimum reinforcement:</div> <div>$A_{s,min} = k_c k (f_{ctm} - f_{Ftms}) \frac{A_{ct}}{\sigma_s}$</div>	<div>In many areas, the durability of concrete can be significantly improved by the use of fiber reinforcement (ACI 544.5R). Fiber reinforcement has also been shown to improve the resistance of concrete in exposure to freezing-and-thawing cycles. Using macrofibers in concrete alters the crack widths and spacing that can positively affect the long-term durability.</div> <div>Moreover, there exists a lot of research and practical experience showing significant reduction in crack width in environmental structures using hybrid reinforcement (bars plus fibers).</div> <div>To ensure proper serviceability, cracking should be examined so that the flexural crack width is not greater than the allowable crack width. ACI 224R limits the allowable crack width to 0.012 in. (0.3 mm) for concrete structures exposed to soil. This value may vary for different applications in various environments.</div>	<div><table><tr><th colspan="5">Table 3 - Criteria for crack width</th></tr><tr><th rowspan="2">Exposure class (*)</th><th rowspan="2">Steel fibres</th><th rowspan="2">Steel fibres + ordinary reinforcement</th><th colspan="2">steel fibres +</th></tr><tr><th>post-tensioning</th><th>pre-tensioning</th></tr><tr><td>1</td><td>(****)</td><td>(****)</td><td>0.2 mm</td><td>0.2 mm</td></tr><tr><td>2</td><td>0.3 mm</td><td>0.3 mm</td><td>0.2 mm</td><td>decompression (**)</td></tr><tr><td>3</td><td colspan="4" rowspan="3">Special crack limitations dependent upon the nature of the aggressive environment involved have to be taken.</td></tr><tr><td>4</td></tr><tr><td>5</td></tr></table><div>(*): (**): (***): (****):</div><div>see Appendix 2 the decompression limit requires that, under the frequent combination (***) of loads, all parts of the tendons or ducts lie at least 25 mm within concrete in compression see ENV 1992-1-1 [1] for exposure class 1, crack width has no influence on durability and the limit could be relaxed or deleted unless there are other reasons for its inclusion.</div></div>	Table 3 - Criteria for crack width					Exposure class (*)	Steel fibres	Steel fibres + ordinary reinforcement	steel fibres +		post-tensioning	pre-tensioning	1	(****)	(****)	0.2 mm	0.2 mm	2	0.3 mm	0.3 mm	0.2 mm	decompression (**)	3	Special crack limitations dependent upon the nature of the aggressive environment involved have to be taken.				4	5	<div>The characteristic crack width wk, in FRC elements can be evaluated by using the following relationship:</div> <div>$wk = \beta \cdot s_{rm} \cdot \varepsilon_{sm}$</div>	<div>(1) Cracks in HPFRCC due to bending moments, shear forces, torsional moments and axial forces shall be examined with appropriate methods determining whether safety and serviceability of structure are impaired.</div> <div>(2) Examination of cracks in terms of resistance to environmental actions is essentially a control of crack width in HPFRCC surfaces under specified environmental conditions and not to allow Steel corrosion associated with ingress of chloride ions and carbon dioxide and resulting degradation of required performance of structures during design service life. Examination may be accomplished by confirming the following (i) and (ii) with the method specified in Chapter 9.</div> <div>(3) When water tightness is an important factor, an appropriate permissible crack width may be specified, and then be confirmed that crack widths are less than the permissible value.</div> <div>(4) When appearance is an important factor, an appropriate permissible crack width may be specified, and then be confirmed that any crack widths are less than the permissible value.</div>
Table 3 - Criteria for crack width																																		
Exposure class (*)	Steel fibres	Steel fibres + ordinary reinforcement	steel fibres +																															
			post-tensioning	pre-tensioning																														
1	(****)	(****)	0.2 mm	0.2 mm																														
2	0.3 mm	0.3 mm	0.2 mm	decompression (**)																														
3	Special crack limitations dependent upon the nature of the aggressive environment involved have to be taken.																																	
4																																		
5																																		



ELS – Compresión máxima					
EHE 08	Model Code 2010	ACI	RILEM	CNR	JSCE
-	<p>In structural FRC elements having a tension hardening behaviour after cracking, the tensile stresses verification shall be done by imposing the limitation:</p> $\sigma_t \leq 0.6 \cdot f_{tsk}$	-	-	<p>(1) The compressive stresses at SLS shall be limited in accordance to the current Codes.</p> <p>(2) When structural elements with softening FRCs are considered, the verification of the tensile stresses is satisfied if the element is verified at ULS.</p> <p>(3) When structural elements with hardening FRCs are considered, the tensile stresses verification shall be done by imposing the limitation:</p> $\sigma_t \leq 0.6 \cdot f_{tuk}$	<p>Compressive stress of HPFRCC due to bending moments and axial forces and tensile stress of steel shall not exceed the limit values given in (1) and (2).</p> <p>(1) Limit value of compressive stress due to bending moment and axial forces of HPFRCC are $0.4f'_{ck}$ under permanent load where f'_{ck} is a characteristic value of compressive strength of HPFRCC.</p> <p>(2) Limit value of steel tensile stress is f_{yk}, where f_{yk} is a characteristic value of tensile yield strength of steel.</p>



Cuantías mínimas - Flexión					
EHE 08	Model Code 2010	ACI	RILEM	CNR	JSCE
<p>Los valores de la tabla 42.3.5 relativos a las cuantías geométricas mínimas que, en cualquier caso, deben disponerse en los diferentes tipos de elementos estructurales, en función del acero utilizado, se podrán reducir, en el caso de hormigones con fibras, en una cuantía mecánica equivalente:</p> $A_c f_{ctR,d}$	$A_{s,min} = k_c k (f_{ctm} - f_{Ftsm}) \frac{A_{ct}}{\sigma_s}$	$M_n \approx m_{\infty} M_{cr}$ $= \frac{6 \rho_g n k (\mu \alpha - \mu + \alpha \omega) + 3 \omega \mu - 3 (\rho_g n k)^2}{\omega + \mu} M_{cr}$ $\rho_{min} = \frac{9 \alpha - \sqrt{81 \alpha^2 - 6}}{2 \alpha n k}$  <p>Normalized Ultimate Moment, $M'(\lambda=\lambda_{cu})$</p> <p>Reinforcement Ratio, ρ_g</p> <p>Grade 60</p> <p>Grade 80</p> <p>Grade 40</p> <p>$\mu=0.00$</p> <p>$\mu=0.33$</p> <p>$\mu=0.67$</p> <p>$\mu=1.00$</p> <p>balance failure</p> <p>$f'_c=30$ MPa, $\gamma=1.00$, $\omega=8.5$, $\alpha=0.80$, $\kappa=16.0$, $\lambda_{cu}=28.0$</p>	$A_s = (k_c k k_p f_{fct,ef} - 0.45 f_{Rm,1}) \frac{A_{ct}}{\sigma_s}$	<p>For cracking control in the elements under bending, a minimum reinforcement should be present, its area should be present and greater than:</p> $A_{s,min} = (k_c k_s k_p f_{ctm} - f_{Ftsm}) \frac{A_{ct}}{\sigma_s}$	<p>In principle, structural details shall be determined based on section 6.2.2 “Structural details” of Standard Specifications for Concrete Structures –<i>Structural Performance Verification</i>.</p> <p>[Commentary] When the tension reinforcement ratio becomes extremely small in a reinforced concrete member, the yielding load becomes smaller than the cracking load, and steel bars may yield or fracture immediately after cracking and the bending member shows brittle failure mode. Only one crack may occur and it may show a failure mode like unreinforced concrete. This requires the tension reinforcement ratio of a rectangular member, where flexural moment is dominant, should be larger than 0.2 percent as specified in Standard Specifications for Concrete Structures –<i>Structural Performance Verification</i>. HPRCC on the other hand is a highly ductile material showing pseudo strain-hardening characteristics and can bear tensile stress in a stable manner. Experimental results showed that cracking did not result in a brittle failure even though tension reinforcement ratio is smaller than 0.2 percent. However, this “Recommendations” document follows Standard Specifications for Concrete Structures –<i>Structural Performance Verification</i> because sufficient data is not yet available.</p>



Cuantías mínimas - Cortante					
EHE 08	Model Code 2010	ACI	RILEM	CNR	JSCE
<p>Armaduras transversales</p> <p>La cuantía mínima de refuerzo a cortante, ya sea en forma de Hormigón Reforzado por Fibras de acero y/o estribos verticales se verifica siempre que se cumpla la relación:</p> $V_{su} + V_{fu} > \frac{f_{ct,m}}{7,5} b_0 d$	<p>It is possible to prevent the use of the minimum amount of conventional shear reinforcement (stirrups) if the following condition is fulfilled:</p> $f_{Ftuk} \geq 0.08 \sqrt{f_{ck}}$ <p>where:</p> <p>f_{Ftuk} [MPa] is the characteristic value of the ultimate residual tensile strength for FRC, by considering $w_u = 1.5$ mm</p>	<p>According to this code, it is possible to eliminate minimum amount of conventional shear reinforcement (stirrups) if the ultimate tensile residual strength of FRC is sufficiently high—that is, $f_{ut-FRC} > (0.6) f_c$ (1/2) psi (f_c (1/2)/20 MPa).</p>	-	<p>It is possible to avoid the presence of conventional shear reinforcement (stirrups) if the following limitation is respected:</p> $f_{Ftuk} \geq \frac{\sqrt{f_{ck}}}{20} [f_{ck} \text{ in MPa}]$ <p>This limitation allows limiting the development and the diffusion of the inclined cracking and, as a consequence, can ensure a sufficient member ductility.</p> <p>When the above-mentioned limitation is violated, a conventional shear reinforcement (stirrups) shall be introduced, sufficient to ensure an ultimate shear resistance greater than the first cracking one, V_{cr}:</p> $V_{cr} = 0.67 \cdot f_{ctk} \cdot b_w \cdot d.$ <p>The part of the shear resistance due to the shear reinforcement is equal to the difference:</p> $V_{Rds,min} = V_{cr} - V_{Rd,F}.$ <p>The longitudinal spacing between the shear reinforcements (stirrups), s, shall not exceed the value $0.8 \cdot d$.</p> <p>When a great amount of longitudinal reinforcement in the compressive zone is present, adequate stirrups reinforcement shall be applied in order to prevent rebar instability.</p>	<p>(1) No particular specifications are prescribed for the minimum number of stirrups when the design tensile yielding strength of HPFRCC is larger than 1.5 N/mm². However in the other case, amount of shear reinforcement greater than 0.15% shall be arranged throughout the length of the linear member. The stirrup spacing shall in principle be less than 3/4 of the effective depth of the member and less than 400mm. This rule is not applicable to planar members</p> <p>(2) Where the calculation results show that the linear member needs shear steel reinforcement, the stirrup spacing shall be less than 1/2 of the effective depth and less than 300 mm. In addition, the same amount of shear steel reinforcement shall be provided over a distance equal to the effective depth of member from the end of the region that is found to be in need of shear Steel reinforcement in calculation.</p> <p>(3) When stirrups are anchored in a tension region, an appropriate confirmation process such as testing shall be followed.</p>



Tras analizar la normativa internacional para el diseño del hormigón reforzado con fibras pueden extraerse las siguientes conclusiones:

Caracterización mecánica

Módulo de elasticidad

El módulo de elasticidad del hormigón reforzado con fibras, según las normativas consideradas, no varía significativamente respecto al del hormigón convencional a menos que se incluya un alto porcentaje de fibras. Por lo tanto, deben de aplicarse los valores de hormigón convencional que propone cada normativa. La normativa japonesa indica que el método de ensayo puede ser el utilizado para hormigón convencional, además muestra como el módulo de elasticidad es menor que para el hormigón convencional.

Coeficiente de Poisson

Si bien no todas las normativas recogen específicamente el coeficiente de Poisson, de manera general todas ellas indican que las propiedades mecánicas no deben de modificarse respecto al hormigón convencional, salvo que se añada un alto porcentaje de fibras. La normativa japonesa indica que debe de basarse en ensayos o datos existentes, y refleja que el coeficiente es ligeramente superior para el hormigón reforzado con fibras.

Tracción

Para la caracterización a tracción todas las normativas recurren al ensayo a flexión para la obtención del diagrama carga-apertura de fisura. De este diagrama se obtienen las resistencias residuales a tracción que definen los diferentes diagramas de cálculo propuestos. Tanto la EHE 08 como el Model Code 2010, recurren al ensayo normalizado EN 14651 del marco europeo. La normativa ACI hace referencia al ensayo propuesto por RILEM cuyas características son similares a las de EN 14651 con un ensayo a flexión en tres puntos. La norma CNR propone el ensayo UNI 11039, en el que se aplican dos cargas puntuales a diferencia de los ensayos nombrados anteriormente. Se observa que el comportamiento a tracción varía significativamente con la adición de fibras.

Compresión

El comportamiento a compresión, como recogen las distintas normativas, no varía notablemente respecto al hormigón convencional, tanto la EHE como la JSCE proponen recurrir al diagrama parábola rectángulo.



Estado Límite Último

Flexión compuesta

El refuerzo con fibras supone que en flexión compuesta la zona fisurada de la sección, desarrolle resistencia, a diferencia de en hormigón convencional, de esta forma las distintas normativas recogen la contribución de este área a la resistencia de la sección frente a flexión compuesta.

Cortante

Para la capacidad frente a esfuerzo cortante las normativas proponen la consideración de un término adicional en la tradicional fórmula de cortante. La formulación de las distintas normativas es similar, teniendo en cuenta los mismos factores.

Torsión

La capacidad a torsión no está lo suficientemente desarrollada en ninguna de las normativas analizadas, la única condición impuesta por la normativa es la limitación de tensión. Para el resto de aspectos la normativa indica que se recurra a métodos apropiados, como ensayos.

Fatiga

La normativa actual no profundiza en el tratamiento del comportamiento a fatiga, si bien indica que la adición de fibras mejora este comportamiento. La normativa japonesa propone un estudio de daño acumulado.

Estado Límite de Servicio

Fisuración

Como se ha comentado anteriormente la inclusión de fibras de refuerzo disminuye la propagación de fisuras, el código modelo plantea la formulación para el cálculo del ancho de fisura cuando existe refuerzo convencional, además requiere una armadura mínima para controlar la fisuración. La norma ACI no propone ninguna formulación.

Por su parte la norma RILEM establece el criterio de ancho de fisura según el tipo de exposición y el tipo de refuerzo como plantea en su tabla. Además, indica que el cálculo debe de hacerse de manera similar al de hormigón convencional, pero considerando que la tensión de tracción tras la fisuración no es cero, si no $0.45 f_{Rm,1}$.

Por otro lado, la norma CNR propone su propia formulación, mientras que la norma japonesa se limita a hacer recomendaciones sin establecer una formulación específica.

Compresión máxima

Tanto el Model Code como CNR, limitan la tensión de compresión máxima al 60% de la resistencia última residual de tracción del hormigón reforzado con fibras para una



apertura de fisura de 1.5mm. La normativa japonesa limita la tensión de compresión debida a flexión o esfuerzo axial al 40% de la resistencia característica a compresión. El resto de normativas no incluyen disposiciones específicas.

Cuantías mínimas

Flexión

El Model Code, RILEM y CNR recurren a una formulación similar para las cuantías mínimas de flexión, cuya misión principal es el control de la fisuración. La EHE reduce la cuantía mínima en una cuantía mecánica equivalente $A_c f_{ctR,d}$. Por último, la norma ACI propone una cuantía de refuerzo en función del momento último normalizado.

Cortante

Para la cuantía mínima de cortante, tanto el Model Code, como ACI y CNR, permiten prescindir de refuerzo convencional si la resistencia característica última residual de tracción supera cierto umbral, que depende de cada normativa. Del mismo modo la EHE permite sustituir la armadura de cortante mínima por el refuerzo con fibras.

Torsión

Ninguna de las normativas consideradas especifica la cuantía mínima de torsión para el hormigón reforzado con fibras.



3.8. COMPORTAMIENTO EN TORSIÓN

Debido a la falta de desarrollo de la normativa del comportamiento en torsión se ha realizado un análisis más detallado de las investigaciones y desarrollos experimentales bajo este esfuerzo.

La normativa ACI en su publicación ACI 544.9R Report on Measuring Mechanical Properties of Hardened Fiber- Reinforced Concrete [11] indica lo siguiente sobre la caracterización a torsión: Para el comportamiento a torsión, solo ensayos en elementos estructurales han sido desarrollados (di Prisco et al. 2014). La figura 11a muestra el montaje para ensayos de torsión en vigas, con el detalle de la articulación de torsión en extremos (Fig. 11b). El fallo de las vigas ocurre según el modelo estructural dimensional (3D). Un contenido hasta 1.2 de porcentaje en volumen de fibras no es capaz de inducir un comportamiento multifisura, sin embargo, si se añade un porcentaje superior al 0.9 por ciento, las fibras son capaces de mejorar la ductilidad de las vigas, evitando así la separación abrupta de la vida en dos segmentos tras la fisuración

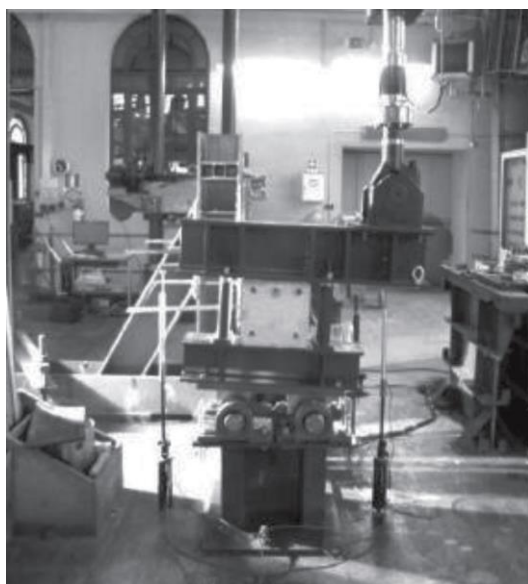


Ilustración 52.- ACI 544.9R - Fig. 11a Schematic of setup for torsion test on FRC beams (di Prisco et al. 2014).

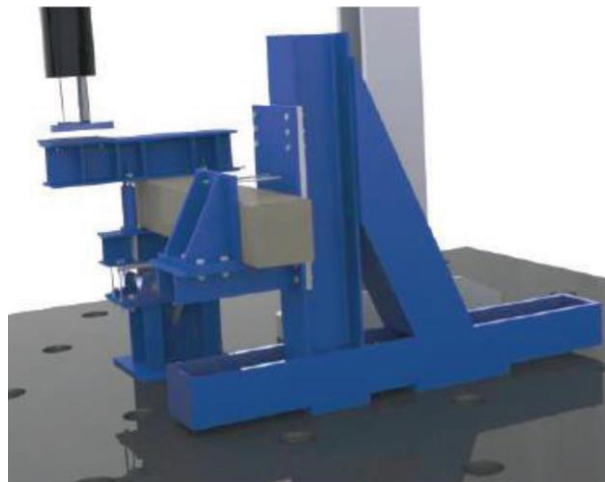


Ilustración 53.- ACI 544.9R - Fig. 11b Torsional hinge (*di Prisco et al. 2014*).

La publicación “TORSIONAL STRENGTH OF STEEL FIBER REINFORCED CONCRETE” [12] trata de aportar una formulación para la resistencia a torsión, a continuación, se presentan los extractos más relevantes:

Según Rao [13], como el estado de tensión es cortante puro acompañado de la misma intensidad de tensiones de compresión y tracción en direcciones ortogonales, la resistencia aparente de tracción disminuye ligeramente respecto a la del hormigón. De esta forma la resistencia efectiva de tracción del hormigón en torsión pura es:

$$1/f_t = 1/f_c + 1/f_{spt}$$

Donde:

f_t : resistencia de tracción efectiva del hormigón en torsión pura

f_{spt} : resistencia de tracción del cilindro de deslizamiento

f_c : resistencia cúbica del hormigón

Por otra parte, según ACI, una viga sometida a torsión se idealiza como un tubo de pared delgada despreciando el núcleo de hormigón a través de la sección, con analogía del entramado espacial, el momento torsor es función de $\sqrt{f'_c} \left(\frac{A_{cp}^2}{p_{cp}} \right)$

Donde:

f'_c : resistencia específica a compresión del hormigón.

A_{cp} : área encerrada por el perímetro exterior de la sección de hormigón.

p_{cp} : perímetro exterior de la sección de hormigón.



Los parámetros anteriores se aplican introduciéndolos en la expresión general:

$$T = \alpha \left(\frac{A_{cp}^2}{p_{cp}} \right) f_t$$

Donde:

f_t : resistencia de tracción efectiva del hormigón en torsión pura

T: resistencia a momento torsor, kNm

El análisis de regresión conduce a la siguiente ecuación:

$$T = 0.833 \left(\frac{A_{cp}^2}{p_{cp}} \right) f_t$$

La siguiente figura ilustra la comparación entre la torsión calculada según la expresión obtenida y la recogida en la norma ACI.

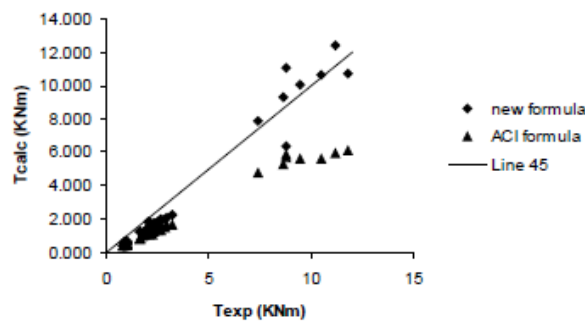


Ilustración 54.- Figure 1 Experimental values of torsion (Texp) versus calculated torsion (Tcal) according, first according to proposed equation, then according to ACI equation.

El artículo “Minimum torsional reinforcement ratio for reinforced concrete members with steel fibers” [14], propone un refuerzo mínimo transversal de torsión:

$$A_{t,min} = \lambda \frac{1}{4} \frac{\sqrt{f'_c}}{f_{yt}} \frac{A_{cp}^2}{A_0} \frac{s}{p_{cp}} \tan \theta$$

Además, el refuerzo transversal mínimo a torsión es el siguiente:

$$A_{l,min} = \lambda \frac{1}{4} \frac{\sqrt{f'_c}}{f_{yl}} \frac{A_{cp}^2}{A_0} \frac{p_h}{p_{cp}} \cot \theta$$



4. CONCLUSIONES

La tendencia del sector eólico conduce a torres más altas en las cuales el hormigón resulta competitivo, para ello es necesario el desarrollo de tecnologías que mejoren las propiedades y optimicen el costo económico. Una de estas técnicas es el uso de hormigón reforzado con fibras en lugar del hormigón convencional.

Es necesario comprender el comportamiento y las características de este tipo de hormigón para lo cual se ha recurrido al estudio de la normativa existente.

El análisis de la normativa refleja que la inclusión de fibras en el hormigón resulta beneficiosa para los estados límites últimos y límite de servicio. El comportamiento a compresión del hormigón reforzado con fibras no varía significativamente, a diferencia del comportamiento a tracción que mejora debido al endurecimiento que provocan las fibras al coser las fisuras.

De forma general las distintas normativas reflejan la contribución de las fibras a la capacidad desarrollada para los diferentes esfuerzos sin profundizar en su uso como único refuerzo, lo cual supone uno de los grandes avances en esta tecnología.

Si bien los principales apartados analizados están contemplados en la normativa, el comportamiento a torsión no queda definido en ninguna de ellas, limitándose a indicar que deberán de realizarse estudios específicos como ensayos. De igual forma para el comportamiento a fatiga solo la norma japonesa profundiza en el cálculo, limitándose el resto de normativas a indicar que la inclusión de fibras mejora este comportamiento.

De lo anterior podemos concluir que la línea de investigación del hormigón reforzado con fibras debe de dirigirse hacia la completa caracterización a torsión y fatiga, para la posterior inclusión en las diferentes normativas que deben de actualizarse.



5. REFERENCIAS

- [1] W. E. Foundation, «Wind Energy Foundation,» [En línea].
- [2] G. -. G. W. E. Council, «Global Wind Report, Annual Market Update 2017».
- [3] A. I. T. G. 9, «Report on Design of Concrete Wind Turbine Towers».
- [4] T. C. Centre, «Concrete Towers for Onshore and Offshore Wind Farms».
- [5] A. 544.1R-96, «Report on Fiber Reinforced Concrete,» R2009.
- [6] M. Joshua A. McMahon and Anna C. Birely, «Experimental Performance of Steel Fiber Reinforced Concrete Bridge Deck,» 2018.
- [7] J. V. N. A. J. B. H. R. Paulo A. L. Fernandes, «Study of a self-compacting fiber-reinforced concrete to be applied in the precast industry,» 2018.
- [8] P. P. J. M. X. S. Y. R. AC Birely, «Fiber Reinforced Concrete for Improved Performance of Transportation Infrastructure,» 2018.
- [9] M. d. Fomento, Instrucción de Hormigón Estructural EHE-08, 2008.
- [10] JSCE, «Recommendations for Design and Construction of High Performance Fiber Reinforced Cement Composites with Multiple Fine Cracks (HPFRCC),» 2008.
- [11] 544.9R-17, «Report on Measuring Mechanical Properties of Hardened Fiber-Reinforced Concrete,» 2017.
- [12] M. A. M. Muhammad I. Rjoub, «TORSIONAL STRENGTH OF STEEL FIBER,» Journal of Engineering Sciences, Assiut University, Vol. 35, No.1, pp.1-8, 2007.
- [13] D. R. S. T.D. Gunneswara Rao, «Torsion of steel fiber reinforced concrete members,» Cement and Concrete Research 33, 2003.
- [14] D. H. L. K. S. K. Hyunjin Ju, «Minimum torsional reinforcement ratio for reinforced concrete members with steel fiber,» Composite Structures, 2018.



- [15] R. T. 1. TDF, «Test and design methods for steel fibre reinforced concrete,» 2003.
- [16] CNR, «Guide for the Design and Construction of Fiber-Reinforced Concrete Structures,» 2007.
- [17] A. 544.2R-17, «Report on the Measurement of Fresh State Properties,» 2017.
- [18] A. 544.3R-08, «Guide for Specifying, Proportioning, and Production of Fiber-Reinforced Concrete,» 2008.
- [19] A. 544.4R-18, «Guide to Design with Fiber Reinforced Concrete,» 2018.
- [20] A. 544.R-10, «Report on the Physical Properties and durability of fiber reinforced concrete,» 2010.
- [21] A. 544.6R-15, «Report on Design and Construction of Steel Fiber-Reinforced Concrete Elevated Slabs,» 2015.
- [22] A. 544.7R-16, «Report on Design and Construction of Fiber-Reinforced Precast Concrete Tunnel Segments,» 2016.
- [23] ACI.8R-16, «Report on Indirect Method to Obtain Stress-Strain Response of Fiber-Reinforced Concrete,» 2016.